UV-Vis and MCD Spectroscopy and TDDFT investigations into N-Confused porphyrins and properties of mono-functionalized tetraferrocenyl porphyrins in solution and on a gold surface: assessment of the influencing factors for photoelectrochemical applications

A THESIS SUBMITTED TO THE GRADUATE SCHOOL OF THE UNIVERSITY OF MINNESOTA BY

Nathan Robert Erickson

IN PARTIAL FULFILLMENT OF THE REQUIREMENTS FOR THE DEGREE OF MASTER OF SCIENCE

Advised by Dr. Victor N. Nemykin

August 2014

Acknowledgements

I would like to thank Dr. Victor Nemykin for all of his support and guidance during my time working with him. I would not have been able to complete these projects without him. I am grateful of all the support that I received from my colleagues in the Nemykin lab, they were excellent help when I was frustrated. I would like to thank all of the collaborators I have worked with on my projects, their work has kept me busy. I also need to thank my family for their support and understanding during my time working in the lab. I finally would like to thank the NSF for their grant NSF (CHE-1110455) and the Minnesota Supercomputing Institute for their support of this research.

Abstract

N-confused porphyrin (NCP) and its externally methylated variant (MeNCP) were investigated using UV-visible and magnetic circular dichrosim (MCD) spectroscopies. In addition to evaluating the spectroscopy of the neutral compounds, the acid/base chemistry of these macrocycles was examined by the same methods. NCP exhibits two tautomeric states depending on the polarity of the solvent, and their protonation/deprotonation chemistries also differ depending on solvent polarity. DFT and TDDFT calculations were employed to evaluate the observed spectroscopic changes. Using both experimental and calculated results, we were able to determine the sites of protonation/deprotonation for both tautomeric forms of NCP. Inspection of the MCD Faraday B terms for all of the macrocycles presented in this report showed that the ΔHOMO > ΔLUMO condition is maintained in all cases and these observations were in good agreement with the DFT calculations.

Various methylated N-confused tetraphenylporphyrins (MeNCTPP) were investigated using UV-Vis and magnetic circular dicrhoism (MCD) spectroscopy in polar and apolar solvents as well as the protonation and deprotonation of the compounds. The MeNCTPPs were also investigated using time-dependent density functional theory (TDDFT) methods in the gas phase. Experimentally, the MCD spectra showed that all the molecules investigated had transitions with the ΔHOMO > ΔLUMO. TDDFT results confirmed these energy gaps. TDDFT calculations also showed that nearly all low energy transitions were from the HOMO to the LUMO and LUMO+1, except in the case of **2c**, **5a,** and **5c**. Otherwise, results show that the addition of a methyl group to the N-

confused tautomer of tetraphenylporphyrin effectively regulates the proton tautomerization of the N-confused tautomer. MeNCTPPs are unaffected by the polarizability of the solvent.

Two unsymmetric *meso*-tetraferrocenyl-containing porphyrins of general formula $H_2Fc_3Fc(COR)P$ [Fc = ferrocenyl, R = $-CH_3$ or $-(CH_2)_5Br$, P = porphyrin(2-)] have been prepared and characterized by variety of spectroscopic methods, while their redox properties were investigated using cyclic voltammetry (CV) and differential pulse voltammetry (DPV) approaches. Spectroscopic signature of the mixed-valence $[H_2Fc_3Fc(COR)P\ ]^{n+}$ (n = 1, 3) were investigated using spectroelectrochemical as well as chemical oxidation methods and corroborated with DFT and TDDFT calculations. Inter-valence charge-transfer (IVCT) transitions in $[H_2Fc_3Fc(COR)P\ ]^{+}$ were analyzed using band deconvolution analysis in the borders of Hush model. The resulting data from the mixed-valence $[H_2Fc_3Fc(COR)P\ ]^{+}$ derivatives matched very closely to the previously reported MTFcP and metal-free poly(ferrocenyl)porphyrins complexes and were assigned as Robin and Day Class II mixed-valence compounds. Following previous results indicating the ability of gold supported TFcP monolayers in photo-catalytic reduction of dioxygen, self-assembled monolayers (SAMs) of a thioacetyl derivative ($H_2Fc_3Fc(CO(CH_2)_5SCOCH_3)P$) were also prepared and characterized using UV-vis spectroscopy and CV methods. Photoelectrochemical properties of SAMs in different electrolyte systems were investigated by electrochemical techniques and photocurrent generation experiments, showing that the choice of electrolyte is critical for efficiency of redox-active SAMs.

Table of Contents

List of Tables

List of Figures

Chapter One: Magnetic Circular Dichroism Spectroscopy of N-Confused Porphyrin and its Ionized Forms

Introduction

Since its discovery in 1994,[1,2] the properties of the porphyrin isomer N-confused porphyrin (also known as 2-carba-21-azaporphyrin and inverted porphyrin, Scheme 1) have intrigued chemists.[3-8] Accordingly, the chemical and physical properties of this porphyrinic macrocycle have received a considerable amount of attention. In large part, this attention is the result of the striking similarities and differences between N-confused porphyrin and normal porphyrin. Essentially, N-confused porphyrin has an identical structure to normal porphyrin but with two atom positions swapped; a carbon atom occupies one of the four internal positions, and a nitrogen atom resides at the periphery of the ring. As a result, the overall shapes of N-confused porphyrin and normal porphyrin are nearly identical, and the two macrocycles share many of the same characteristics, including the presence of an 18 electron annulene ring and two ionizable protons.

However, in spite of the similarities in steric footprint, N-confused porphyrins and normal porphyrins exhibit markedly different electronic structures and chemical reactivities, as seen in their metal binding properties.[5,7,8] One particular notable difference can be seen in the tautomerization of N-confused porphyrin.[9] Normal porphyrins exhibit multiple tautomeric states, but in symmetric porphyrins (e.g. H_2TPP, **1**,

Scheme 1), the two most stable tautomers are identical. In N-confused porphyrin (NCP), tautomerization of the ionizable protons results in two separate and stable isolable forms: an external tautomer (**2**) where one proton resides at the external nitrogen position and two protons are found at the core of the ring and an internal tautomer (**3**) where three protons are located in the core of the ring. These two tautomers, both shown in Scheme 1, exhibit different degrees of planarity, vary in the bond lengths in the inverted pyrrole region, and most notably show different UV-visible spectra.[9,3] The tautomeric state of N-confused porphyrin can be controlled by solvent polarity; the external tautomer is stable in polar media that can hydrogen bond the external NH group, while the internal tautomer forms under non-polar conditions. One method for controlling the tautomeric states of N-confused porphyrin is to alkylate the external nitrogen position, such as via a methyl group, (**4)** which effectively forces the macrocycle to adopt an external tautomeric structure.[10] The notable difference in the UV-visible spectra included a broadening of the Soret band, a very intense $\pi \rightarrow \pi^*$ transition normally found between 400 nm and 450 nm, and sifts in the weaker Q-bands, which are lower intensity $\pi \rightarrow \pi^*$ transitions that are indicative of different porphyrins.

The disparities between normal and N-confused porphyrin and between the tautomers of N-confused porphyrin have spurred theoretical and photophysical investigations comparing the two macrocycles.[10-16] To date, there has only been a limited amount of analysis of the spectral features of either tautomer of free base N-confused porphyrins or their corresponding metal complexes. One methodology that has proven invaluable for the investigation of macrocycles related to porphyrins and phthalocyanines is magnetic circular dichroism (MCD).[17-29]

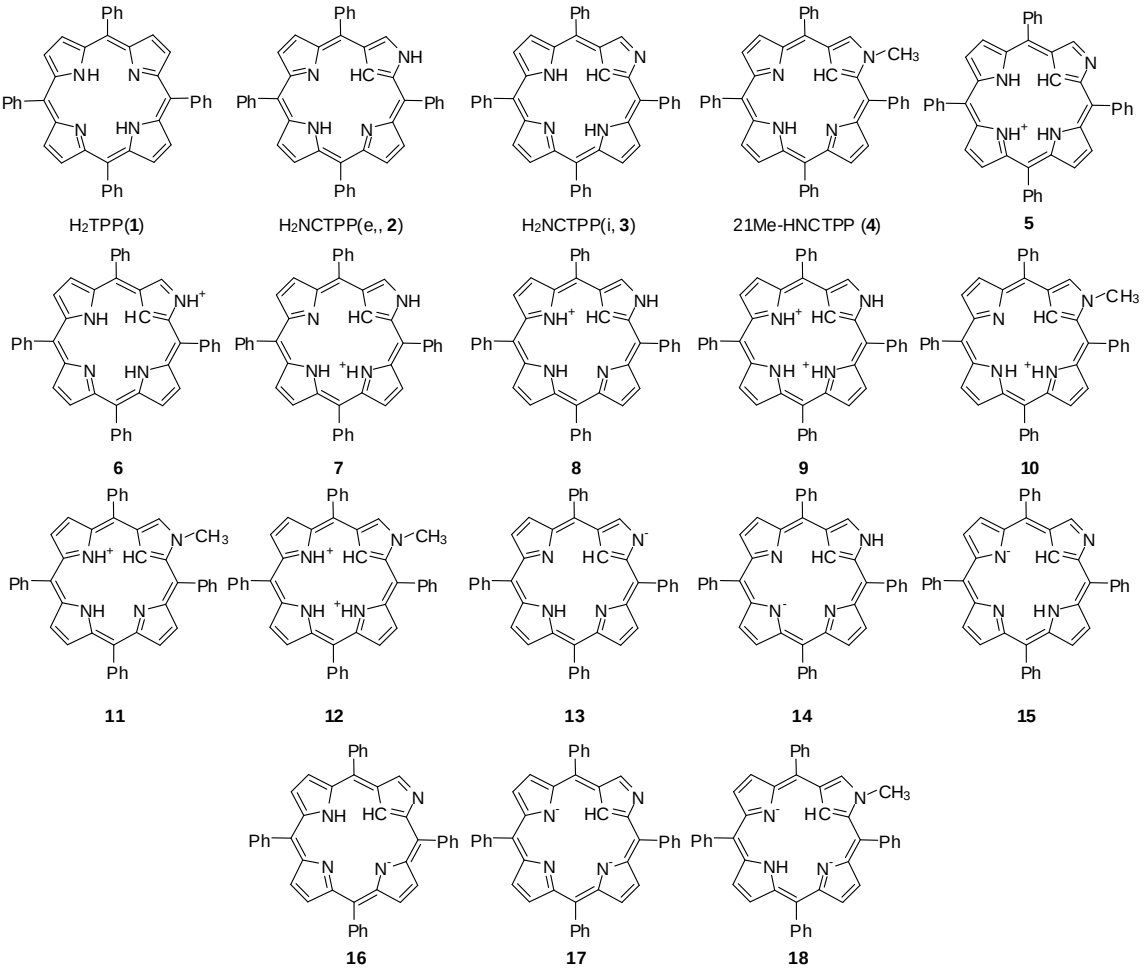

Scheme 1

Recently, we presented an investigation into the MCD of nickel N-confused porphyrin, and observed striking "sign reversed" spectra in its neutral form.[30] A normal porphyrinic MCD spectra could be achieved by deprotonation of the external NH group, indicating that the relative magnitudes of the ΔHOMO and ΔLUMO can be switched by a simple protonation/deprotonation reaction.

In this report, we present the first MCD study of free base N-confused porphyrin and its externally N-methylated variant (Scheme 1). We have collected MCD spectra for free base, protonated and deprotonated N-confused porphyrin in non-polar solvents (dichloromethane, DCM, and toluene) and a polar solvent (dimethylformamide, DMF), as

well as the corresponding spectra for 21-N-methyl-N-confused porphyrin. Scheme 1 also shows the various protonation/deprotonation states for these two macrocycles. As part of our interpretation of the data, we have carried out new theoretical calculations on these molecules using a TD-DFT approach. In particular, since the UV-visible spectroscopy and MCD spectra of porphyrinoids can be described in large part via Goutermann's four orbital and Michl's perimeter models,[31-36] we shall present calculated relative ΔHOMO and ΔLUMO values as they pertain to the observed MCD Faraday B terms.

Experimental

Synthesis and Instrumentation. All solvents were purchased from commercial sources and dried using standard approaches prior to experiments. A methanol solution of $(NBu_4)OH$ and trifluoracetic acid were purchased from Aldrich used without future purification. 5,10,15,20 tetraphenyl N-confused porphyrin (2-aza-21-carbaporphyrin, NCP) free base was synthesized by using Geier's method[37] and purified via

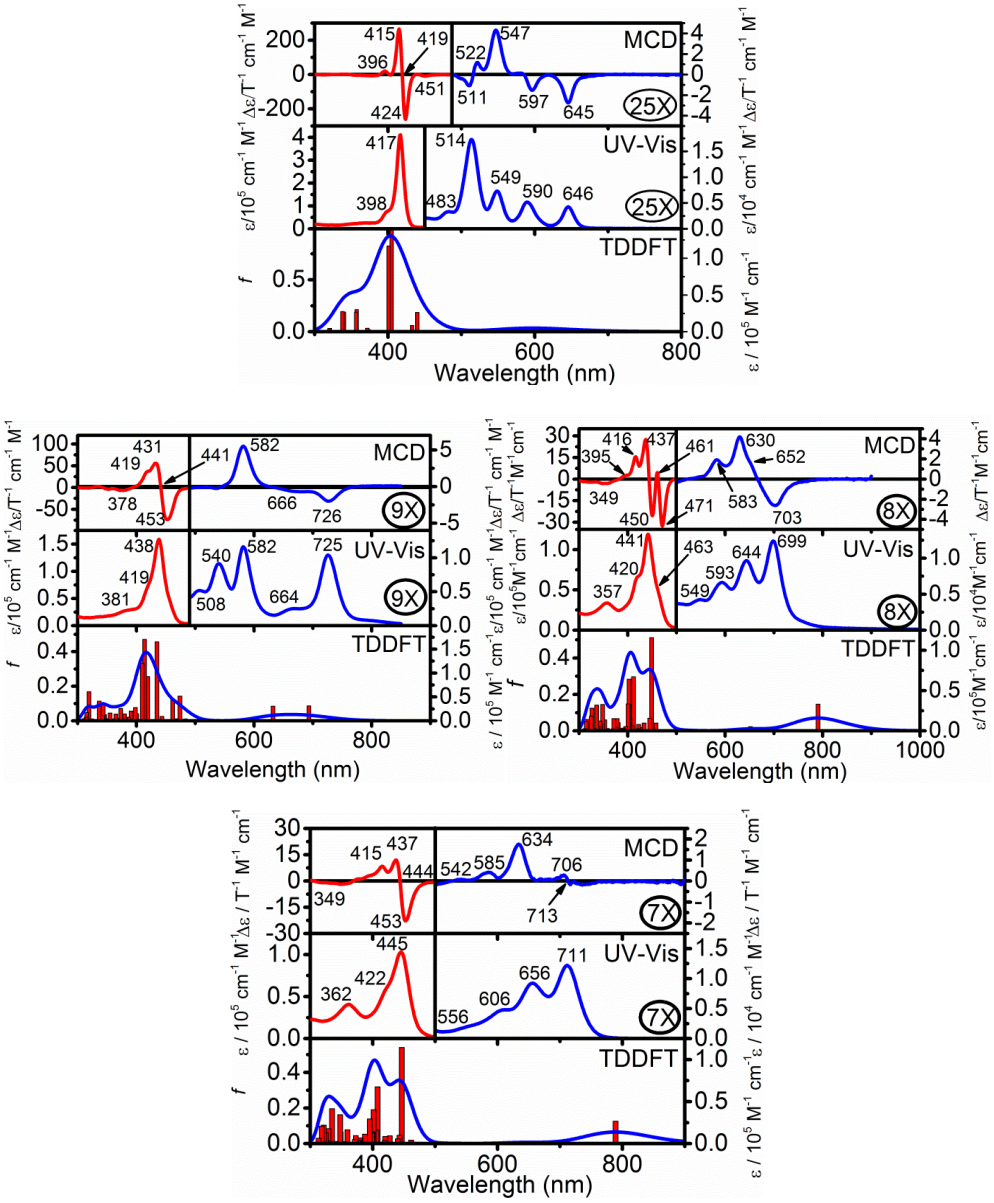

Figure 1: The UV-visible, MCD and TDDFT predicted spectra of TPP (top), NCP in DCM (middle left), NCP in DMF (middle right) and Me-NCP in DCM (bottom).

chromatography by using activity III basic alumina and chloroform/hexane as the eluents. 21-N-methyl 5,10,15,20-tetraphenyl N-confused porphyrin (MeNCP) was generated via alkylation with iodomethane using the cesium carbonate method described by Ziegler and co-workers.[38] UV-vis-NIR data were obtained on Jacso V-670 or spectrometer in DCM, DMF, or toluene as solvents. MCD data were recorded using an OLIS DCM 17 CD

spectropolarimeter using a permanent 1.4 T DeSa magnet. The spectra were recorded twice for each sample, once with a parallel and an antiparallel fields.

Computational Aspects: All DFT and TDDFT calculations were conducted using the Gaussian 03 and 09 software package running under either a Windows or UNIX OS.[39] The molecular geometries were obtained via optimization with Becke's exchange functional[40] and Perdew 86 nonlocal correlation functional (BP86)[41] coupled with 6-31G(d) basis set[42] for all atoms. For all optimized structures, frequency calculations were carried out to ensure that optimized geometries represented local minima. When necessary, the percent contributions of atomic orbitals to molecular orbitals were calculated using the VMOdes program.[43] TDDFT calculations were conducted at the same level of theory as geometry optimizations and single point calculations. The first 50 excited states were calculated in order to ensure that both Q- and B-band regions of the UV-Vis spectrum are covered.

Results and Discussion

Neutral macrocycles: N-confused porphyrin can be readily synthesized in high yield via the method developed by Lindsey and Geier.[37] By using methane sulfonic acid as both the acid catalyst and the template, reasonably high yields (>35%) of N-confused porphryins can be produced. Methylation of the exterior nitrogen position can be carried out by using Ziegler's method via the reaction of iodomethane and 5,10,15,20-tetraphenyl N-confused porphyrin in THF/DMSO solution with Cs_2CO_3 as the base[38]

As previously reported, the UV-visible spectra of N-confused porphyrin are highly solvent dependent, and regardless of the polarity conditions differs from that of

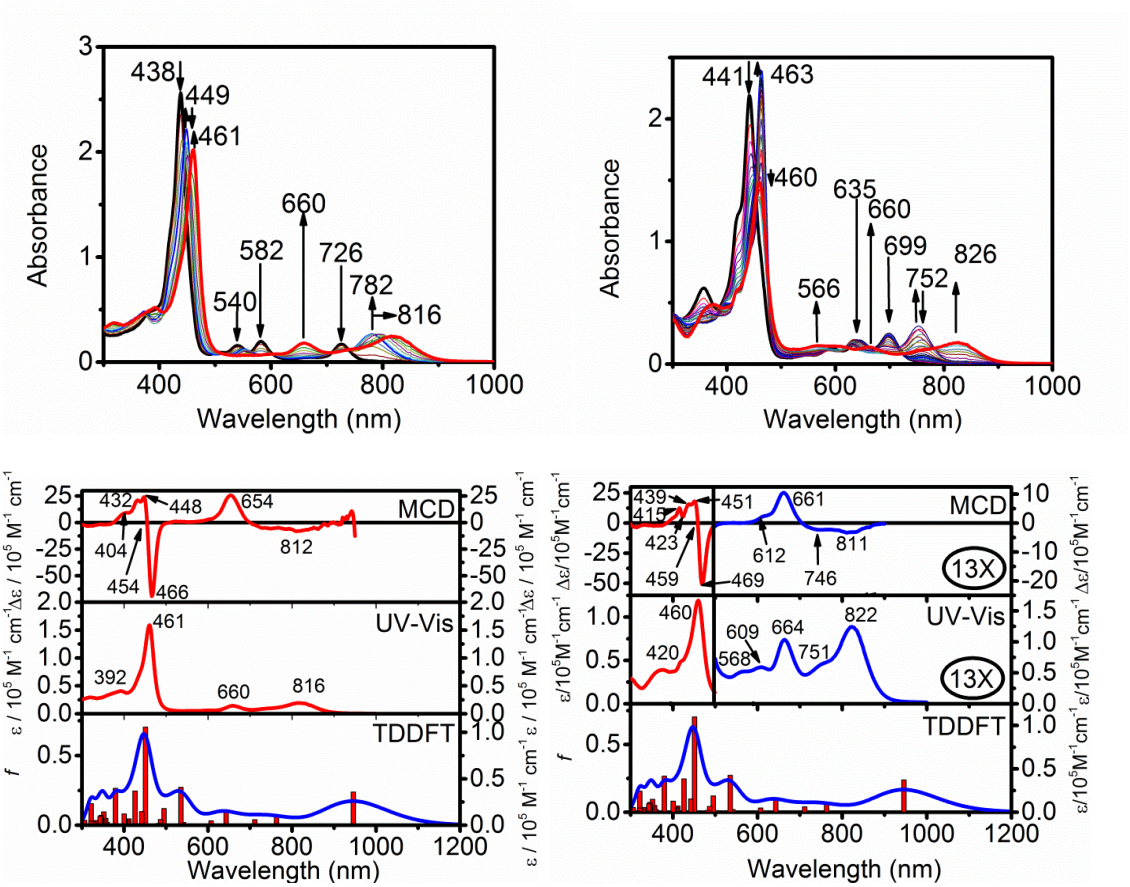

Figure 2: The UV-visible, MCD and TDDFT predicted spectra for NCP upon reaction with trifluoroacetic acid. Top: Protonation of NCP in DCM (left) and DMF (right). Bottom: MCD spectra of diprotonated forms in DCM (left) and DMF (right).

normal 5,10,15,20-tetraphenyl porphyrin.[8,9] In non-polar media, such as DCM (Figure 1), the spectra of **3** exhibits a red-shifted Soret band at 438 nm with a shoulder at 417 nm as well as an asymmetric set of Q bands. Two Q bands appear at 539 and 582 nm, and there is a highly red-shifted peak at 725 nm with a shoulder at 665 nm. The MCD spectrum for NCP in DCM shows the typical negative to positive in ascending energy MCD Faraday B terms, as seen in normal porphyrins. This suggests that in non-polar

media, a ΔLUMO < ΔHOMO relationship holds true for the frontier π orbitals. Previous work has supported that the internal tautomer of NCP exist under non-polar conditions. In DMF solution, the spectrum of form **2** of NCP has a similarly red shifted Soret band (441 nm) similar to that seen DCM (Figure 1). However, the energies and intensities of the Q band transitions differ significantly from the internal tautomeric form. Four bands appear (549, 593, 644 and 699) with increasing intensity as the energies of the transitions decrease. As in the internal tautomeric form, the MCD spectrum shows a typical MCD Faraday B term that goes from negative to positive with increasing energy. Therefore, as in the externally tautomeric form, we observe the same ΔLUMO < ΔHOMO relationship for the frontier π orbitals. So, although changing solvent polarity does modify the spectrum of free base NCP, the frontier orbital energy differences remain unchanged. Additionally, the MCD Faraday pseudo A term is split in this spectrum, with peaks at 450 and 471 nm. This splitting may result from the presence of an equilibrium in solution between the two tautomeric forms of the macrocycle.

Alkylation of the external nitrogen position of N-confused porphyrin forces the macrocycle to adopt a structure similar to that of the external tautomer observed in polar media. The spectrum of MeNCP (**4)** in DMF is virtually identical to that of unmodified NCP, except with a slight red shift of the transitions (Figure 1). Due to the presence of the N-methyl group, MeNCP is unable to "tautomerize" to a structure analogous to the internally protonated form, and as a result, the spectrum in non-polar solvents (such as DCM) is effectively identical to that seen in polar

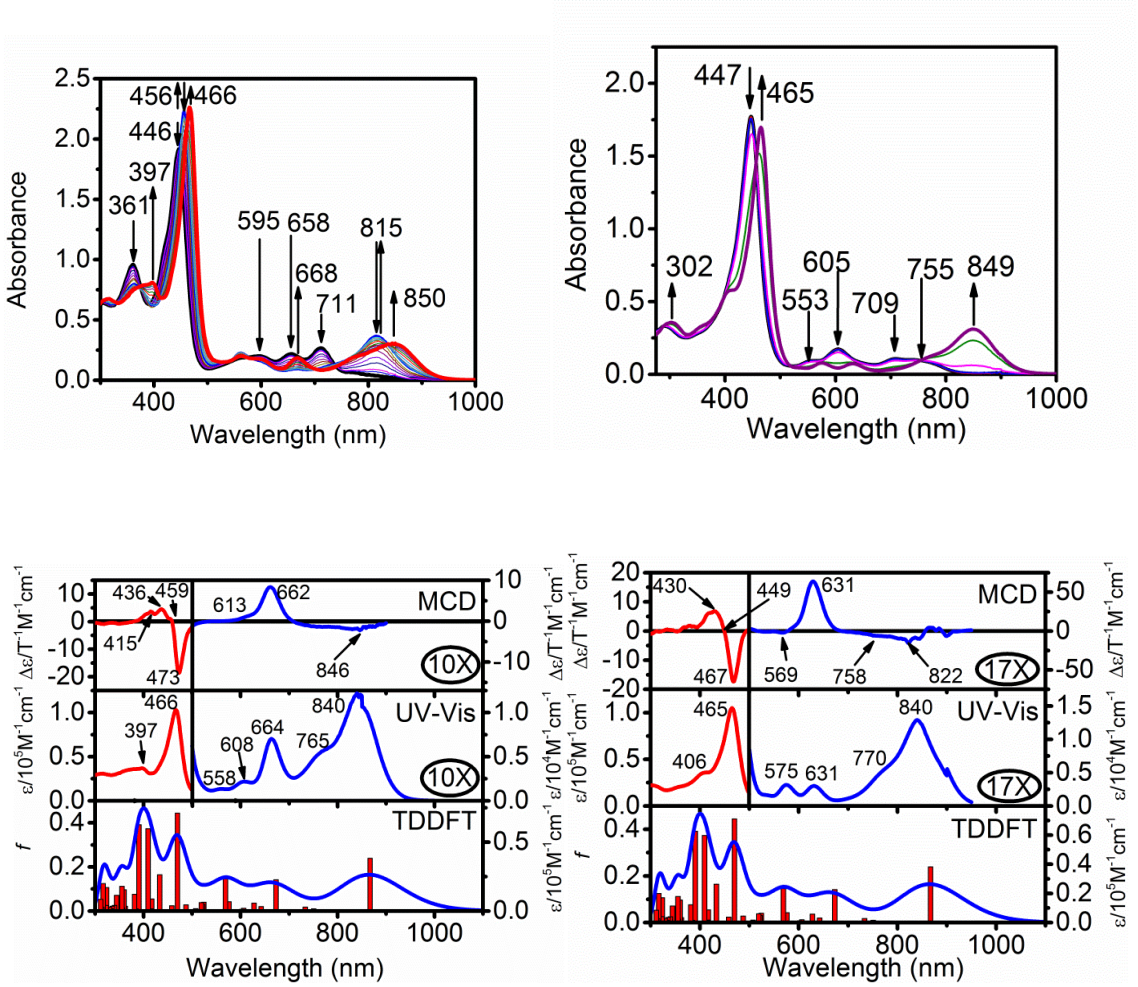

Figure 3: The UV-visible, MCD, and TDDFT predicted spectra for MeNCP upon reaction with acid. Top: Protonation of MeNCP in DCM (left) and DMF (right). Bottom: MCD spectra of diprotonated forms of MeNCP in DCM (left) and DMF (right).

media. The Soret band appears at 445 nm, and the four Q bands at 551, 606, 656 and 711 nm. The MCD spectrum of MeNCP, not surprisingly, resembles that of the external tautmoeric form of unmodified NCP, however the MCD Faraday B terms are much weaker in intensity. Also, the MCD Faraday pseudo A term in the Soret band region is notably not split in the MCD spectrum; this may result from the inability of the externally methylated form to engage in external/internal tautomerization as seen in the free base macrocycle 2 or 3.

Protonation of NCP and MeNCP: Both tautomers of free base N-confused porphyrin can be protonated with strong acids such as trifluoroacetic acid, and not surprisingly we observe different behavior between the two forms of NCP. The protonation of N-confused porphyrin free base was first investigated by Latos-Grazynski for both the unmodified and externally N-methylated forms.[2,44] More recently, Furuta and coworkers presented a report on the acid base chemistry of water soluble NCPs.[45] However, in these studies, the UV-visible spectroscopy of the protonated/deprotonated forms of NCP and MeNCP were not extensively explored, and additionally we now have the opportunity to investigate these ions via MCD spectroscopy.

In dichloromethane, reaction of free base NCP with trifluoracetic acid results in the appearance of a new spectra as the two nitrogen sites become protonated. (Figure 2). Not surprisingly, the spectra of the titrations differ depending on the tautomeric form. Scheme 1 shows the different possible monoprotonation states for the two tatuomeric forms (compounds **5** and **6**); as can be seen in the scheme, the monocations for each form exhibit different structures. In DCM, titration with acid results in the transient

appearance of a band at 782 nm, along with a red shift of the Soret band to 449 nm. The addition of additional acid eventually results in the fully protonated dicationic form, which exhibits a very bathochromically shifted Q band at 816 nm as well as a similarly shifted Soret at 461 nm. For a polar solvent such as DMF, we would expect the monocationic form to adopt one of two possible configurations (compounds **7** and **8**). In DMF, protonation also results in the formation of a transient band at 752 nm and a slightly diminished Soret at 460 nm. Continued reaction with acid results in the dicationic form, with features similar to that seen for the form in DCM. In their

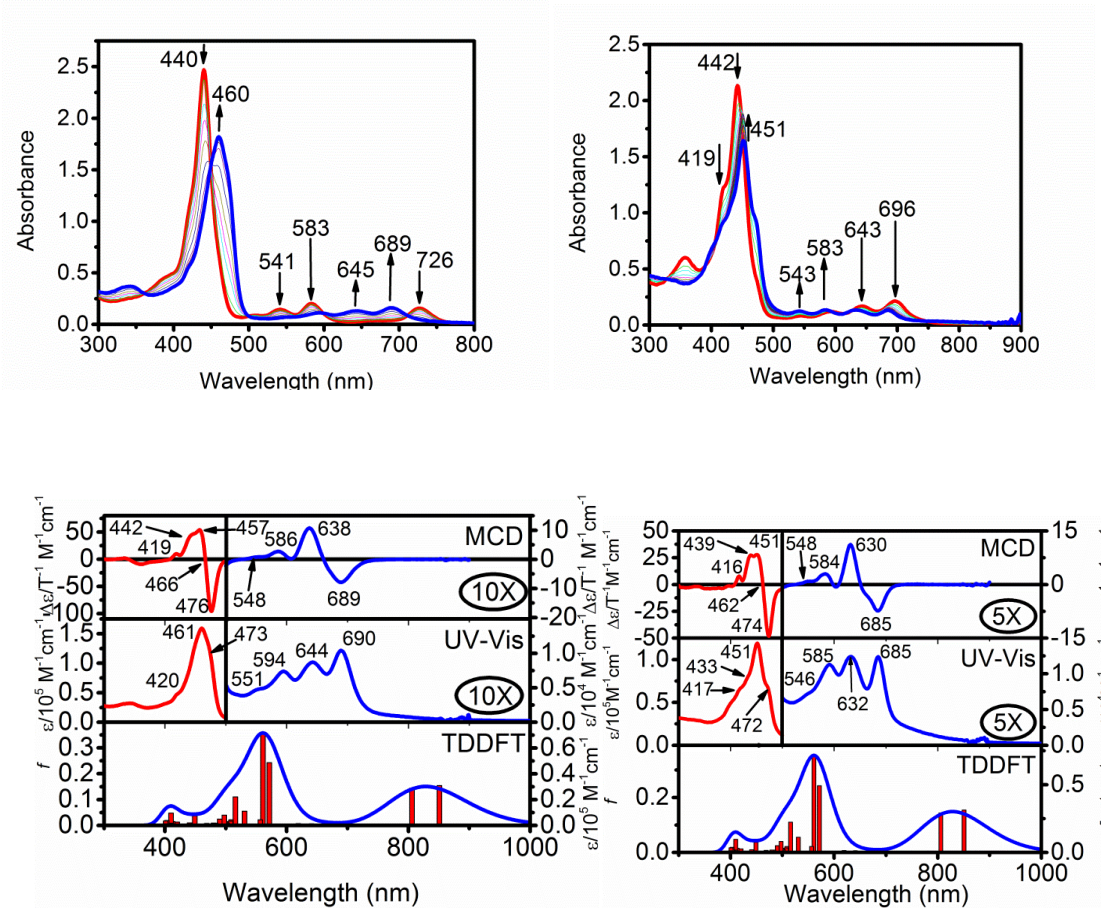

Figure 4: The UV-visible, MCD, and TDDFT predicted spectra for NCP upon reaction with base. Top: Deprotonation of NCP in toluene (left) and DMF (right). Bottom: MCD spectra of deprotonated forms of NCP in toluene (left) and DMF (right).

absorption spectra, the dications in both solvent exhibit red shifted Soret bands near 460 nm, and two primary Q bands (660 and 816 nm in DCM and 664 and 822 nm in DMF). The bathochromic shift in the DMF spectrum Q bands relative to the DCM bands may arise due to the increased dielectric constant of the more polar solvent. The MCD spectra of both compounds show MCD Faraday B terms with negative to positive progression with increasing energy, indicating that even upon formation of the fully protonated products, the ΔLUMO < ΔHOMO relationship still holds true for the frontier orbitals. For the fully protonated form in either solvent, we would expect identical protonation structures, represented by compound **9**.

We also investigated the protonation of MeNCP, shown in Figure 3. In this macrocycle, the only position available for the initial binding of an equivalent of H^+ is an internal nitrogen position, as shown in Scheme 1, although there are two possible configurations (**10** and **11**). The fully protonated form has only one possible structure (**12**). Accordingly, the titrations with acid for in DCM and DMF solutions proceed similarly, resulting in nearly identical spectra for the diprotonated compounds. The Soret band is red shifted to ~465 nm in both solvents, and the primary Q band appears near a red shifted value of ~850 nm. The primary difference between the two spectra is seen in the intermediary Q bands; the DCM spectra shows only one major feature at 664 nm, whereas in DMF two bands appear at 575 and 631 nm. As in the protonated forms of NCP, the MCD Faraday B term shows the same negative to positive progression as one goes to higher energy. Therefore, the protonated forms of MeNCP continue to maintain a ΔLUMO < ΔHOMO energy relationship.

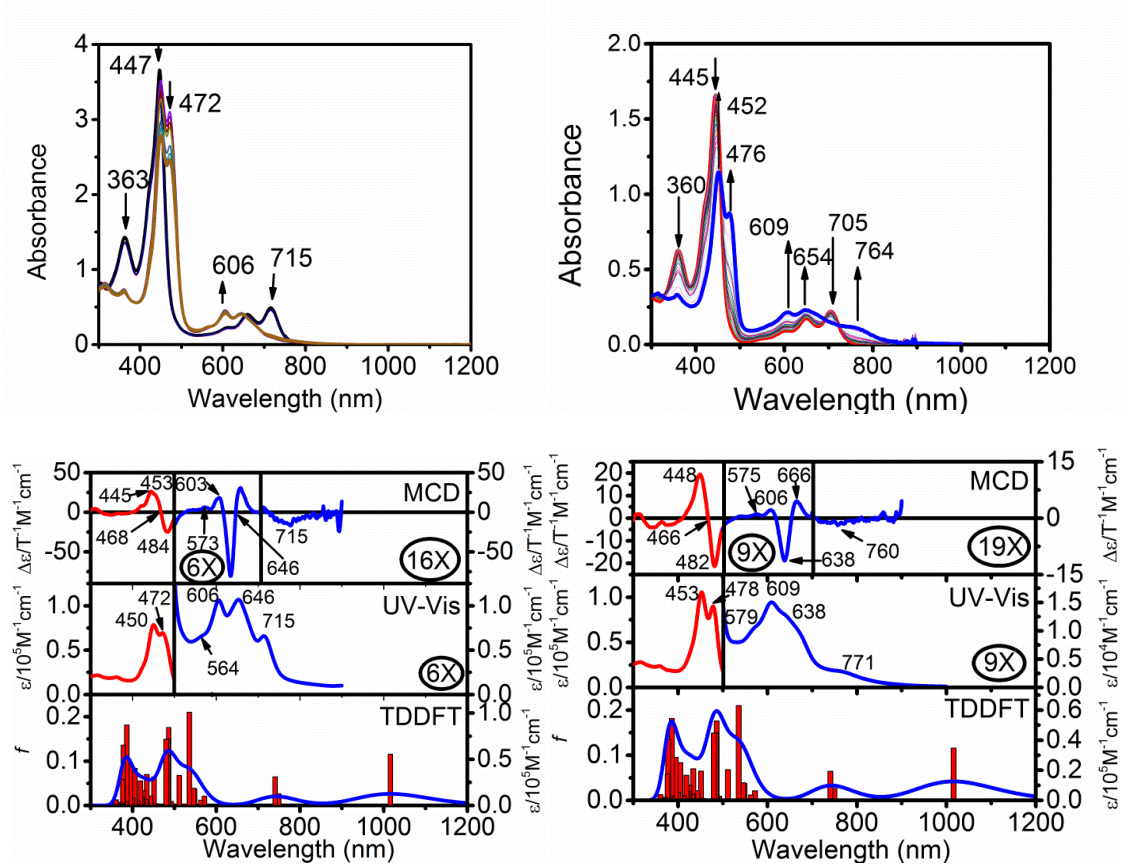

Figure 5: The UV-visible, MCD, and TDDFT predicted spectra for MeNCP upon reaction with base. Top: Deprotonation of MeNCP in toluene (left) and DMF (right). Bottom: MCD spectra of deprotonated forms of MeNCP in toluene (left) and DMF (right).

Deprotonation of NCP and MeNCP: We were able to readily deprotonate NCP by use of tetrabutylammonium hydroxide. Both tautomers of NCP have two ionizable hydrogen atoms that can be removed, whereas MeNCP has only one such hydrogen. Scheme 1 also shows the possible monodeprotonated structures for the two tautomeric forms of NCP (compounds **13**-**16**); the fully deprotonated form would be identical in either polar or non-polar media (compound **17**). Figure 4 shows the deprotonation spectra of NCP. We did not observe clean deprotonation spectra in DCM, most likely due to the reactivity of the solvent, so we moved to toluene as the non-polar solvent for these experiments. In

toluene, titration with base results in the formation of a more normal-type spectrum in the Q band region, with peaks that resemble the exterior tautomeric form. The Q bands appear at 551, 594, 644 and 690 nm, and increase in intensity with decreasing energy. In DMF, deprotonation does not greatly change the Q band region; the four primary absorptions remain but are blue shifted. In both toluene and in DMF, the Soret band loses intensity and is red shifted to 460 in toluene and 451 in DMF. In the deprotonated spectra in both solvents, the MCD Faraday B terms show clear negative to positive progression with increasing energy, showing that once again the $\Delta LUMO < \Delta HOMO$ energy relationship continues upon loss of protons.

For MeNCP, removal of the single ionizable proton results in the spectrum shown in Figure 5, and the monodeprotonated structure is shown in Scheme 1 as **18.** Deprotonation of this macrocycle in toluene results in the the appearance of a split Soret and new Q bands at 606 and 646 nm. In DMF, a similar spectrum is produced, which is not surprising as the structure of the resultant anion should be the same in both solvents. However, in DMF, a red shifted tail like band appears above 750 nm that is not as pronounced in the toluene spectra. Inspection of the MCD Faraday B term initially appears to undergo a positive to negative shift with increasing energy, which would imply that the frontier orbital energy relationship is inverted, i.e. $\Delta HOMO < \Delta LUMO$. However, we cannot rule out the presence of weak negative bands (more clearly seen in the DMF spectra), which would correlate to a $\Delta LUMO < \Delta HOMO$ relationship. Modern DFT methods can be used for the prediction of the spectroscopic signatures and relative energies of NH tautormers in porphyrinoids. [46,11-13-47]

Calculations: Early computational studies have supported the hypothesis that both tautomeric states of N-confused porphyrin (**2** and **3**) have less stabilization than normal porphyrin, and that the two tautomeric states differ in energy. Latos-Grażyński first reported a difference between the internal tautomer of tetraphenyl N-confused porphyrin and normal tetraphenyl porphyrin of 21.5 kcal mol^{-1},[16] while Ghosh calculated a 17.7 kcal mol^{-1} increase in energy for the same tautomer for N-confused porphine.[14] Ghosh also presented a difference in energy between the two tautomeric states for N-confused porphine, with the external tautomer having a 5.7 kcal mol^{-1} higher energy than the internal tautomer. More recently, Ziegler and Modarelli carried out B3LYP/3-21G(d) and B3LYP/6-31G(d)//B3LYP/3-21G(d) level calculations on both tautomers, and found relative stabilities to normal porphyrin of 17.1 and 13.2 kcal mol^{-1} respectively for the internal tautomer and 20.4 and 18.8 kcal mol^{-1} respectively for the external tautomer[10] Modarelli recently revisited these calculations at the B3LYP/6-31+G(d)//B3LYP/6-31G(d) and B3LYP/6-311+G(d)//B3LYP/6-31G(d) level, and observed similar relative stabilities between the two tautomers of 4.9 and 4.8 kcal mol^{-1} respectively.[11] This later calculation also determined the energy difference between the tautomeric states of N-confused porphine, and found a larger difference in energy (9.0 kcal mol^{-1} at the B3LYP/6-31G(d) level and 6.9 kcal mol^{-1} with single-point energy calculations at the B3LYP/6-31+G(d)//B3LYP/6-31G(d) and B3LYP/6-311+G(d)//B3LYP/6-31G(d) levels of theory). This difference in energy is appreciably larger than that seen by Ghosh, which was attributed to the use of a non-planar conformation for the macrocycle.

Theoretical investigations into the molecular orbital energies have provided insight into the differences in electronic structure between N-confused and normal

porphyrin that result in the observed destabilizations of the two tatuomers. In the initial study by Ziegler and Modarelli,[46] for both the internal (**3**) and external tautomeric form (**2**), the HOMO and HOMO-1 orbitals (which correspond to the a_{1u} and a_{2u} of normal D_{4h} porphyrin) are inverted and separated by a larger energy than seen in H_2TPP. The energies of the LUMO and LUMO+1 orbitals (which correspond to the e_g orbitals in D_{4h} porphyrin) differ significantly between the two tautomeric forms. In both tautomers, the LUMO and LUMO+1 are non-degenerate, as expected for the reduction in symmetry in the macrocycle versus normal porphyrin. However, in the external tautomer, the difference in energy between the LUMO and LUMO+1 is appreciably larger than that seen in the internal tautomer. The later calculations carried out by Modarelli on tetraphenyl N-confused porphyrin are in agreement with the initial theoretical study and correlate well to N-confused porphine.

For this study, we have calculated the electronic structure of the two tautomeric forms of NCP (**2** and **3**), MeNCP (**4**) and the various protonated and deprotonated states (**5**-**18**). The structures of the four Gouterman-type frontier orbitals for our calculations can be found in the supporting information. Overall, our calculated energies and the features of these orbitals are in agreement with the previous MO calculations carried out using the B3LYP/6-31G(d)//B3LYP/3-21G(d) methodology.[4] When comparing the overall structures of the frontier orbitals of the two tautomers of NCP to MeNCP, as expected the externally protonated form bears greater resemblance to MeNCP in terms of orbital structures than the internally protonated form. When considering the energies of these orbitals, it is useful to consider the relative magnitudes of the ΔLUMO and ΔHOMO separations, as these correlate directly to the observed spectroscopic features of

these macrocycles, in particular the MCD Faraday B terms. The values for ΔLUMO and ΔHOMO for the tautomers of NCP, MeNCP and their various protonated/deprotonated forms are listed in the supporting information, Table 6. We calculate the ΔHOMO values for the external tautomer and internal tautomer of NCP to be ~0.7519 and ~0.5690 eV respectively, and the ΔLUMO values to be ~0.5197 and ~0.0963 eV respectively. Previously, the ΔHOMO values for the external tautomer and internal tautomer were calculated at 0.7516 and 0.6144 eV respectively and the ΔLUMO values as 0.6024 and 0.0887 eV for the B3LYP/6-31G(d)//B3LYP/3-21G(d) approach. We calculated ΔHOMO and ΔLUMO values for MeNCP as ~0.7426 and 0.5206 eV, which matches the values observed for the external tautomer. Based on our calculations, we predict that all three neutral macrocycle forms should have MCD Faraday B terms that progress from negative to positive with increasing energy, which is in agreement with spectroscopic observation.

When calculating the energies and frontier orbital structures of the protonated and deprotonated forms of NCP for both tautomers, we considered the various sites of reaction in our calculations. For the internal tautomer, there are two possible protonation states for the monocation: protonation at the internal nitrogen position and protonation (**5**) at the peripheral nitrogen atom (**6**). For the external tautomer, there are also two possible states: protonation at the nitrogen that is adjacent to the inverted pyrrolic nitrogen atom (**7**), and protonation on the nitrogen that is oriented away from the inverted pyrrolic nitrogen (**8**). In addition to the changes in orbital structure, the ΔHOMO and ΔLUMO values change depending on the site of protonation. For the internal tautomeric form, the ΔHOMO does not change very much between internal and external protonation (~0.7059 versus ~0.7309 eV), but the ΔLUMO changes appreciably, moving from ~0.1012 to

~0.5271 eV. We can also calculate the relative stabilities of the different protonation states, shown in supporting information Table 6. Protonation at the external nitrogen position is also slightly less favorable than protonation at the internal position, with a calculated difference of 0.5990 kcal/mole. This would correspond to an equilibrium constant between the internal and external forms that would be very close to unity; therefore exposure of the internal tautomer of N-confused porphyrin produces equal concentrations of internally and externally protonated monocations, in spite of the differences in electronic structure. With regard to the external tautomeric form of NCP, the ΔHOMO and ΔLUMO values do not change very much based on protonation location, although the structures of the orbitals do change. Additionally, the calculated energy difference between the two protonation sites is minimal (1.430 kcal/mmol), so we would also predict an equilibrium mixture of protonation between the adjacent and opposite nitrogen sites. In all cases regarding the monoprotonated tautomers of NCP, we predicted that the ΔHOMO > ΔLUMO condition would be maintained, and for all of the monoprotonated spectra we observe negative to positive MCD Faraday B terms.

For the monoprotonated form of MeNCP, once again there are two sites for the binding of an equivalent of H^+: the interior nitrogen adjacent to the inverted pyrrolic nitrogen (**10**), and the one on the opposite side (**11**). The structures of the molecular orbitals show some minor mirror image type changes between the two protonation states. The energies of the two protonation states are very close based on our calculation, differing by only ~0.5476 kcal/mole. The frontier orbitals also maintain the same ΔHOMO > ΔLUMO differences for both possible protonation states, in good agreement

with observed MCD Faraday B terms. Based on the small size of the energy difference, we hypothesize that both states are in equilibrium in solution.

The diprotonated dicationic form of NCP (**9**) has significantly perturbed frontier orbital structures. In particular, the HOMO-1 is no longer a macrocycle localized orbital, but rather resides on two of the four meso phenyl rings. The HOMO-4 orbital can be considered as contributing to the aromaticity; however even in this case the orbitals are highly delocalized onto the phenyl rings. Additionally, the lack of planarity observed in this molecule is also indicative of significant π overlap between the confused porphine core and the meso phenyl rings. In spite of this, the ΔHOMO > ΔLUMO condition remains unchanged (even though the HOMO-1 is not one of the Gouterman-type orbitals) and thus the MCD Faraday B term shows the expected negative to positive progression. For doubly protonated MeNCP (**12**), the structures of the frontier orbitals closely resemble those of the diprotonated form of NCP, however the ΔHOMO and ΔLUMO energies do change between the two macrocycles (~0.8008 and ~0.4357 eV for H_4NCP^{2+} and ~0.5638 and ~0.4095 eV for H_3MeNCP^{2+}). In both cases, ΔHOMO > ΔLUMO values were calculated in agreement with the observed MCD Faraday B terms in their spectra.

We also investigated the deprotonation of NCP and MeNCP via computational methods. As in the monoprotonated case, deprotonation can take place at different positions for each tautomeric form. For the external tautomer of NCP, a proton can be removed either from the external nitrogen position (**13**) or from the internal NH unit (**14**). For the internal tautomer, the proton can be removed either opposite to the inverted pyrrolic nitrogen (**15**), or from the adjacent pyrrole on the same side as the inverted

nitrogen atom (**16**). For the external tautomer, inspection of the frontier orbital structures reveals small differences, but the energy calculations show that removal of the proton from the external NH position is preferred. When the proton resides on the internal position in the singly deprotonated NCP, the resultant monoanionic macrocycle is 28.68 kcal/more stable than when the proton resides on the internal NH position. The acidity of the external nitrogen NH position in N-confused porphyrin is well known, and the external nitrogen position has been observed to readily bind to metal ions upon deprotonation.[5]

In the internal tautomer, inspection of the frontier orbital structures also reveals some small differences, but unlike the external tautomer, there is little difference energy between the internal adjacent and far nitrogen positions. Our calculations indicate that the two monoanionic tautomeric forms differ by only 1.430 kcal/mole. For the MeNCP macrocycle, only one proton can be removed (**18**), and only one product can be produced upon formation of the monoanion. Not surprisingly, the structures of the frontier orbitals closely resemble those of the external tautomer with the interior proton removed. For all of the monodeprotonated structures of NCP and MeNCP, we predict the ΔHOMO > ΔLUMO conditions, which is observed for all of the corresponding experiments.

For the doubly deprotonated system in NCP (**17**), there is of course only one possible structure as all of the ionizable protons are removed. The frontier orbital structures do differ significantly between the two macrocycles, in particular in the structure of the HOMO-1 orbital. For fully deprotonated NCP, the ΔHOMO and ΔLUMO values are calculated as ~0.6087 and 0.0841, which are close to those calculated for fully deprotonated TPP (~0.5806 and ~0 respectively). As for all of the examples investigated

in this report, the ΔHOMO > ΔLUMO condition is maintained, producing the observed MCD Faraday B term behavior.

Conclusions

In this report, we have carried out a comprehensive investigation into the UV-Vis and MCD spectra of NCP and MeNCP, as well as spectroscopic studies into the protonation/deprotonation properties of these two macrocycles. In all cases for the neutral or ionic macrocycles, the ΔHOMO > ΔLUMO condition is retained despite the changes in electronic structure, as observed via the MCD Faraday B terms. This is in contrast to our previously reported observations on NiNCP, which undergoes reversible ΔHOMO/ΔLUMO changes upon changing the protonation state. Additionally, we have used computational and spectroscopic methods to investigate the sites of protonation/deprotonation in NCP and MeNCP, and have observed that in NCP solvent polarity does affect the site of addition or loss of a single proton. Additionally, we calculated that the interior and exterior nitrogen sites in the internal tautomer of NCP are nearly equivalent in basicity, but deprotonation in the exterior tautomer occurs preferentially at the exterior nitrogen position. We are continuing our investigations into the fundamental electronic structures of N-confused porphyrin, its metal complexes and other porphyrin isomers and analogs.

Chapter Two: UV-Vis and MCD Spectroscopy, DFT, and TDDFT Investigations into the Regulation of Methylated N-Confused Porphyrins.

Introduction

Regulation of the aromaticity and protonation of N-confused porphyrins (NCTPP) was further investigated by methylating various positions of the NCTPP. Tetraphenylporphyrin (TPP), NCTPP, and 2-methyl-N-confused tetraphenylporphyrin (2-MeNCTPP) were investigated using MCD, DFT, and TDDFT in chapter one. Those same techniques have been used to investigate the electronic properties of other NCTPPs. Through alkylation, tautomer switching can be prevented intrinsically due to the presence of a methyl group. Six tautomers with a methyl group attached to a different nitrogen in each case were investigated with the nomenclature used in this paper shown in Scheme 2**.** 22-methylated-N-confused tetraphenyl porphyrin (MeNCTPP) and 24-MeNCTPP were used to investigate the asymmetry of the N-Confused porphyrin while 21-MeTPP was used as a standard reference for the N-confused porphyrins.

Depending on the tautomer of the N-confused porphyrin (NCP), the aromaticity of the molecule can be dampened[9]. When the protons are located inside of the porphyrin ring, the tautomer possesses an [18]annulenic circuit and shows strong aromaticity, but when a proton is located on the "confused" nitrogen, this tautomer only shows moderate aromaticity and it no longer possesses the [18]annulenic circuit[47]. Previous work with metallated N-confused porphyrins has shown them to have controllable and reversible electronic structures when investigated using magnetic circular dichroism (MCD)

spectroscopy[48]. To further investigate this trend, methylated N-confused porphyrins were selected in an attempt to regulate the tautomerism of the N-confused porphyrins.

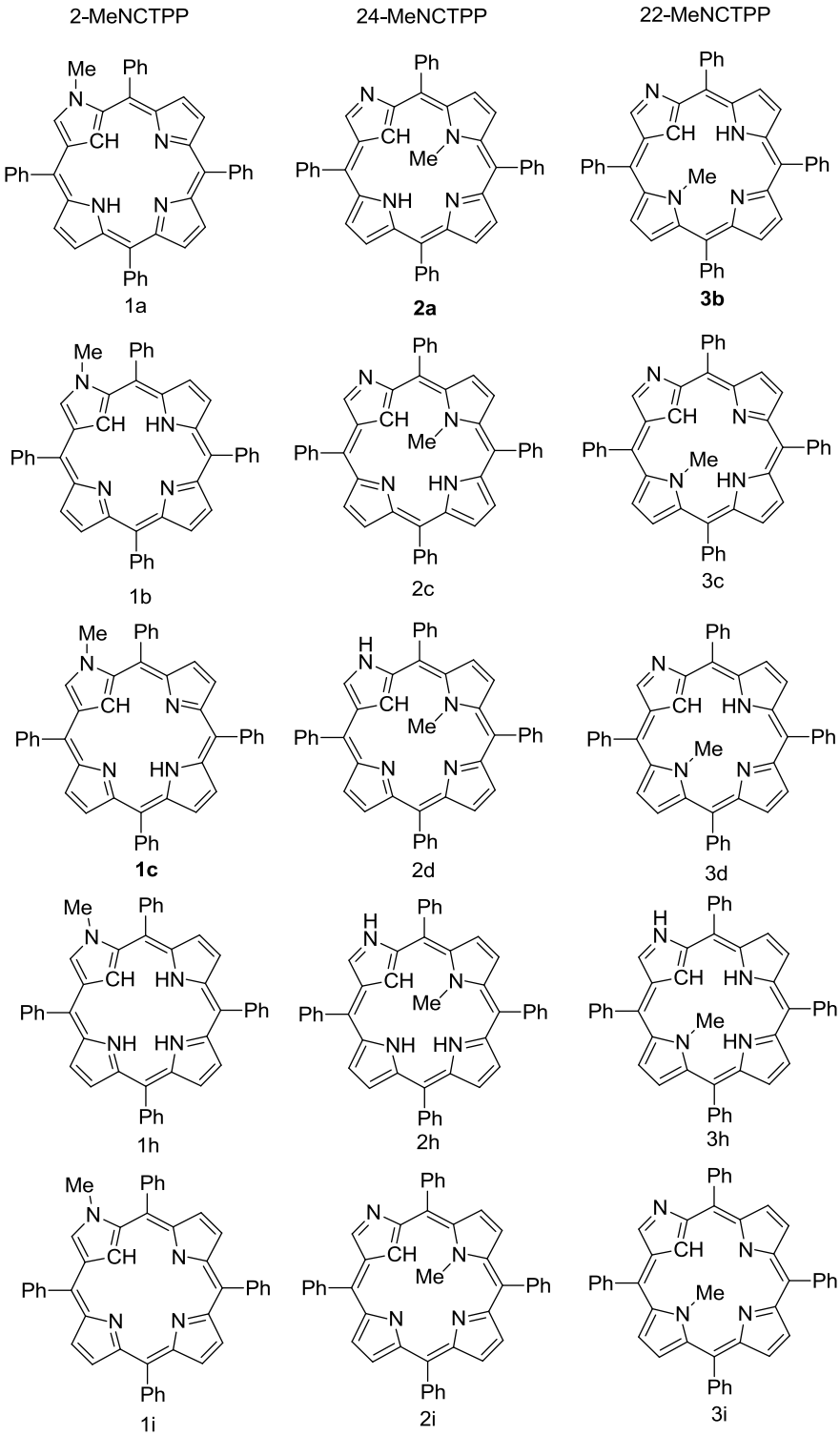

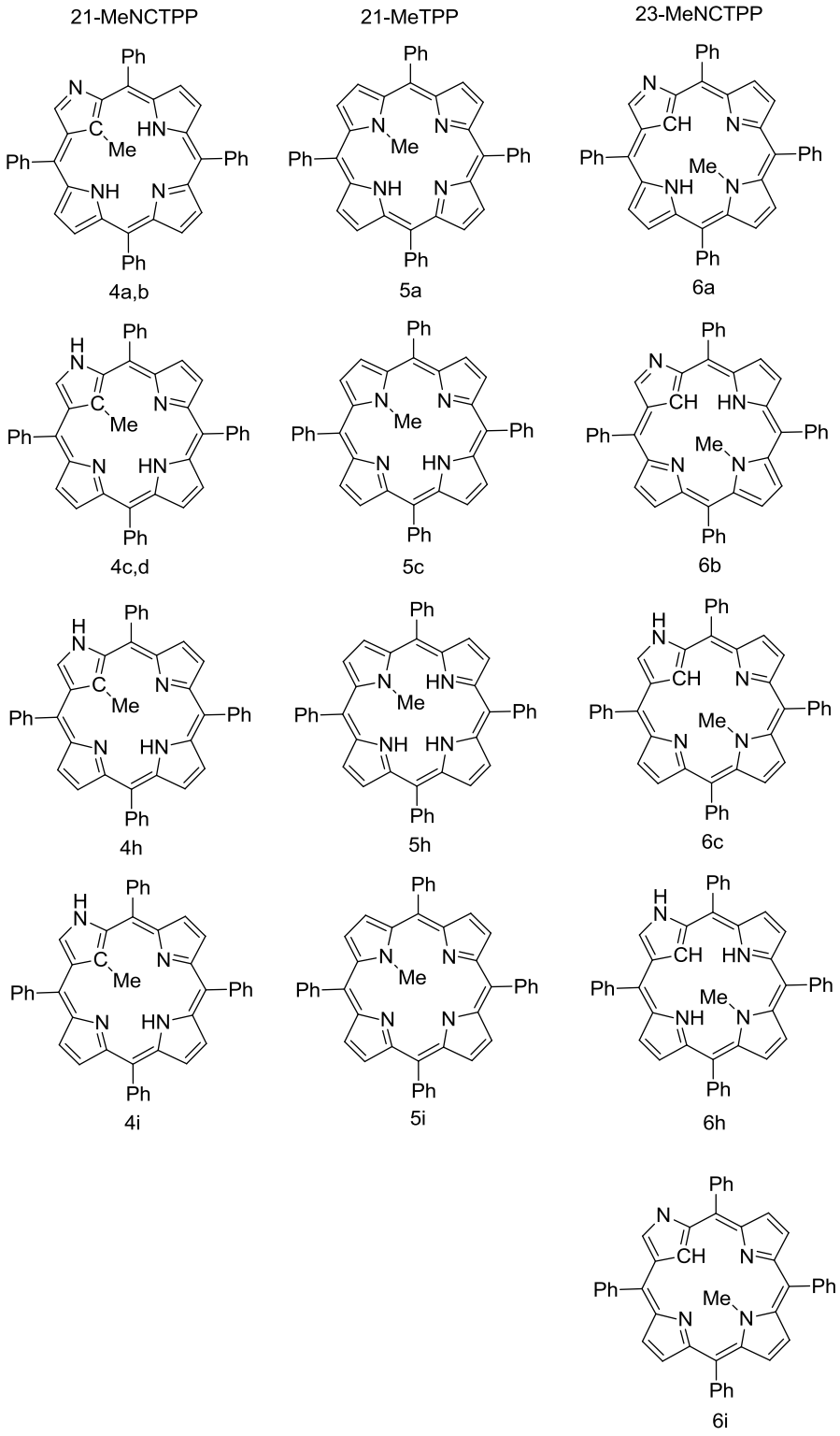

Scheme 1: Nomenclature usage when describing the possible locations of the methyl and proton locations during the DFT calcuations for the tautomers of NCTPP.

UV-vis, MCD Spectroscopy, and DFT calculations were used to investigate the electronic structure of methylated-N-confused porphyrins and their respective protonated and deprotonated forms. All N-confused and methyl-N-confused porphyrins were investigated in polar protic and non-polar solvents (DMF and Toluene respectively). It is expected that the type of solvent plays a large part in the tautomeric location of the nitrogen bound hydrogens[9]. Figure 6 and 7 shows the neutral form of the porphyrins investigated in toluene and DMF respectively. NCP and MeNCPs have UV-vis absorbances which are highly solvent dependent. Compared to tetraphenylporphyrin (TPP), N-confused tetraphenylporphyrin (NCTPP) and the various MeNCTPPs all have red-shifted B-bands. In all cases the MCD spectra of the Q-bands goes from negative to positive suggesting that ΔHOMO is greater than ΔLUMO. DFT calculations further confirm this electronic structure as shown in Table 1.

Computational Details

All Density Functional Theory (DFT) and Time-Dependent DFT (TDDFT) computational investigations were done using the Gaussian 09 software packages running on either a Windows or UNIX operating systems. Molecular geometries were obtained view optimization via Becke, 3-parameter, Lee-Yang-Parr (B3LYP)[49,50] correlation functional theory coupled with the 6-31G(d) basis set[42]. For all optimizations frequency calculations were carried out to ensure the optimized geometries had reached local minima. TDDFT and single point (SP) calculations were carried out on the optimized geometries using the same level of theory and basis set and the molecules were optimized with. The first 50 excited states were calculated for TDDFT in order to ensure that both

the Q- and B-band regions of the UV-vis spectrum were covered. The calculations were carried out under vacuum conditions with the tautomerization, protonation, and deprotonation states imposed on the compounds.

Experimental Details

All solvents were purchased from commercial sources and dried using standard approaches prior to experiments. A methanol solution of $(NBu_4)OH$ and trifluoroacetic acid was purchase from Aldrich and used without further purification. The MeNCTPP macrocycles were provided by Dr. H. Furuta and were synthesized as decribed by Toganoh and Furuta[47]. UV-vis-NIR data were obtained using a Jasco V-670 spectometer in toluene and DMF as solvents. MCD dadta were recorded using an OLISDCM 17 CD spectopolarimeter using a permanent 1.4 T DeSa magnet. The MCD spectra were measured in mdeg = [θ] and converted to $\Delta\varepsilon = \theta/(32980 \text{ X } Bdc)$, where *B* is the magnetic field, *d* is the path length, and *c* is the concentration of the solution. The spectra were recorded twice for each sample, once with a parallel and once with an antiparallel field.

Results and Discussion

Neutral Macrocycles: Previous work on NCTPP has shown that the UV-vis spectra are highly solvent-dependent and, regardless of the polarity conditions, differ from that of normal 5,10,15,20-tetraphenyl porphyrin[9,51]. The Soret band of NCTPP is red-shifted in both polar and non-polar solvents[51]. The Q-bands of NCTPP is highly responsive to the polar environment[51].

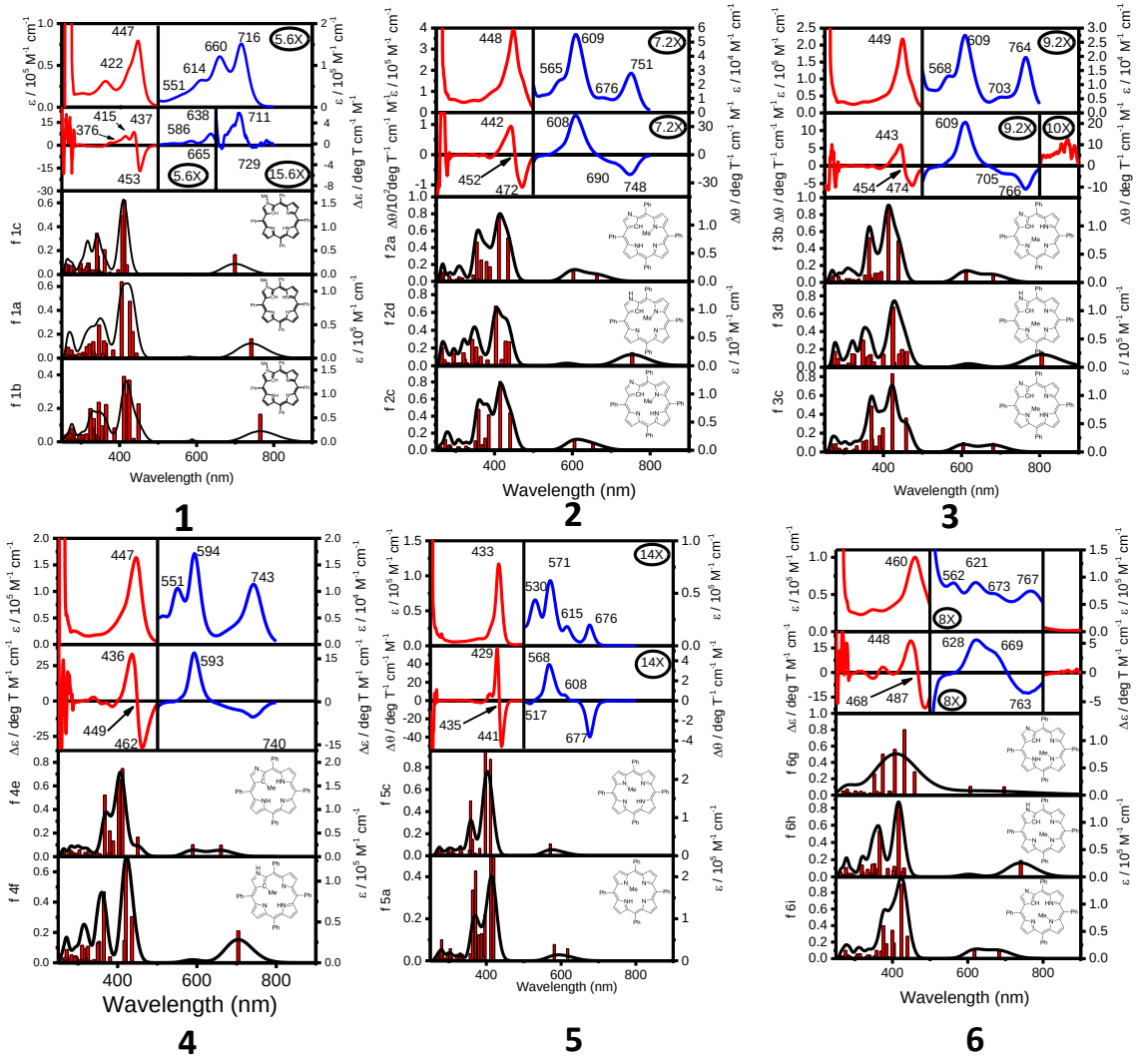

Figure 6: The UV-Vis, MCD, and TDDFT of the spectra for 2-MeNCTPP (**1**), 24-MeNCTPP (**2**), 22-MeNCTPP (**3**), 21-MeNCTPP (**4**), 21-MeTPP (**5**), 23-MeNCTPP (**6**). Experimental data collected in Toluene.

The solvent affects to the UV-Vis spectra of the methylated NCTPPs controlled by location of where the methyl group is attached to the NCTPP. Figure 6 compares 2-MeNCTPP (**1**), 24-MeNCTPP (**2**), 22-MeNCTPP (**3**), 21-MeNCTPP (**4**), 21-MeTPP (**5**), and 23-MeNCTPP (**6**), in toluene, showing that in the tautomers that support the imino form (**1**, **2**, **3**, and **4**), the Soret band is relatively stable (about 3 nm difference). While in tautomers that force the molecule into the amino form (**5** and **6**), the Soret band has a greater variance (about 44 nm difference). These band shifts agree

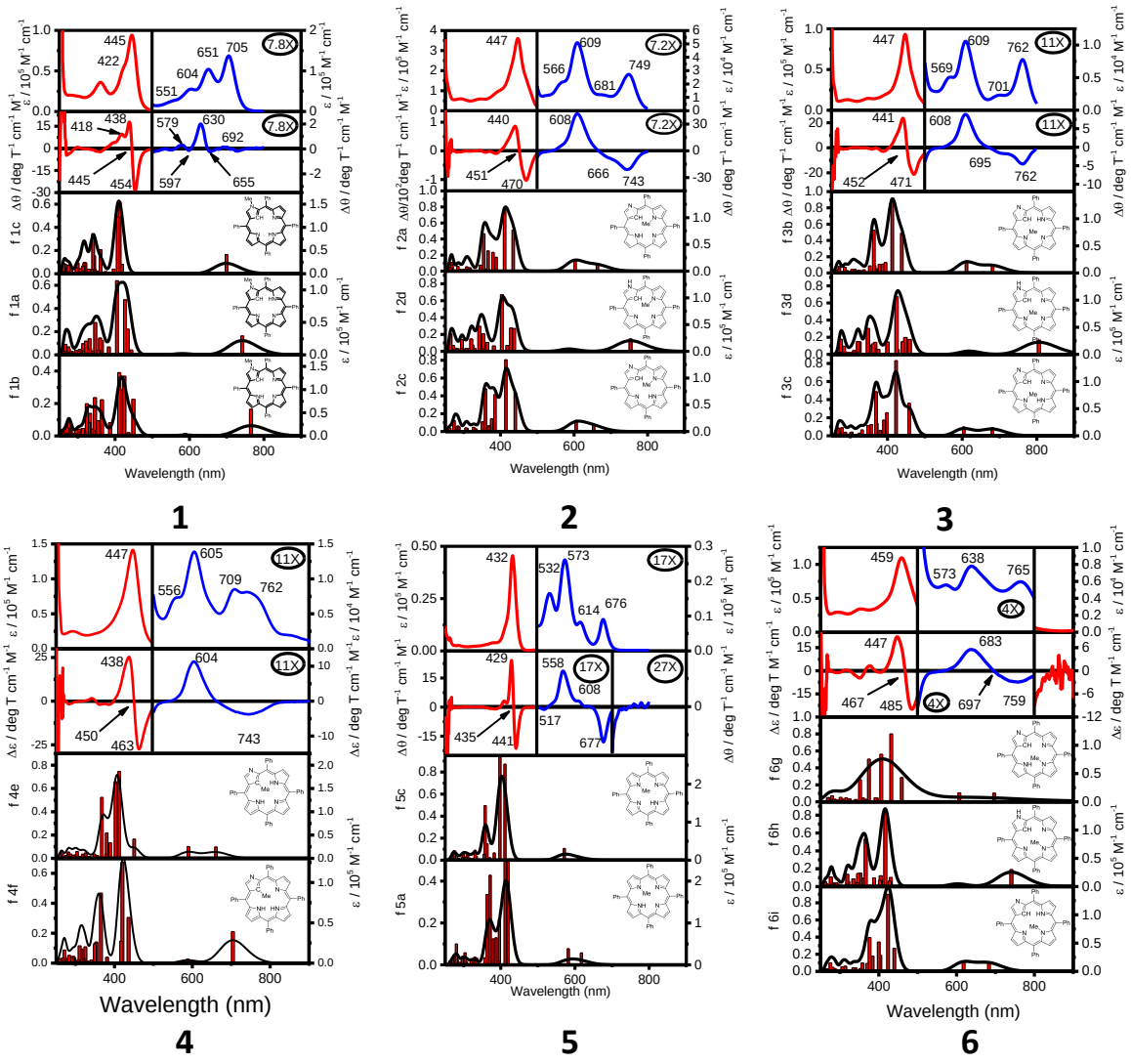

Figure 7: The UV-Vis, MCD, and TDDFT of the spectra for 2-MeNCTPP (**1**), 24-MeNCTPP (**2**), 22-MeNCTPP (**3**), 21-MeNCTPP (**4**), 21-MeTPP (**5**), 23-MeNCTPP (**6**). Experimental data collected in DMF.

with previous work[47]. Figure 7 shows the same MeNCTPP tautomers in DMF, and interestingly, there is very little movement of the Soret band locations between the solvents. This suggests that the methyl group has a stronger effect toward the stability of the tautomer than the solvent polarity does as the Soret band only changes by a few wavenumbers (>3 nm) for each tautomer. Q-band structure and relative intensities remain similar between the two solvents as well. The four Q-bands are retained in the NCTPP UV-Vis spectra (compared to TPP) but the relative intensities are affected

depending on the location of the methyl group. When then methyl group is located internally on the NCTPP or TPP, the second and fourth Q-bands are most intense, with the second band being the most intense. This differs from TPP where the first Q-band is the most intense band and then decreases in intensity with decreasing energy. The MCD spectra for all tautomers shows negative to positive signals, meaning that ΔHOMO>ΔLUMO. This is supported by single point calculations which show ΔHOMO>ΔLUMO (Table 1). The separation of the signals in the NCTPP is reduced to the point that several look like pseudo Farday's A-terms, but due to the lack of 4-fold symmetry in the metal free tautomers, A-terms cannot exist in the Q-band region.

Table 1: Difference in the ΔHOMO and ΔLUMO energies. Energies taken from single point calculations based on optimized geometries using B3LYP/6-31G(d) in the gas phase. See scheme 1 for abbreviation usage.

Tautomer	ΔHOMO-ΔLUOMO of tautomer							
	a	b	c	d	a,b	c,d	h	i
2-MeNCTPP (**1**)	0.0051	0.0046	0.0051				0.0160	0.0096
24-MeNCTPP (**2**)	0.0231		0.0223	0.0082			0.0082	0.0195
22-MeNCTPP (**3**)		0.0227	0.0175	0.0098			0.0190	0.0184
21-MeNCTPP (**4**)					0.0172	0.0076	0.0161	0.0230
21-MeTPP (**5**)	0.0132		0.0132				0.0324	0.0140
23-MeNCTPP (**6**)	0.0165	0.0201		0.0104			0.0191	0.0124

The imino tautomers with methyl groups on the inside of the ring (**2** and **3**) have red shifted Q-bands compared to the imino tautomer with the external methyl group (**1**). The amino supporting tautomer **6** has a red-shifted Soret band compared to the imino tautomers and the MeTPP while tautomer **4** is hardly shifted at all. This is most likely due to increased steric strain from the methyl group breaking the planarity of the porphyrin molecule. Single point calculations show that all of the tautomers follow the Gouterman

Four Orbital Theory. Due to the asymmetry of the molecule, the orbitals aren't perfect and the methyl group adds further distortion to the orbitals, but the HOMO-1 has a_{1u} character, the HOMO has a_{2u} character and the LUMO and LUMO+1 have e_g character. But these are metal free compounds with imperfect symmetry due to the protonated nitrogens. The addition of the methyl group further decreases the symmetry. This prevents the LUMO and LUMO+1 orbitals from being degenerate as is supported by the energy diagram in figure 8.

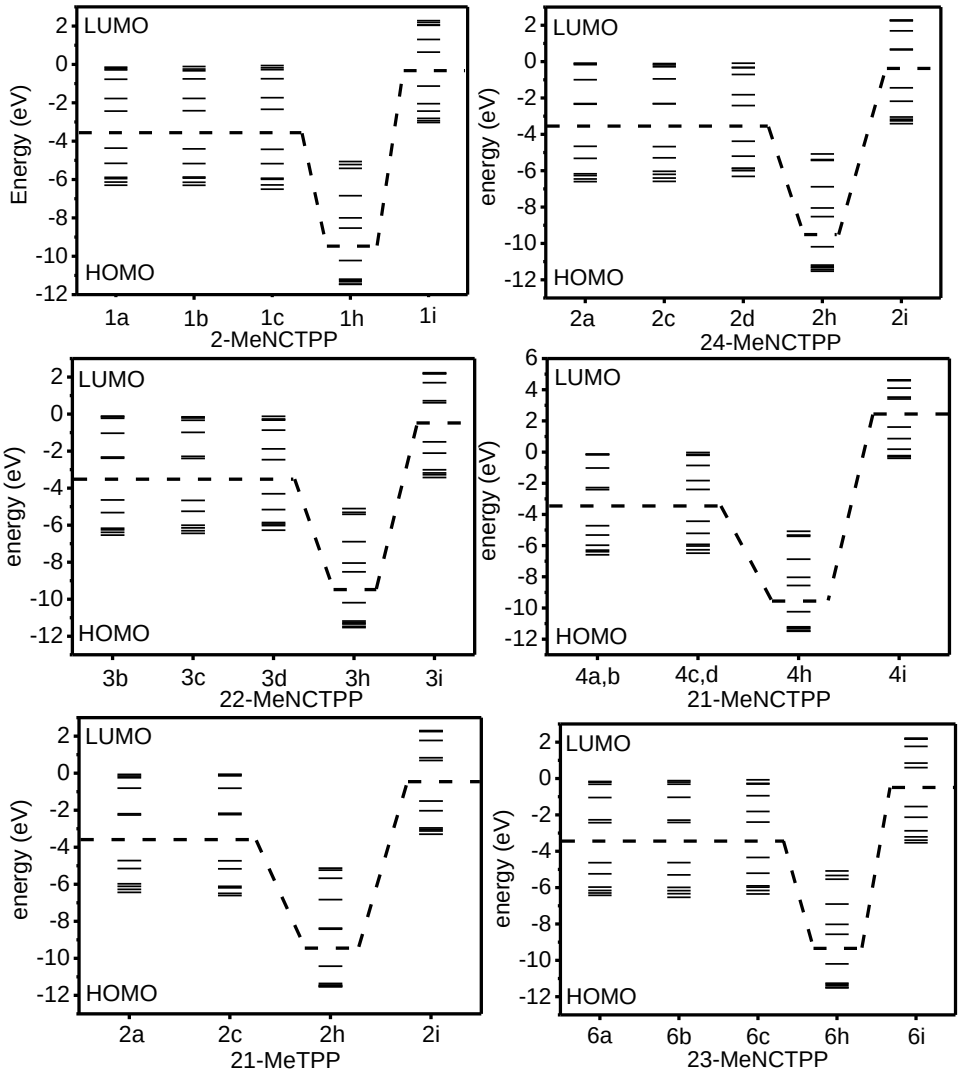

Figure 8: The relative energy levels of the N-confused tautomers from HOMO-5 to LUMO+5.

TDDFT caclulations show that the lowest energy transition for all tautomers is HOMO → LUMO (165 → 166), except for **2c**, **5a,** and **5c,** which are transitions from HOMO → LUMO+1. **5a** is in fact a combination transition, mixing the transitions from HOMO → LUMO and HOMO → LUMO+1 to form the excited state. **5** is the only TPP which does not contain a confused pyrrole ring. This suggests that the LUMO and LUMO+1 are at very similar energy levels for the **5a** tautomer.

Protonated Form: All tautomers of NCTPP were readily protonated using strong acids such as triflouroacetic acid. More differences in the UV-vis spectra for each NCTPP are observed between solvents when protonated form than in the neutral form. Figures 9 and **4** show that the most noticeable difference is that the lowest energy Q-band becomes the highest intensity signal for **2-4**. The lowest energy Q-band of **1** remains the most intense signal. A red shift is also observed in the Soret band and all the Q-Bands of all the protonated tautomers compared to the neutral form. Solvent seems to have its greatest effect on the widths of the Q-band peaks. The imino tautomers **1** and **3** showing the greatest widening of the peaks when in toluene as seen in Figure 9. Figure 10 shows a narrowing of the peaks and more excitations become visible when **1** and **3** are protonated in DMF.

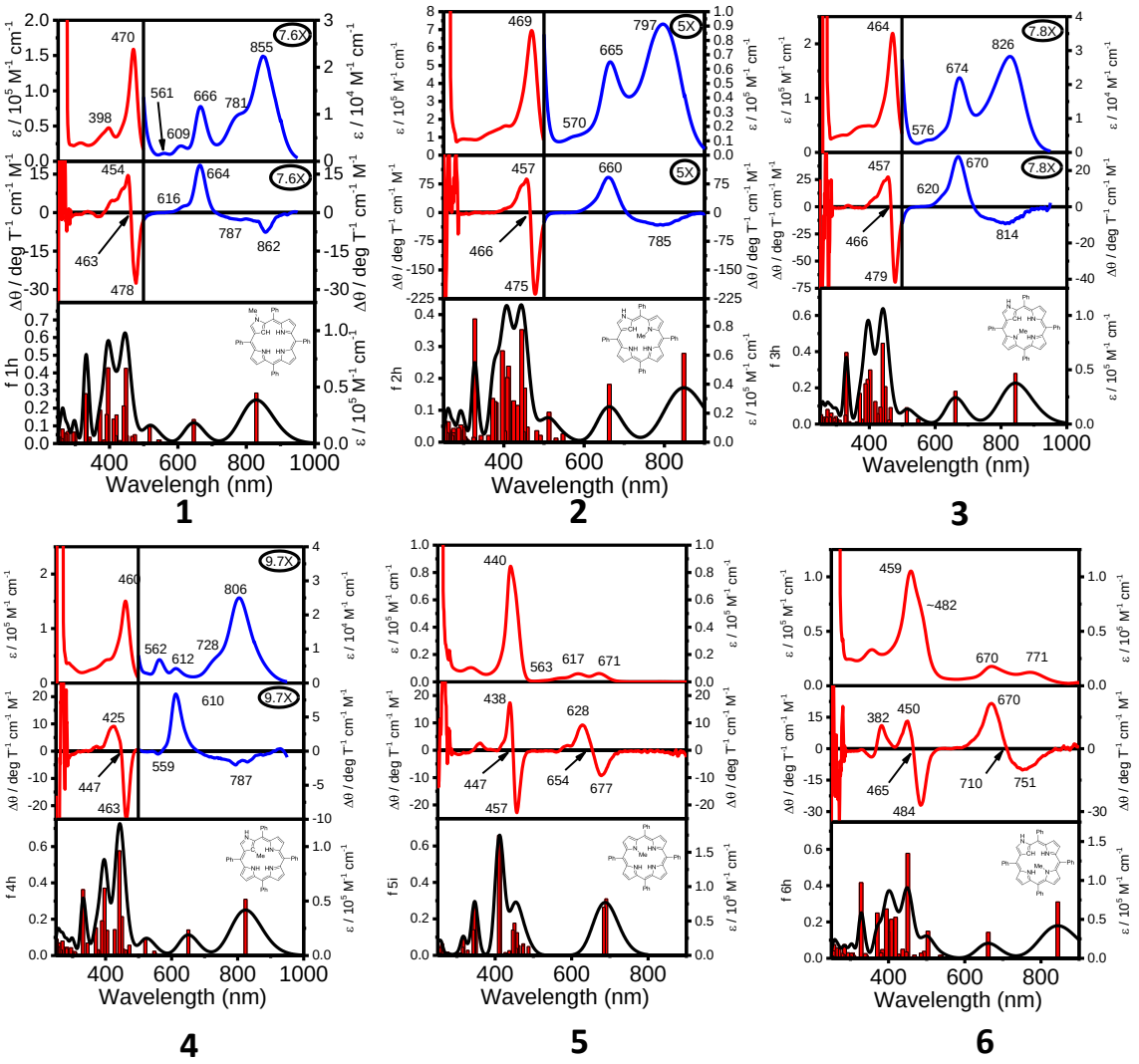

Figure 9: The UV-Vis, MCD, and TDDFT of the protonated spectra for 2-MeNCTPP (**1**), 24-MeNCTPP (**2**), 22-MeNCTPP (**3**), 21-MeNCTPP (**4**), 21-MeTPP (**5**), 23-MeNCTPP (**6**). Experimental data collected in Toluene. Compounds were protonated using trifluoroacetic acid.

MCD spectra show the same negative to positive transition in the Q-bands as energy increases for all tautomers, suggesting that the ΔHOMO>ΔLUMO. **Figures 9** and **4** show that **1-4** have very weak low energy negative Q-band signals. Interestingly, **1** increases its negative low energy signal intensity in both toluene and DMF. **5** results in a pseudo A-term in both toluene and DMF. True A-terms are not expected in this system as there is no four-fold symmetry in the molecule. The adjacent B-terms in **5** are

supported by TDDFT results; predicting that there are excitations within 10nm of each other.

The computational results also correctly predict the relative peak intensity in **1-4** with the lower energy Q-bands being more intense than the higher energy bands. All calculations except for **5** show a clean separation of the highest two excitations. SP calculations of the protonated form show that the molecules still follow Gouterman's four orbital model, but the LUMO and LUMO+1 orbitals are not degenerate. TDDFT calcuations also show that for all protonated species, the lowest energy transition is HOMO ➔ LUMO.

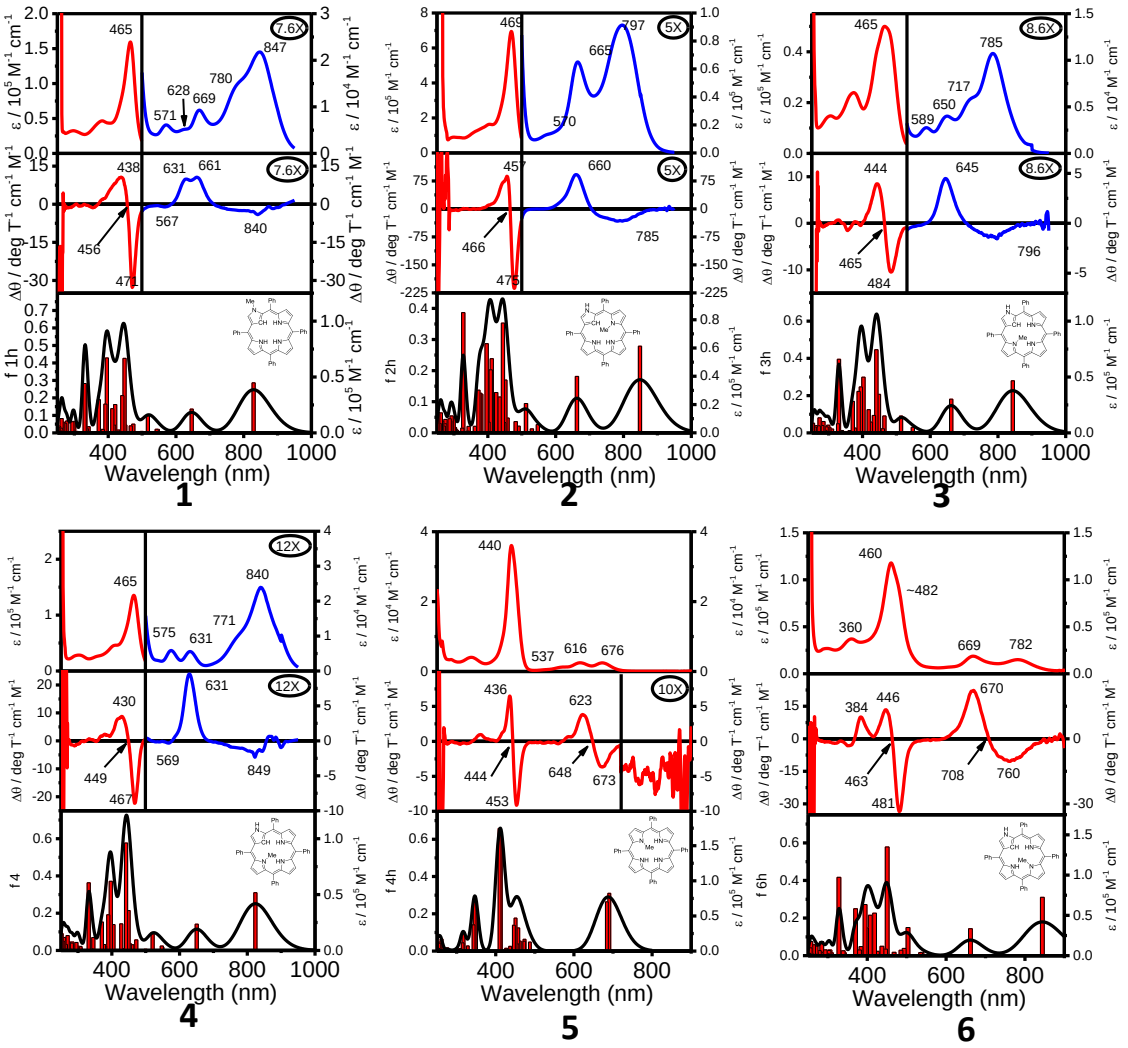

Figure 10: The UV-Vis, MCD, and TDDFT of the protonated spectra for 2-MeNCTPP (**1**), 24-MeNCTPP (**2**), 22-MeNCTPP (**3**), 21-MeNCTPP (**4**), 21-MeTPP (**5**), 23-MeNCTPP (**6**). Experimental data collected in DMF. Compounds were protonated using trifluoroacetic acid.

Deprotonated Form: All tautomers of NCTPP were readily deprotonated using strong bases such as tetrabutylammonium hydroxide. Only compound **4** has two protons to deprotonate. All other compounds have a single proton to remove. Figures 11 and 12 show that upon deprotonation, all Soret bands are red-shifted except for **5** in DMF, which actually has a slight blue shift. **1** develops a second peak in the Soret band area in both toluene and DMF. A shoulder also appears in **2** when in toluene. These peaks and

shoulders seem to be caused by a blue shift in the Q-bands. The blue-shift in the Q-bands could be caused by the addition of extra electrons into the system.

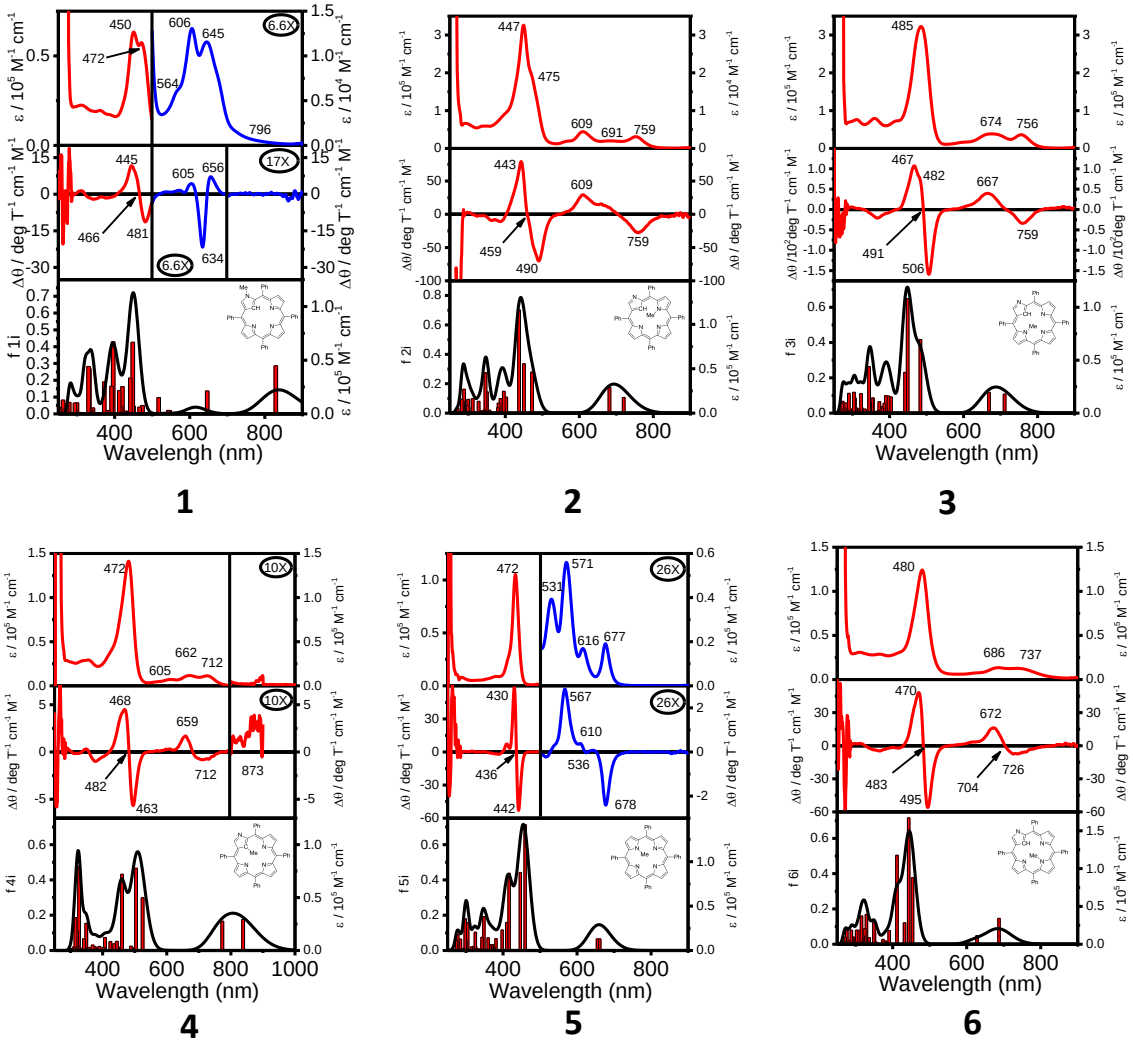

Figure 11: The UV-Vis, MCD, and TDDFT of the deprotonated spectra for 2-MeNCTPP (**1**), 24-MeNCTPP (**2**), 22-MeNCTPP (**3**), 21-MeNCTPP (**4**), 21-MeTPP (**5**), 23-MeNCTPP (**6**). Experimental data collected in Toluene. Compounds were deprotonated using $(NBu_4)OH$.

The MCD spectra for both solvent systems and all tautomers show negative to positive signals, meaning that ΔHOMO>ΔLUMO. This is supported by Single Point calculations which show ΔHOMO>ΔLUMO (table 1). A pseudo A-term is observed in the Q-band region of the MCD spectra due to the close approximation of the

Gouterman's four orbital system. SP calculations support the pseudo A-term by showing nearly degenerate looking π* orbitals. TDDFT collaborates that the energies are not degenerate for the lowest energy excitations. TDDFT calculations show that for all tautomers in the protonated from the lowest energy transition is HOMO → LUMO except for **2i** which is HOMO → LUMO+1. Interestingly, **2c** also shows this transition.

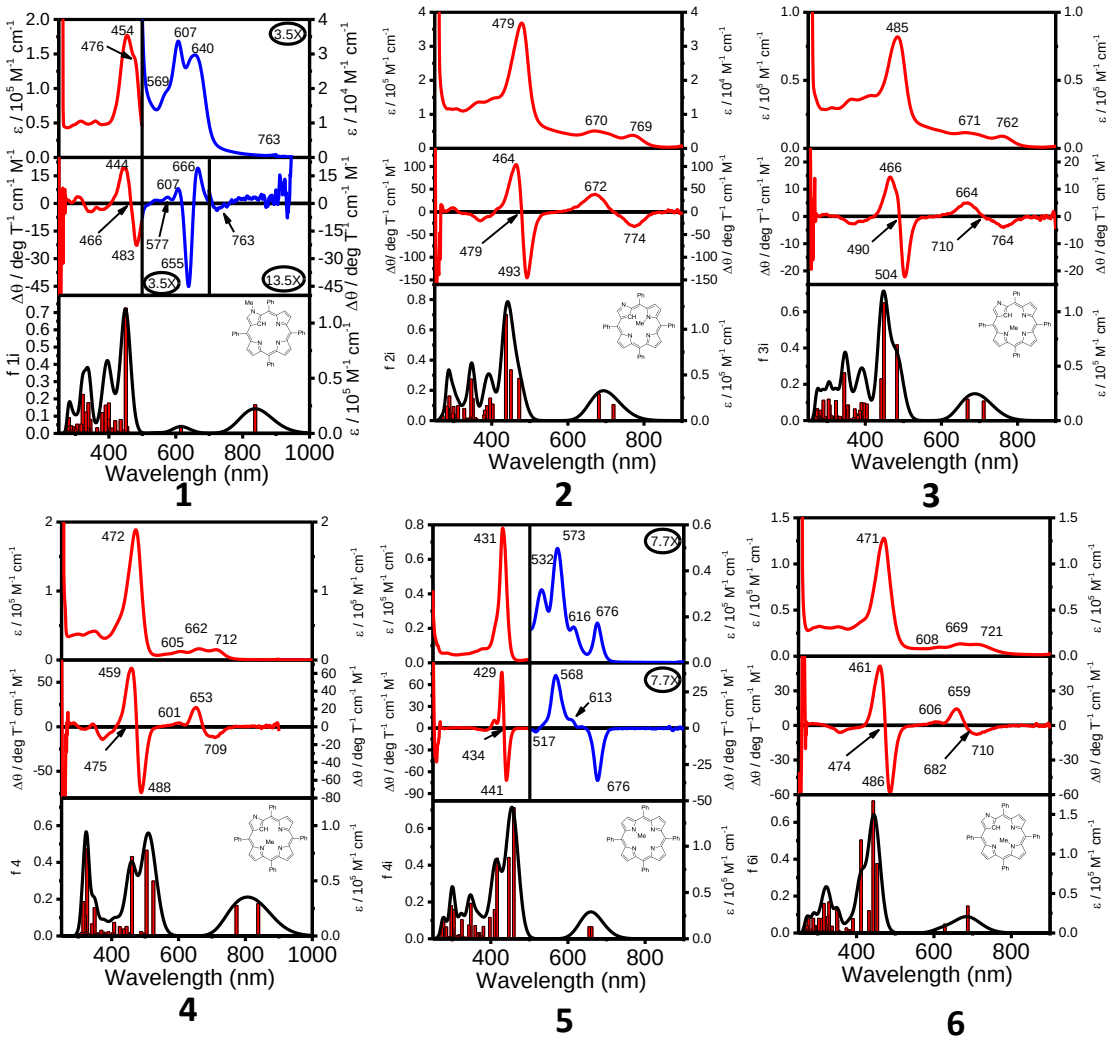

Figure 11: The UV-Vis, MCD, and TDDFT of the deprotonated spectra for 2-MeNCTPP (**1**), 24-MeNCTPP (**2**), 22-MeNCTPP (**3**), 21-MeNCTPP (**4**), 21-MeTPP (**5**), 23-MeNCTPP (**6**). Experimental data collected in DMF. Compounds were deprotonated using $(NBu_4)OH$.

2c is not the predicted stable tautomer in either polar or apolar solvents. This suggests

that the complete absence of protons disrupts the π-system as much as forcing a proton into a location that does not support the [18]annulenic ring system.

Conclusion:

Previous studies have shown that NCTPP contains two tautomers which are highly responsive to the polarity of the solvent environment. The addition of a methyl group in various positions "locks" the NCTPP into a specific proton tautomer regardless of the solvent environment. The methyl group adds steric strain and asymmetry such that Gouterman's four orbital theory cannot be strictly adhered to, the ΔHOMO is consistently larger than the ΔLUMO for all tautomers and solvents, which was seen both experimentally and computationally. This suggests that the steric strain from the added methyl group is not enough to significantly alter the e_g orbitals of the LUMO and LUMO+1. What the methyl group did add was specific functionality for the porphyrin system what will operate independently of the solvent system.

Chapter 3: Electronic properties of mono-functionalized tetraferrocenyl porphyrins in solution and on gold surface: assessment of the influencing factors for photoelectrochemical applications

Introduction

Because of the well-established electron-donor properties, ferrocene-containing donor-acceptor dyads, with strong absorption of the solar spectrum and tunable electron-transfer and redox properties, were intensively studied over the last several decades as prominent light-harvesting blocks for organic photovoltaics (OPVs) and dye-sensitized solar cells (DSSCs).[52-63] In addition, such systems were suggested as potentially useful components for redox-driven fluorescence, molecular electronics, ion-recognition, and optical limiting devices.[64-66] Tetraazaporphyrins,[67-69] phthalocyanines,[70-78] corroles,[79,80] porphyrins,[81-120] and (aza)BODIPYs[121-126] substituted with one or several ferrocenyl groups are of great interest because of their rich redox chemistry and redox-switchable spectroscopic versatility. Potential usage of ferrocene-containing porphyrins and analogues in DSSCs, OPVs, molecular electronics, and photocatalysis require their surface immobilization and, in particularly simple synthetic routes, for formation of well-defined self-assembled monolayers (SAMs). Porphyrin-based SAMs were intensively investigated recently by numerous research groups because of their remarkable electrochemical, electrocatalytic, and photophysical properties.[127-133] In general, such SAMs could be prepared using two strategies: (i) by the linkage of a symmetric or an unsymmetric porphyrin to the surface

through a covalent bond, (ii) by the axial coordination of the porphyrin central ion to a pre-formed donor atom-containing monolayer. Despite of the significant progress in preparation and characterization of porphyrin-containing SAMs, reports on surface immobilization of redox-active ferrocenyl-containing porphyrins and their analogues are rare.[134-136] Moreover, only recently we communicated the first example of ferrocenyl-containing porphyrin, which was linked to SAM by porphyrin-ferrocene-linker-Au covalent bond,[137] while all other SAMs were prepared using porphyrin-linker-Au bonding or axial coordination to Au surface.[134-136] Preliminary photocurrent generation experiments pointed out that the covalently bound metal-free TFcPs are able catalytically reduce dioxygen under photo-stimulation.[137] However, despite this uncommon and promising feature, the light-into-current conversion efficiency is much lower than that of other porphyrin-supported gold electrodes.[138]

Thus, in this paper, we provide complete characterization of the unsymmetric tetraferrocenyl-containing porphyrins of general formula $H_2Fc_3Fc(COR)P$ (R = $-CH_3$, **1**; $-(CH_2)_5Br$, **2**; and $-(CH_2)_5SCOCH_3$, **3**) as well as an investigation on the kinetic of the electron transfer at the SAM/electrode interface in view of photocatalytic applications.

Results and Discussion

Synthesis and characterization of $H_2Fc_3Fc(COR)P$. Classical Friedel-Cratfs conditions for ferrocene provided inadequate yields for the functionalization of ferrocenecarboxyaldehyde (around 10%). This is likely due to two simultaneous effects: *i*) FcCHO is deactivated toward acylation because of the –CHO electron withdrawing group; *ii*) the aldehyde competes for the coordination of $AlCl_3$, thus preventing the formation of the acylium ion. Indeed, as soon as aluminum chloride was added, the

solution turned from orange into violet, which stems from the formation of a Lewis complex. In order to overcome these inconveniences, the acylium carbocation was prepared in a separate flask, while an FcCHO---$AlCl_3$ complex was formed in a second flask. Two equivalents of the acyl chloride were necessary to force the reaction to completion. With these modifications, the conversion was improved up to 60-70% yields, using different acylating agents. The reaction is highly regioselective: among possible isomers, the only product observed was the 1,1'-disubstituted compound. Apparently, the introduction of a keto group at the 1' position deactivates the product, thus making a second substitution disfavoured on both rings.

Mono-functionalized tetraferrocenylporphyrins **1** and **2** were prepared by a mixed condensation of FcCHO and functionalized FcCHO in 5:1 ratio using the standard statistical condensation method under the Lindsey cyclization conditions (Scheme 1). The stoichiometric ratio (3:1) was not adopted to avoid the formation of multi-substituted porphyrins, which would have complicated the isolation of the product. As a matter of fact, only traces of di-substituted isomers were isolated as by-products from the synthesis of 5-[1'-acetyl)ferrocenyl]-10,15,20-triferrocenylporphyrin. On the other hand, a ratio higher than 5:1 would have promoted the formation of an excess of H_2TFcP. Another issue responsible for the observed moderate yields is the scarce stability of the functionalized aldehydes in the reaction conditions employed. No traces of these compounds were recovered after column chromatography, whereas a considerable amount of FcCHO was ubiquitous at the end of the reactions. Such an evidence suggests that the decomposition of the 1'-substituted ferrocencarboxyaldehydes is the main drawback in mono-substituted tetraferrocenylporphyrins synthesis.

After separation of **1** and **2** from side-reaction products, using conventional chromatography approach, complex **2** was transformed into thioacetyl derivative **3**. This derivative undergoes *in situ* cleavage upon exposure to the gold surface to form $H_2Fc_3Fc(COR)P$ (R = $-(CH_2)_5SH$, **4**) containing SAMs, hence avoiding handling unstable free-thiol porphyrin compounds.

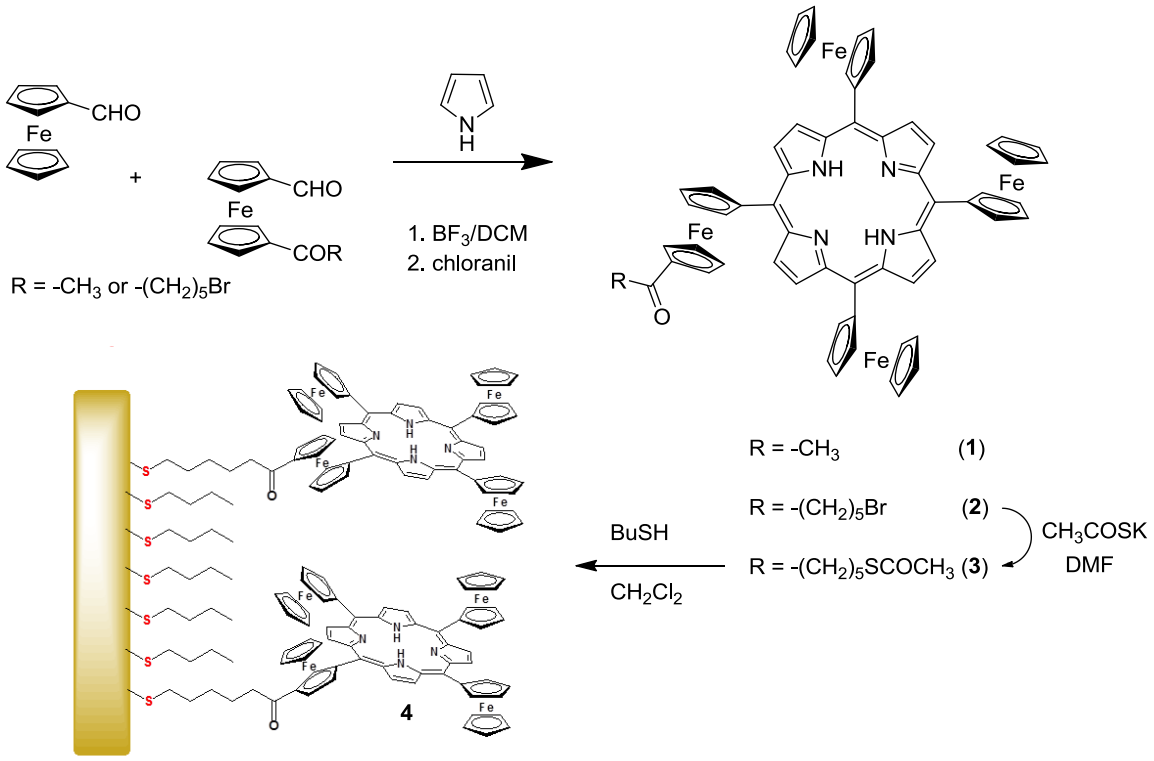

Scheme 3. Synthetic pathways for preparation of the–$H_2Fc_3Fc(COR)P$ derivatives and related SAMs.

The UV-Vis-NIR and MCD spectra of $H_2Fc_3Fc(COR)P$ derivatives **1** and **2** are presented in Figure 13. As expected from similarity of electronic effects of $–COCH_3$ and $–CO(CH_2)_5Br$ groups, both spectra are very close to each other and consist of an intense Soret band located at 434 nm, a shoulder at 490-495 nm range and two prominent Q-

bands observed at ~660 and 725 nm. In both cases, the Soret band located at 437 nm is represented by Faraday pseudo *A* term in their corresponding MCD spectra, while Q-bands are represented by negative (lower energy) and positive (higher energy) Faraday *B*-terms with energies close to the corresponding absorption bands. In addition, most likely another Faraday pseudo *A*-term was observed at 499 nm, which corresponds to a broad shoulder in the absorption spectrum of **1** and **2**. The consistency of MCD spectra of porphyrins **1** and **2** correlates well with the low symmetries of these compounds. Overall, UV-vis and MCD spectra of **1** and **2** are very close to the reported earlier spectra of symmetric H_2TFcP and unsymmetric $H_2Fc_nPh_{(4-n)}P$ derivatives.[20]

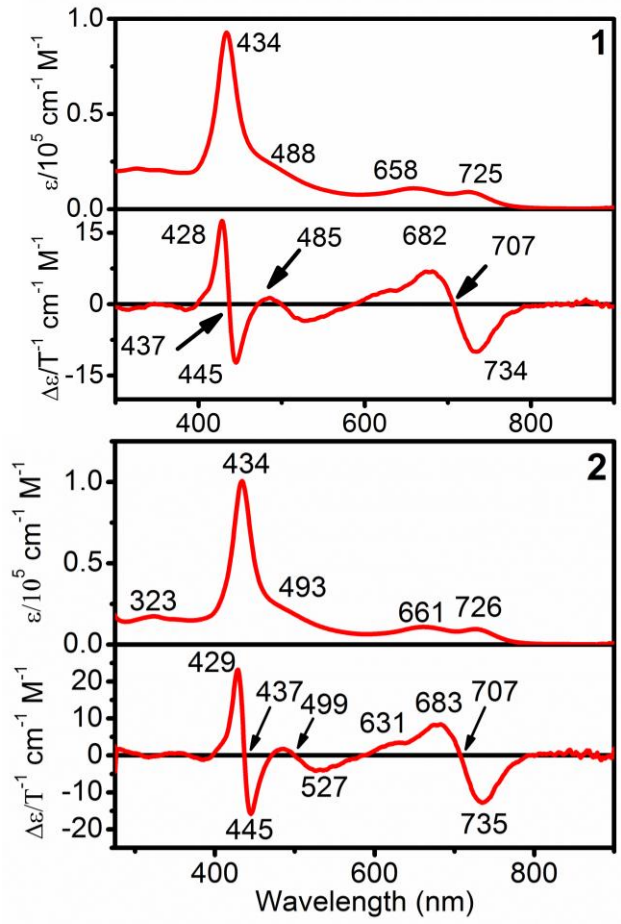

Figure 13. UV-Vis-NIR and MCD spectra of **1** (top) and **2** (bottom) in DCM.

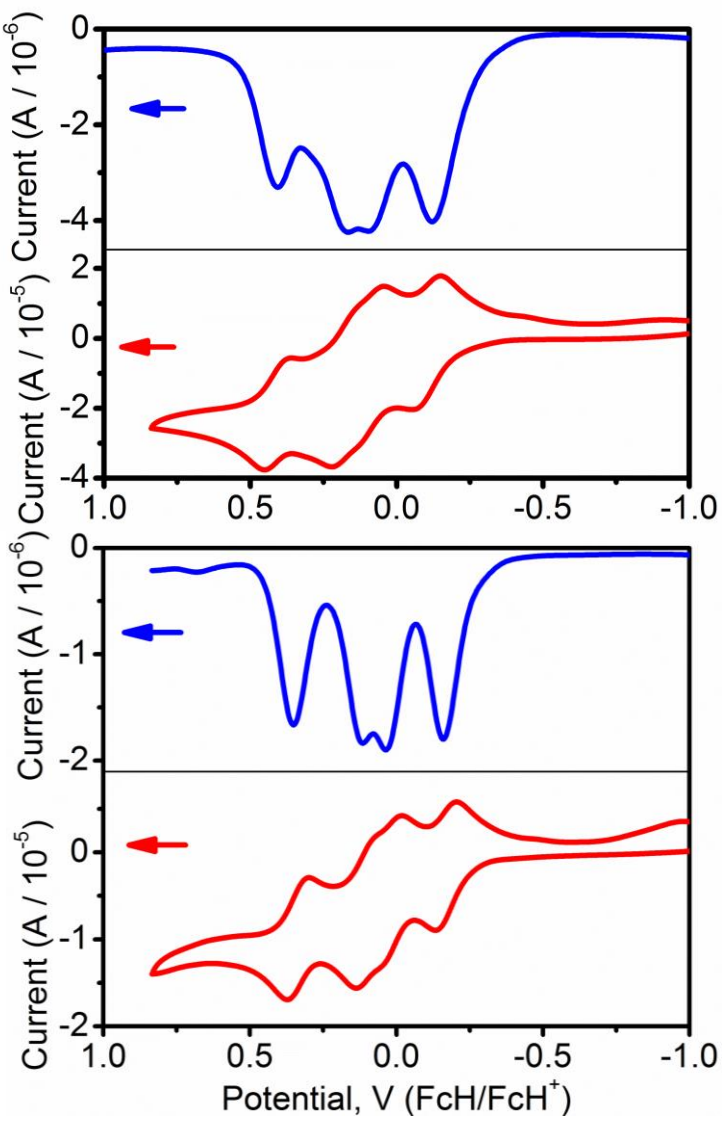

Figure 14. Electrochemical data (CV, 50 mV/s and DPV) of compounds **1** (top) and **2** (bottom) in DCM/0.05M TBAF system in ferrocene substituents' oxidation region.

Similar to the described earlier metal-free and transition-metal tetraferrocenyl porphyrins,[88,93,96,97] the redox properties of $H_2Fc_3Fc(COR)P$ derivatives were initially evaluated using cyclic voltammetry (CV) and differential pulse voltammetry (DPV) approaches. In order to minimize solute-electrolyte ion-pairing and thus improve the resolution between redox processes, all electrochemical and spectroelectrochemical

experiments on $H_2Fc_3Fc(COR)P$ porphyrins were conducted using DCM as a solvent and, as suggested by Geiger and co-workers as well as other research gorups[140-147] tetrabutylammonium tetrakis(perfluorophenyl)borate (TBAF) as the electrolyte. CV and DPV results for $H_2Fc_3Fc(COR)P$ compounds are shown in Figure 14, while redox potentials are listed in Table 2.

Table 2. Redox properties of metal free tetraferrocenyl porphyrins in DCM/0.05M TBAF system at room temperature determined using CV and DPV data. [a]

Porphyrin	Ox_4	Ox_3	Ox_2	Ox_1	Red_1	Red_2
H_2TFcP[b]	0.35	0.21	0.11	-0.15	-1.90	-2.18
$H_2Fc_3Fc(COMe)P$	0.46	0.21	0.15	-0.07	-1.84	-2.10
$H_2Fc_3Fc(CO(CH_2)_5Br)P$	0.44	0.20	0.12	-0.07	-1.82	-2.03

[a] All potentials are versus FcH/FcH^+ couple; [b] Reference 6o.

In agreement with redox data reported previously on H_2TFcP and MTFcP complexes,[88,93,96,97] redox processes in $H_2Fc_3Fc(COR)P$ could be associated with oxidation of ferrocene substituents and oxidation/reduction of the porphyrin core. All reductions are porphyrin-centered, reversible, and observed between -1.82 and -2.1 V, while because of the presence of electron-withdrawing group, the porphyrin-centered oxidation process was not observed within solvent window. It could be expected that an introduction of one ferrocene substituent with electron-acceptor group will result in: (i) shift of redox potentials to more positive region and (ii) a better separation between the ferrocene-centered redox waves of because its higher oxidation potential. Indeed, the

oxidation potential of acetylferrocene was reported to be ~270 mV more positive compared to that of the parent ferrocene.[148] Moreover, an influence of the electron-withdrawing acylferrocene on adjacent and the opposite unsubstituted ferrocene groups should also be slightly different thus resulting in a better separation between redox waves. Not surprisingly, CV and DPV data on $H_2Fc_3Fc(COR)P$ compounds support expected trends. In particular, the first and the second as well as the third and the fourth oxidation waves are very well separated, while separation between the second and the third oxidation waves is much smaller. It is interesting to note that that total span for all four oxidation processes in $H_2Fc_3Fc(COR)P$ compounds is still close to that observed in the parent H_2TFcP although the first oxidation potential in $H_2Fc_3Fc(COR)P$ compounds is ~80 mV more positive because of the electron coupling of the three unsubstituted ferrocene groupf with electro-accepting acylferrocene fragment (Table 2).

Extracted from the electrochemical data, the comproportionation constants (K_c)[149-157] for all possible mixed-valence states in $H_2Fc_3Fc(COR)P$ compounds are presented in Table 2. Based on CV and DPV data, it is expected that the K_c for the following equilibria:

(1) $[H_2Fc_3Fc(COR)P]^0 + [H_2Fc_3Fc(COR)P]^{2+} \rightarrow 2\,[H_2Fc_3Fc(COR)P]^+$

(2) $[H_2Fc_3Fc(COR)P]^{2+} + [H_2Fc_3Fc(COR)P]^{4+} \rightarrow 2\,[H_2Fc_3Fc(COR)P]^{3+}$

indicate higher stability of $[H_2Fc_3Fc(COR)P]^+$ and $[Fc_3Fc^{COR}PH_2]^{3+}$ mixed-valence species in solution. Estimated values of K_c for the second and third oxidation process are significantly smaller (Table 3), reflecting possible difficulties with generation of spectroscopically pure $[H_2Fc_3Fc(COR)P]^{2+}$ mixed-valence species. As usual, it should be noted that although estimated values of K_c could be helpful in characterization of the

mixed-valence species generated under spectroelectrochemical conditions, they should be treated with a great caution because of the well-known fact that the electrochemical redox potentials of potentially mixed-valence compounds are highly dependent on a solvent and electrolyte.[149,150]

Table 3. Summary of comproportionation constants (K_c)[a] in $H_2Fc_3Fc(COR)P$ derivatives estimated from the DPV electrochemical data.

$X^0 + X^{2+} \rightleftarrows 2(X^+)$	$X^{1+} + X^{3+} \rightleftarrows 2(X^{2+})$	$X^{2+} + X^{4+} \rightleftarrows 2(X^{3+})$
	$H_2Fc_3Fc(COMe)P$ (**1**)	
3832	14	13313
	$H_2Fc_3Fc(CO(CH_2)_5Br)P$ (**2**)	
2056	19	11393

[a] comproportionation constants were calculated using $K_c = \exp [\Delta E\ F/RT]$ formula, where $F/RT = 38.92\ V^{-1}$ at 298 K (see Ref. 140).

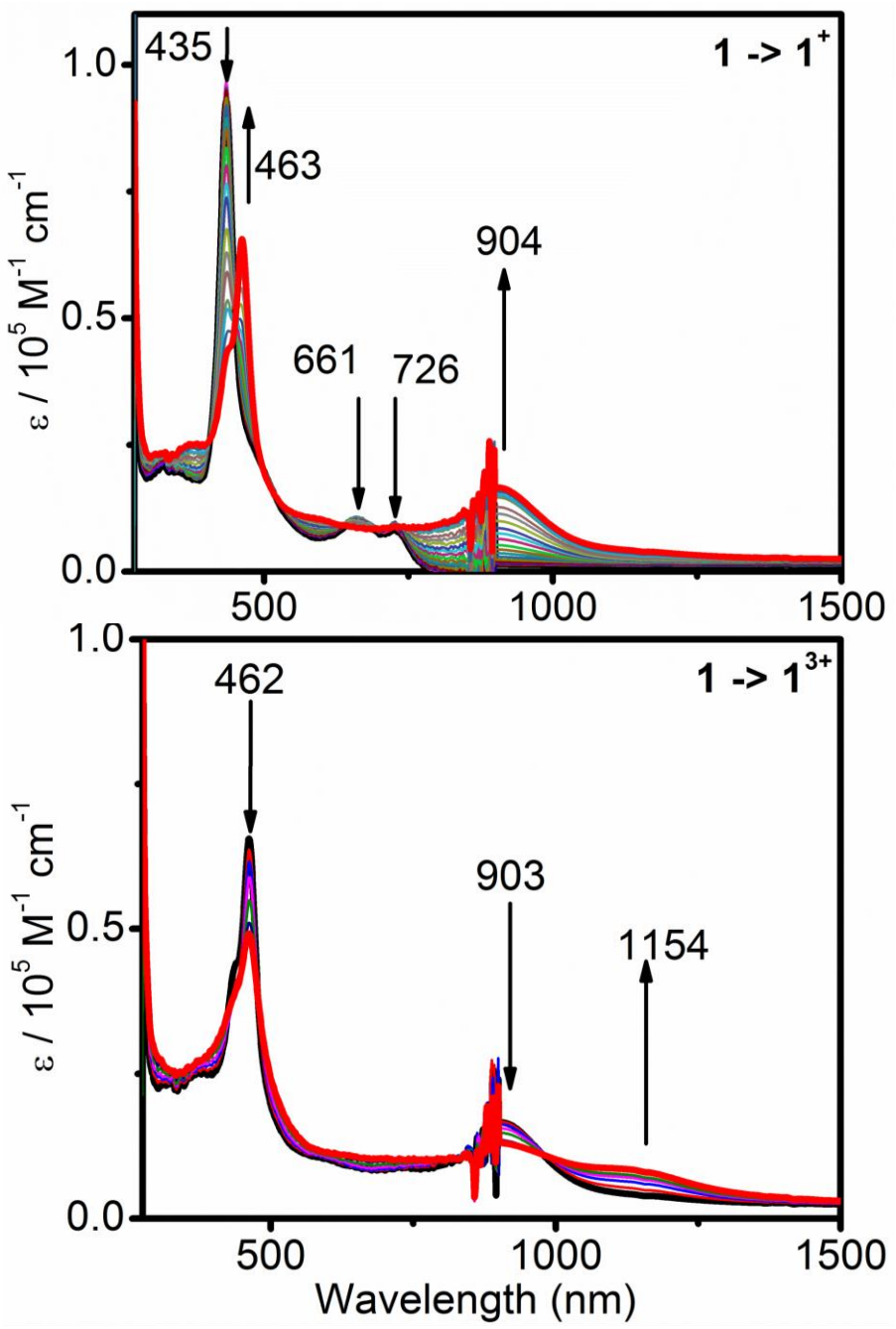

Figure 15. Spectroelectrochemical oxidation of the $H_2Fc_3Fc(COMe)P$ (**1**) at first (top; **1** $\rightarrow$ $\mathbf{1}^{+}$) and second-third (bottom; $\mathbf{1}^{+}$ $\rightarrow$ $\mathbf{1}^{3+}$) oxidation potentials in DCM/0.15M TFAB system.

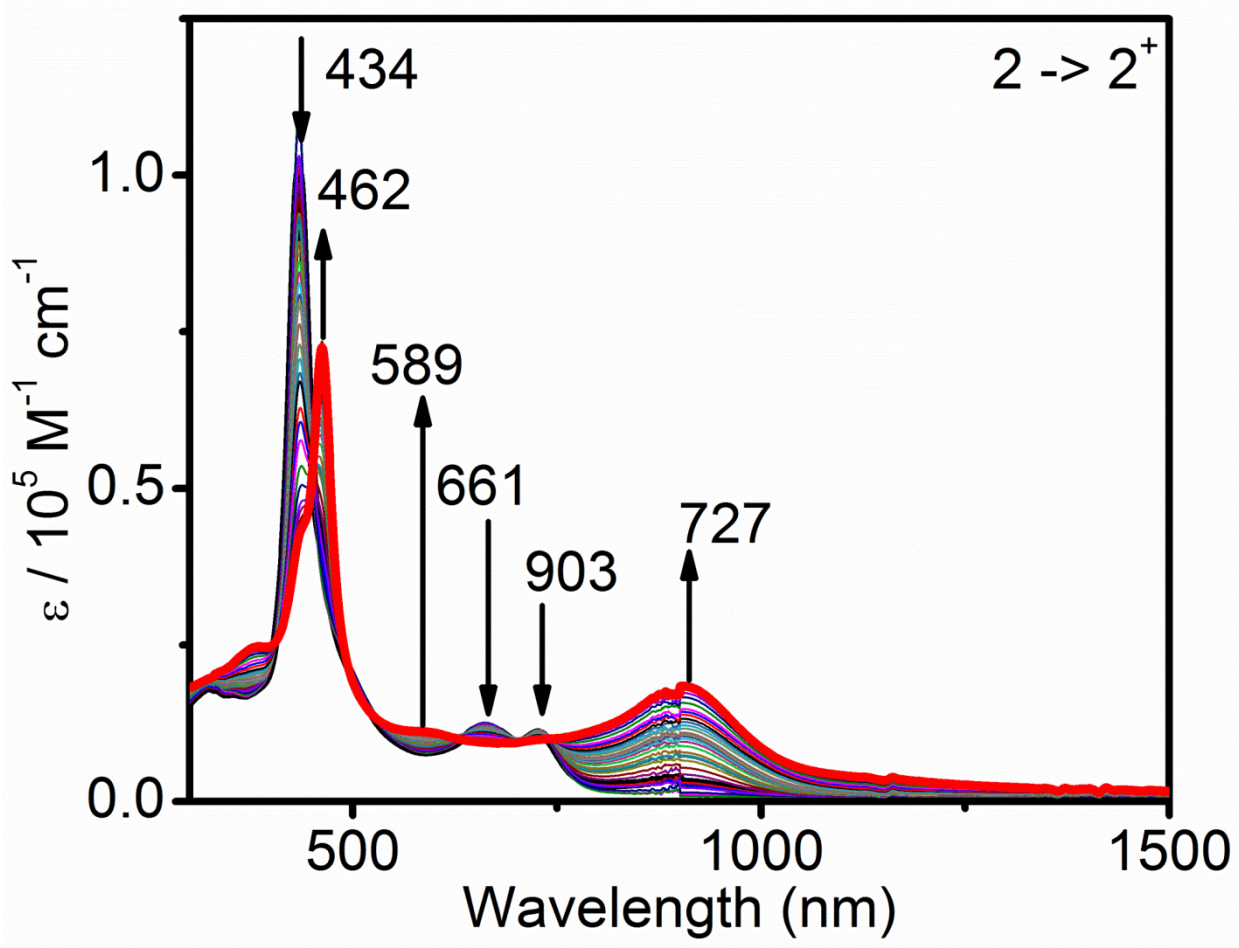

Figure 16. Spectroelectrochemical oxidation of **2** at first oxidation potential in DCM/0.15M TFAB system.

In order to obtain spectroscopic signatures of $[H_2Fc_3Fc(COR)P]^{n+}$ species as well as to provide an accurate assignment of electrochemically observed redox processes, $H_2Fc_3Fc(COR)P$ derivatives **1** and **2** were further investigated by spectroelectrochemical approach. In both cases, during oxidation under the first oxidation potential, the Soret band of **1** and **2** at ~435 nm was found to decrease in intensity and undergo a red shift of 28 nm, while the Q-band was found to decrease in intensity without energy change. In addition, a very characteristic inter-valence charge-transfer (IVCT) band appeared at ~905 nm (Figures 15 and 16). The IVCT band energy and intensity are similar to those observed in the earlier described $[H_2TFcP]^+$ and $[MTFcP]^+$ mixed-valence

complexes.[88,93,96,97] Thus, the first transformation process could be confidently assigned to a $H_2Fc_3Fc(COR)P \rightarrow [H_2Fc_3Fc(COR)P]^+ + e^-$ transformation. Further oxidation of the $[H_2Fc_3Fc(COR)P]^+$ species under spectroelectrochemical conditions resulted in the Soret band intensity decrease, a drop in intensity of the IVCT band and the development of a new broad IVCT band at ~1150 - 1200 nm (Figures 15 and 16). Taking into consideration the small difference between second and third oxidation waves as observed in electrochemical experiments and thus the relatively small values of comproportionation constants for $[H_2Fc_3Fc(COR)P]^+ + [H_2Fc_3Fc(COR)P]^{3+} \rightarrow 2\ [H_2Fc_3Fc(COR)P]^{2+}$ process, we did not attempt to obtain spectroscopic signature for $[H_2Fc_3Fc(COR)P]^{2+}$ mixed-valence complex, but rather convert it to more stable $[H_2Fc_3Fc(COR)P]^{3+}$ compound (Figure 15). The resulting spectra of the mixed-valence $[H_2Fc_3Fc(COR)P]^{3+}$ species characterized by the presence of a very broad NIR IVCT band. Further oxidation of the previously generated mixed-valence species results in gradual disappearance of the entire spectrum, which can be attributed to the decrease in solubility of highly charged $[H_2Fc_3Fc(COR)P]^{4+}$ species in low polarity solvent (DCM). Such behavior was observed earlier with H_2TFcP and MTFcP complexes. [88,93,96,97]

Spectroelectrochemical data were further supported by chemical oxidation of $H_2Fc_3Fc(COR)P$ **1** and **2**. In particular, chemical oxidation of $H_2Fc_3Fc(COR)P$ derivatives by a controlled amount of 2, 3-dichloro-5, 6-dicyanobenzoquinone (DDQ), I_2, Br_2, or $[NO]BF_4$ results in transformation of initial compounds **1** and **2** into mixed-valence $[H_2Fc_3Fc(COR)P]^+$ cations (Figures 16, 18, and 19). During these oxidations, Soret band shifts to ~460 nm region, Q-bands decrease in intensity, and a new, counter-ion dependent IVCT band at ~900 nm appears in the UV-Vis-NIR spectra of

$[H_2Fc_3Fc(COR)P]^+$ cations. Such transformation is in excellent agreement with the spectroelectrochemical data. Further oxidative titrations of the mixed-valence $[H_2Fc_3Fc(COR)P]^+$ compounds result in the rise of a second broad IVCT band at ~1150 nm and decrease of the Soret band intensity, again in agreement with the spectroelectrochemical data (Figures 16, 17, and 18).

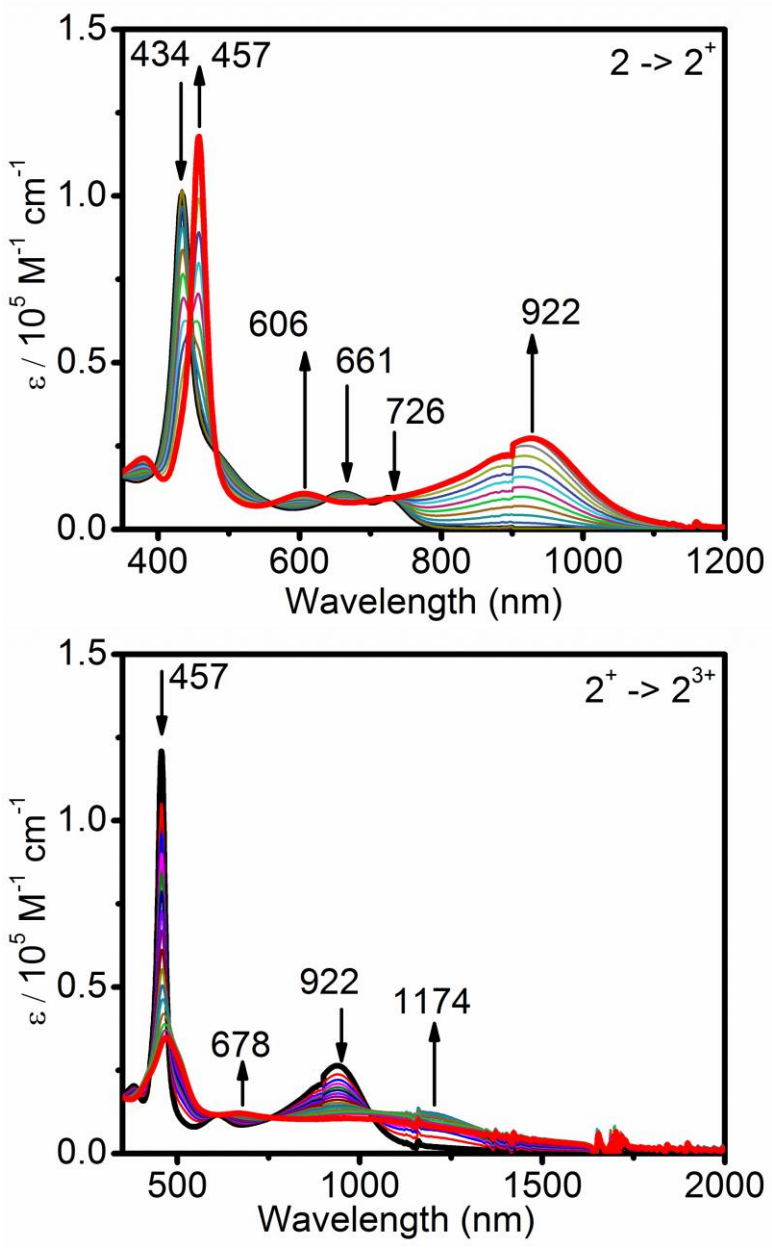

Figure 17. Stepwise chemical oxidation of derivative **2** by $[NO]BF_4$ in DCM.

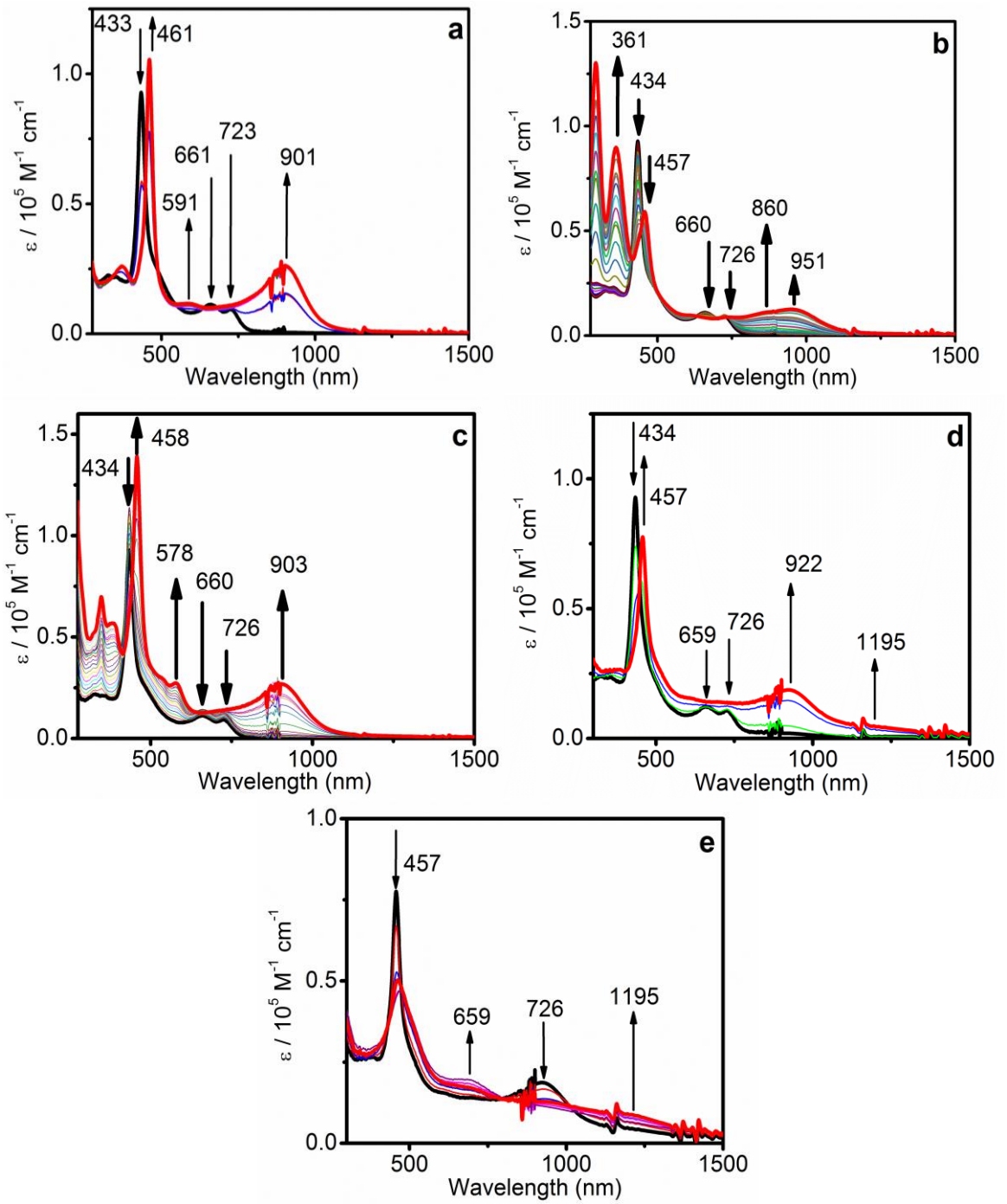

Figure 18. Chemical oxidation of complex **1** in DCM by Br_2 (A), I_2 (B), DDQ (C), and $[NO]BF_4$ (D and E).

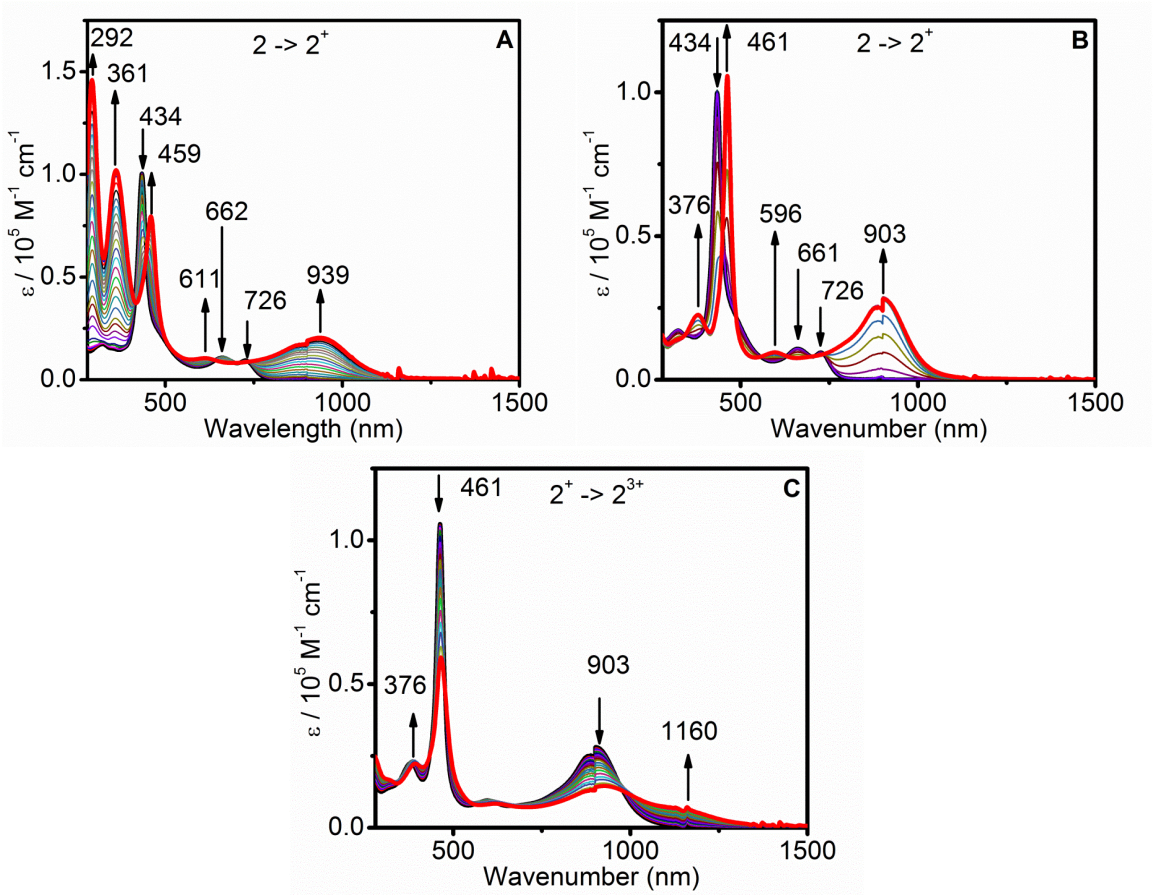

Figure 19. Chemical oxidation of complex **2** in DCM by I_2 (A) and Br_2 (B and C).

The Hush method[158] is typically used for the initial analysis of experimental data in mixed-valence compounds. In the case of $H_2Fc_3Fc(COR)P$ compounds, such analysis could be applied to the spectroelectrochemically or chemically generated mixed-valence $[H_2Fc_3Fc(COR)P]^+$ only because of the presence of a better-defined IVCT band in the NIR region of their UV-Vis-NIR spectra. The two key parameters that are estimated using the Hush model are: the electronic coupling matrix element (H_{ab}) and the degree of delocalization (α^2). These parameters can be estimated using equations 1, 2, with the Fe-Fe distances extracted from the corresponding DFT predicted geometry of neutral $H_2Fc_3Fc(COMe)P$ compound.

$H_{ab} = 2.05 \times 10^{-2} [(\nu_{max} \varepsilon_{max} \Delta\nu_{1/2})^{1/2} / r_{ab}]$ equation 1

$\alpha^2 = 4.24 \times 10^{-4} [(\varepsilon_{max} \Delta\nu_{1/2}) / (r_{ab}^2 \nu_{max})]$ equation 2

The energy of the IVCT at band maximum in cm^{-1} is ν_{max}, $\Delta\nu_{1/2}$ is the width at the band maximum in cm^{-1}, ε_{max} is the molar extinction coefficient of the IVCT, and r_{ab} is the distance between redox centers in Å.

Table 4 displays the parameters obtained from the IVCT band fits. These parameters should be considered with caution because of the relatively broad nature of the IVCT band in $\mathbf{1}^+$ and $\mathbf{2}^+$, uncertainly factor in band deconvolution analysis, and possibility of the protonation to contribute into absorption in IVCT region. Thus, values listed in Table 3 are rough estimates that add support to the other spectroscopic data discussed above. In all cases, the H_{ab} and α^2 values closely match the values obtained for the previously reported polyferrocenyl porphyrins, [88,93,96,97] and are in the range of Class II (Robin and Day classification) mixed-valence compounds.[161]

Table 4. Estimated H_{ab} and α^2 values for mixed-valence states of ferrocenyl-containing porphyrins generated under chemical- and electrochemical conditions.

Compound/Oxidant [a]	ν_{max}, cm^{-1}	ε_{max}, M^{-1} cm^{-1}	$\Delta\nu_{1/2}$, cm^{-1}	R_{ab}, Å [b]	H_{ab}, cm^{-1}	$\alpha^2 x\ 10^3$
1$^+$ / Br_2	11023	23383	1518	9.755	1315	14.21
1$^+$ / DDQ	11024	24670	1724	9.755	1439	17.03
1$^+$ / SEC	11004	12947	1560	9.755	1008	8.10
2$^+$ / I_2	10650	20500	2001	9.755	1389	17.00
2$^+$ / Br_2	11023	25583	1588	9.755	1406	16.27
2$^+$ / NO^+	10688	25129	1655	9.755	1401	17.17
2$^+$ / SEC	11000	15000	1660	9.755	1100	9.99

[a] SEC = spectroelectrochemistry; [b] the shortest Fe-Fe distance from DFT calculations on $H_2Fc_3Fc(COMe)P$. All data are based on band deconvolution analysis of the IVCT region.

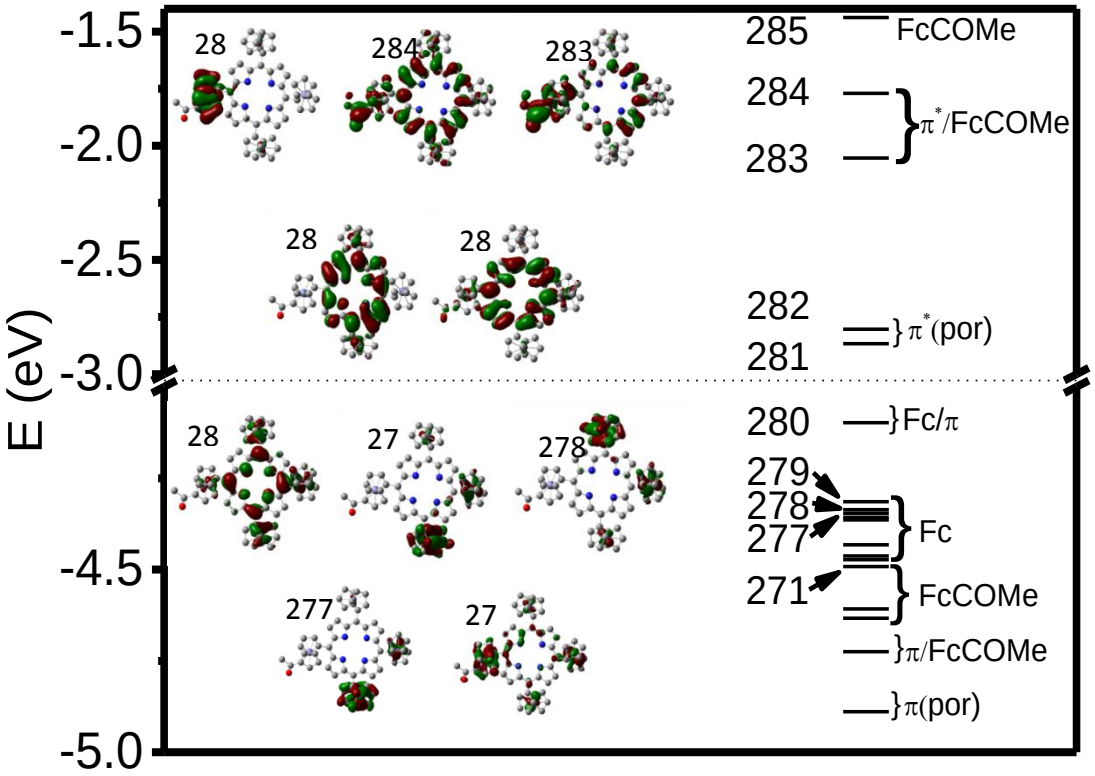

Figure 20. Molecular orbital diagram of $H_2Fc_3Fc(COMe)P$ (**1**) calculated at BP86 DFT level.

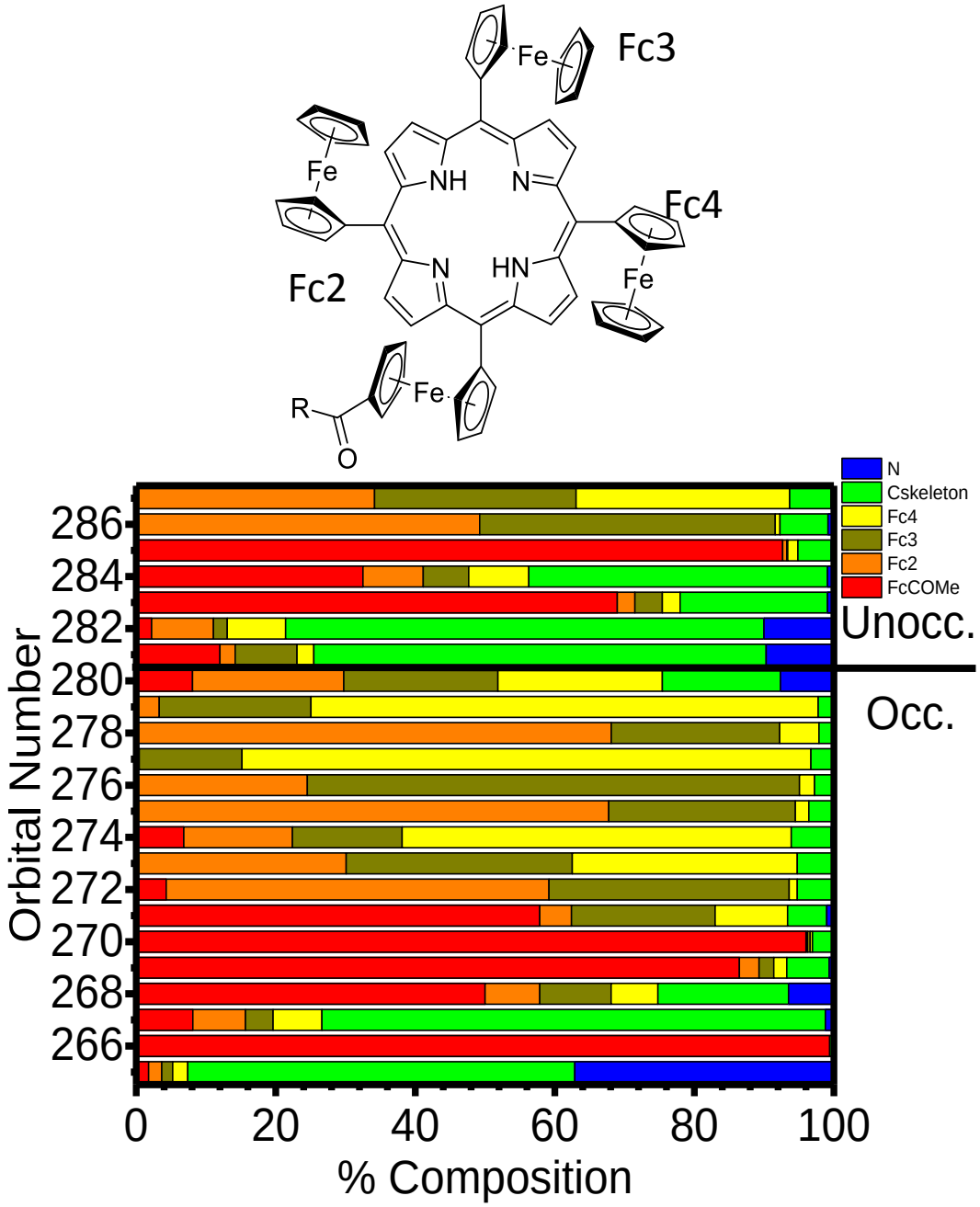

Figure 21. Molecular orbital compositions of $H_2Fc_3Fc(COMe)P$ (**1**) calculated at BP86 DFT level.

Electronic Structures of $H_2Fc_3Fc(COR)P$. Density functional theory (DFT) calculations were performed to acquire insight into nature of the electronic structure, spectroscopy, and redox properties of $H_2Fc_3Fc(COR)P$ derivatives. Because of the great

similarities in properties of **1** and **2**, the electronic structure and excited state energies of only complex **1** were calculated. Similar to the reported earlier H_2TFcP,[139] $H_2Fc_3Fc(COMe)P$ compound predicted to be highly non-planar and adopt the most stable α,β,α,β-conformation. The molecular orbital energy diagram, molecular orbital compositions, and representative shapes of important molecular orbitals predicted using the BP86 exchange-correlation functional and 6-311G(d) basis set are shown in Figures 16 and 17. Electronic structure of $H_2Fc_3Fc(COMe)P$ **1** have many similarities with previously reported electronic structure of the parent H_2TFcP.[139] In particular: (i) the LUMO and LUMO+1 are predominantly porphyrin-centered π* orbitals, that resemble Gouterman's[162] classic e_g symmetry MO pair; these orbitals are well-separated from the LUMO+2, which has large contribution from acylferrocene group; (ii) similar to all previously described MTFcP and H_2TFcP compounds,[88,93,96,97] predominantly ferrocene-containing MOs have higher energies in comparison with the porphyrin-centered occupied π-orbitals; (iii) the HOMO with predominant equatorial ferrocene group character has ~25% porphyrin π-system character mostly located at *meso*-carbon and nitrogen atoms; (iv) the "a_{2u}"-type (with most electron density located at the *meso*-carbon and nitrogen atoms) porphyrin-centered π-orbital (HOMO) has a higher energy than the "a_{1u}"-type (with most electron density located at the α- and β-carbon atoms) porphyrin-centered π-orbital (HOMO-12). Introduction of electron-withdrawing group in one of the ferrocene substituents results in large energy stabilization of the MOs associated with acylferrocene. Although, acylferrocene group contributes ~8% into HOMO, predominantly acylferrocene-centered MOs are located between HOMO-9 and HOMO-11. On the other hand, the three more electron-rich unsubstituted ferrocene groups left

behind dominate in HOMO to HOMO-8 region. Interestingly, DFT predicts that the contribution from adjacent and opposite to acylferrocene group ferrocene substituents contribute nearly equally, which makes it difficult to clearly associate the first oxidation process with specific ferrocene substituent. In contrary, a large stabilization of acylferrocene MOs clearly suggestive that the fourth oxidation process in $H_2Fc_3Fc(COR)P$ derivatives **1** and **2** should be centered on substituted ferrocene group. Unlike in the parent H_2TFcP,[139] HOMO is well-separated (~0.22 eV) from the HOMO-1.

Similar to calculations on parent H_2TFcP,[139] TDDFT predicts a large number of predominantly metal-to-ligand charge transfer (MLCT) bands in Q-band region of **1** heavily mixed into the porphyrin-centered π–π* transitions (Figures 22 and 23). In agreement with its electronic structure, the majority of unsubstituted ferrocene-to-porphyrin MLCT transitions were predicted in 700 - 900 nm region, while those that originated from acylferrocene were calculated in ~600 nm region.

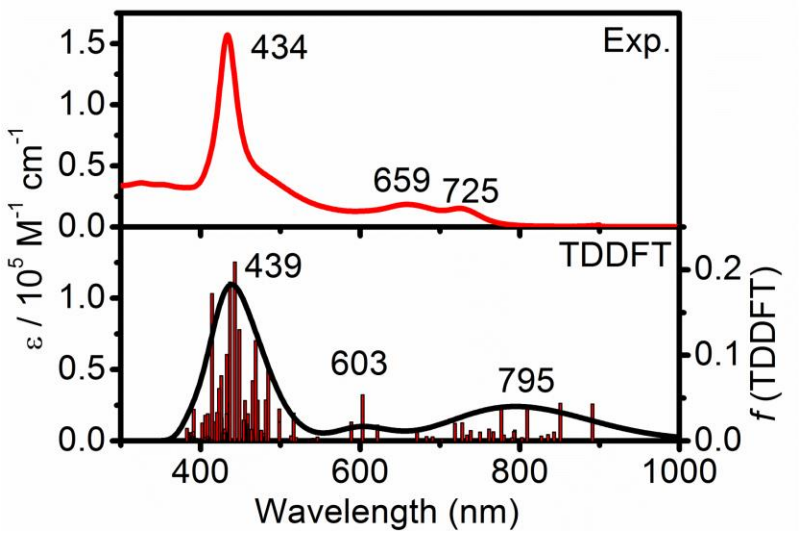

Figure 22. Experimental (top) and TDDFT predicted (bottom) UV-vis spectra of **1** calculated at BP86 DFT level.

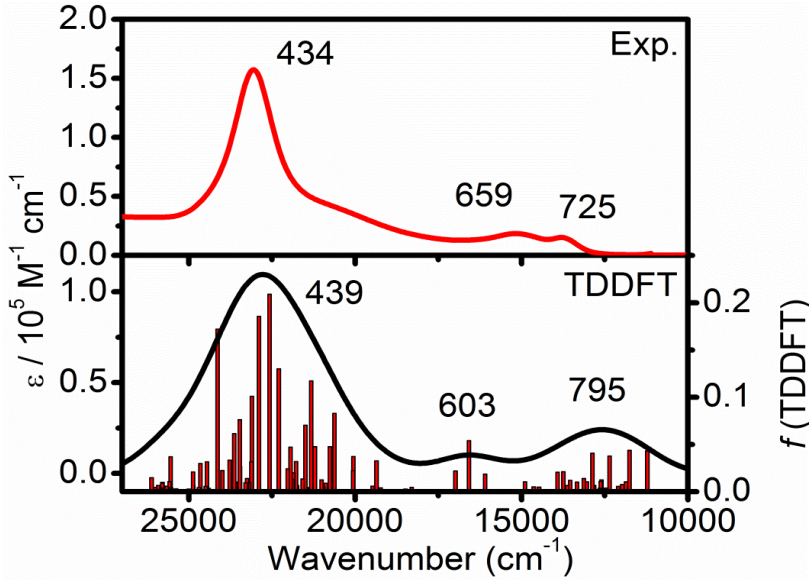

Figure 23. Experimental (top) and TDDFT predicted (bottom) UV-vis spectra of $H_2Fc_3Fc(COCH_3)P$ (**1**) calculated at BP86 DFT level.

Electrolyte-tunable photo-catalytic efficiency of the mixed monolayer

In a previous work we have shown that TFcPs are able to form stable and well-packed self-assembled monolayers.[137] In particular, a mixed SAM of 1-butanethiol and 5-[1'-(6-thioacetylhexanoyl)ferrocenyl]-10,15,20-triferrocenylporphyrin (see Figure 24) exhibited an interesting electrochemical behavior in which a "3+1" oxidation pattern in acetonitrile/TBAP system was detected.

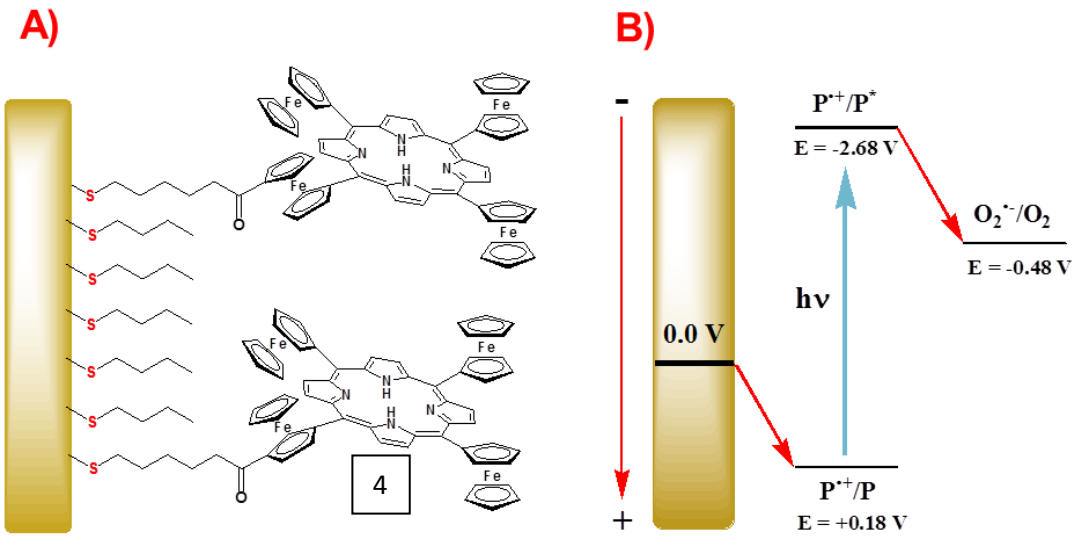

Figure 24. A) Proposed structure of the mixed 5-[1'-(6-thioacetylhexanoyl)]ferrocenyl-10,15,20-triferrocenylporphyirin-butanethiol 1:5. **B)** Scheme of the cathodic photocurrent generation mechanism using dioxygen as the sacrificial electron acceptor.

The same film is able to reduce the atmospheric dioxygen dissolved in water under photo-stimulation in the visible region of the spectrum, using Na_2SO_4 as the supporting electrolyte at 0.0 V applied potential. The reason for this lies in the strong donating character of the porphyrin in the excited state ($E^*_{1/2}$ = -2.68 V *vs* Ag/AgCl) which makes it able to pump electrons into the sacrificial acceptor. The porphyrin is then reduced back to its neutral state by an electron transfer from the gold surface which closes the photoelectrochemical circuit. However, in principle, three electrons are available for O_2 reduction in such a polar environment.

Moreover, as just described in the electrochemical section, mono-functionalized H_2TFcPs undergo four individual single-electron oxidations using a non-coordinating electrolyte in a non-polar solvent. Therefore, a water soluble precursor of TFAB, namely $Li[B(C_6F_5)_4]$,

is supposed to reduce the photo-catalytic activity of the porphyrin, because it is expected to separate the oxidation processes making the second and third process less favorable at applied 0.0 V.

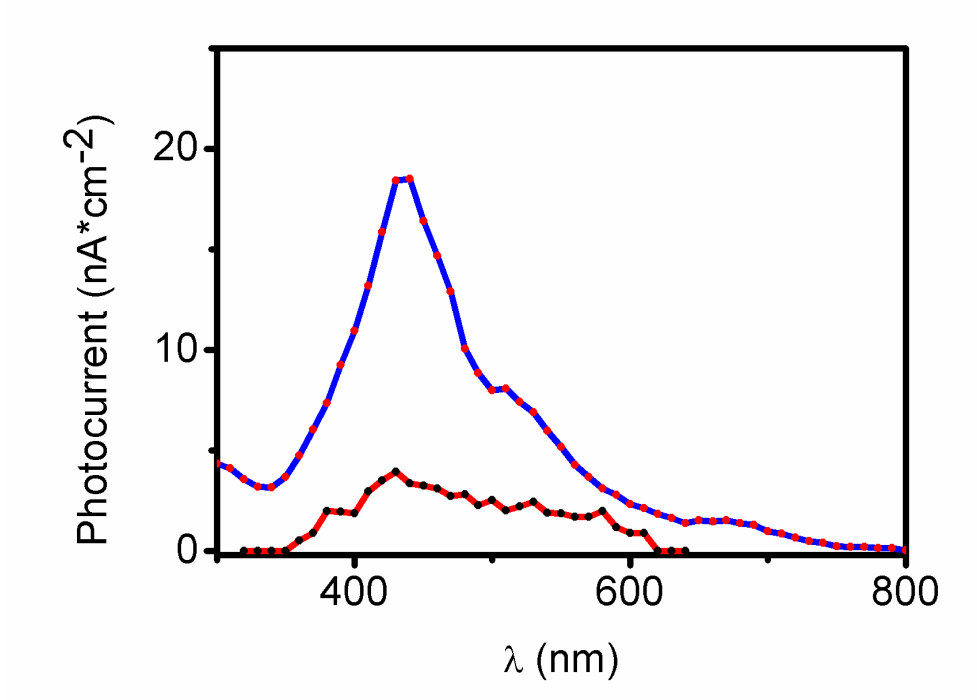

Figure 26. Overlapped action spectra of the mixed SAM obtained in an aqueous solution of Na_2SO_4 0.1 M (blue line with red circles) or in an aqueous solution of $Li[B(C_6F_5)_4]$ 0.05 M. Both photocurrent generation experiments were carried out using O_2 as the sacrificial electron acceptor.

In spite of expectations, the resulting action spectrum (red line in Figure 26) is a noisy, ill-defined plot with a maximum in correspondence of the Soret band, where an 80% loss of intensity was detected with respect to the control experiment carried out using Na_2SO_4 (blue line in Figure 26). Such a remarkable decrease can be explained with a poorer permeability of the bulky tetrakis(pentafluorophenyl)borate anion into the monolayer.

This prevented the association with the redox center, thus increasing the activation energy for the oxidation of the porphyrin.[163] Hence, the photo-catalytic reduction of O_2 was kinetically hindered by the encumbrance of the supporting electrolyte. On the other hand, this simple experiment demonstrated that the photo-catalytic activity of the porphyrin can be easily tuned by the use of different electrolytes, opening the way for new switchable materials.

Electrochemistry of the mixed SAM in aqueous media

In order to confirm the kinetic control over the photo-catalytic activity of the mixed SAM exerted by the electrolytes, CV and DPV experiments were performed using the same solutions employed in photocurrent generation (PG) experiments.

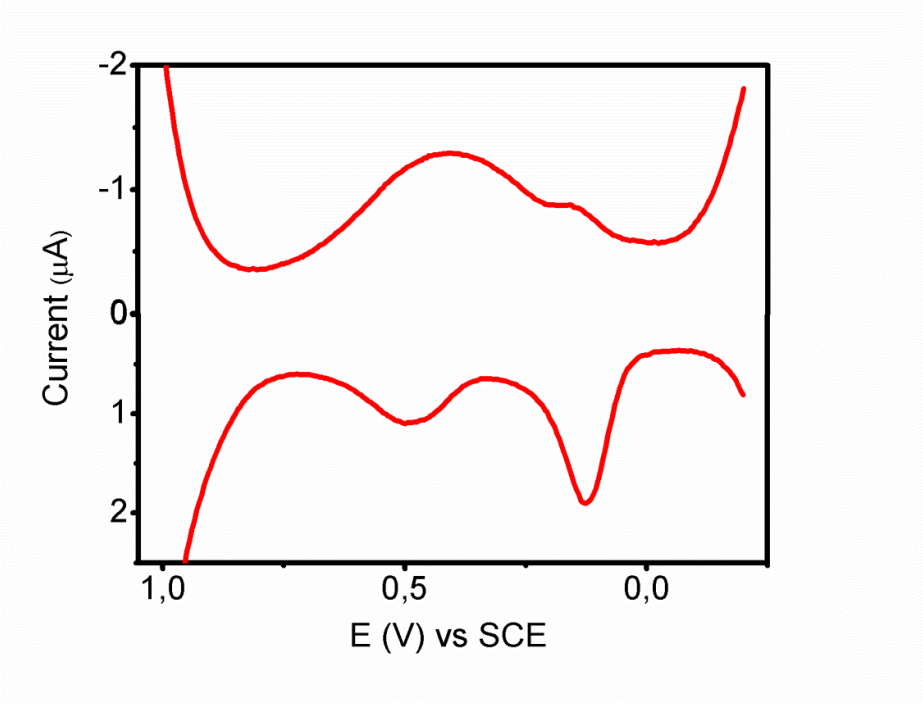

Figure 26. Representative DPV in the oxidative (bottom) and reductive (top) directions of the mixed SAM in an aqueous 0.05 M solution of $Li[B(C_6F_5)_4]$.

In contrast to the above reported well-resolved four individual single electron oxidation processes, the electrochemical profiles of the modified electrodes resemble those reported in acetonitrile/TBAP system,[137] consisting of two redox waves (see the DPV in Figure 26) in which a "3+1" mechanism of electron transfer can be recognized. Moreover, the first process was found to occur at a lower potential using tetrakis(pentafluorophenyl)borate anion, as suggested by the half wave potentials in Table 5. This is reasonable since an organic anion is expected to associate more strongly to a cationic porphyrin than sulphate anions. Although it makes the first process more favorable, $Li[B(C_6F_5)_4]$ is not effective in the resolution of the first three-electrons process and the reduction in the photo-catalytic efficiency cannot be attributed to this effect. Conversely, the kinetic of electron transfer plays a significant role inasmuch as the association with the bulky counterion is too slow to occur during the short lifetime of the excited species. Indeed, CV at different scan rates underlined a quick broadening of the peaks and large values of the overpotential at low scan rates (see Figure 27). Instead, for an ideal electrochemical behavior of adsorbed species, the separation between the peaks ($\Delta E_p = E_{pa} - E_{pc}$) is required to be zero at low scan rates because diffusion does not take place.[164]

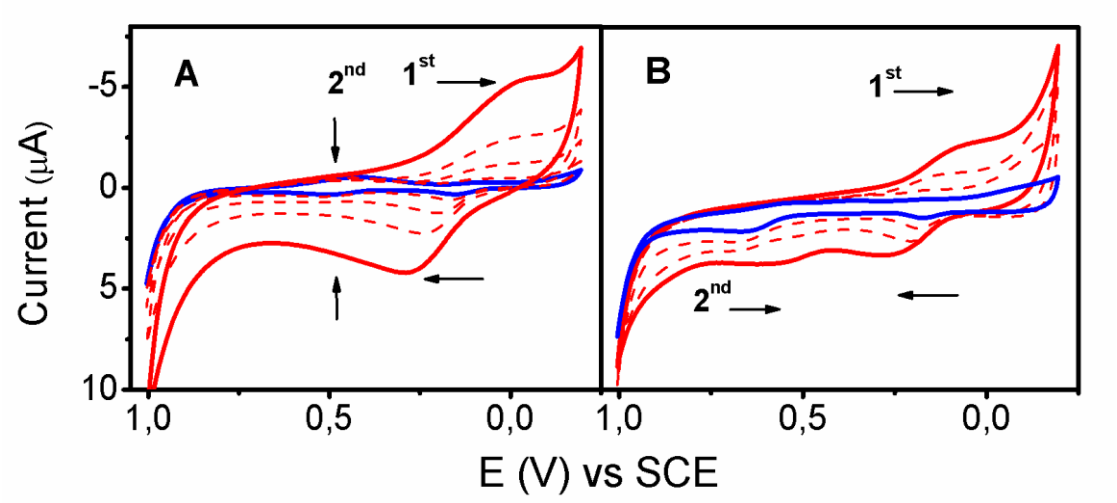

Figure 27. Overlapped CV at different scan rates (5, 10, 25, 50, 100 mV/s) using the mixed SAM as working electrode in a 0.05 M solution of $Li[B(C_6F_5)_4]$ (**A**) and a 0.1 M solution of Na_2SO_4 (**B**) in water.

The large size of $B(C_6F_5)_4^-$ makes the approach and the removal to the redox sites hard, since the monolayer has to reorganize in order to accommodate and release the anions. As a consequence, peaks move in the opposite directions, *i.e.* oxidation and reduction processes get harder as the scan rate increases. In particular, the most hindered site is the substituted ferrocenyl group which lies embedded within the monolayer. As a matter of fact, the second redox wave, attributed to this ferrocenyl group, drops to zero much faster than the first one and is visible only below the scan rate of 25 mV/s (see Figure 15A). A comparison between CV at variable scan rates reveals that peaks move slower with the scan rate when Na_2SO_4 is used as supporting electrolyte (see Figure 26B). Furthermore, the second process is still visible at υ_s > 100 mV/s, a clear indication that both the first and the second process are faster using SO_4^{2-} as a consequence of its better permeability into the monolayer. The rate constants for the electron transfer were calculated through the Laviron method[165] and are reported in Table 5.

Table 5. Electron transfer rates and half wave potentials for the first process of mixed SAM in aqueous solutions of Na_2SO_4 and $Li[B(C_6F_5)_4]$.

	k_{ET} (s^{-1})	$E_{1/2}$ (mV)
Na_2SO_4	$1.6 \cdot 10^{-3}$	180
$Li[B(C_6F_5)_4]$	$2.5 \cdot 10^{-5}$	125

The calculated values are much lower than those reported for other porphyrin-containing SAMs[166,167] probably because of the approximations introduced in the model (see the Experimental section) which are likely to underestimate the value of k_{ET}. However, it should be emphasized that those values refer to the association of a single anion to the *core* of the macrocycle. Instead, regarding to the first process of the TFcP-containing SAM, it requires the simultaneous arrival and accommodation of three anions in a well-packed monolayer. Hence, it should not be surprising that the experimental values are lower than those expected for arylporphyrins.

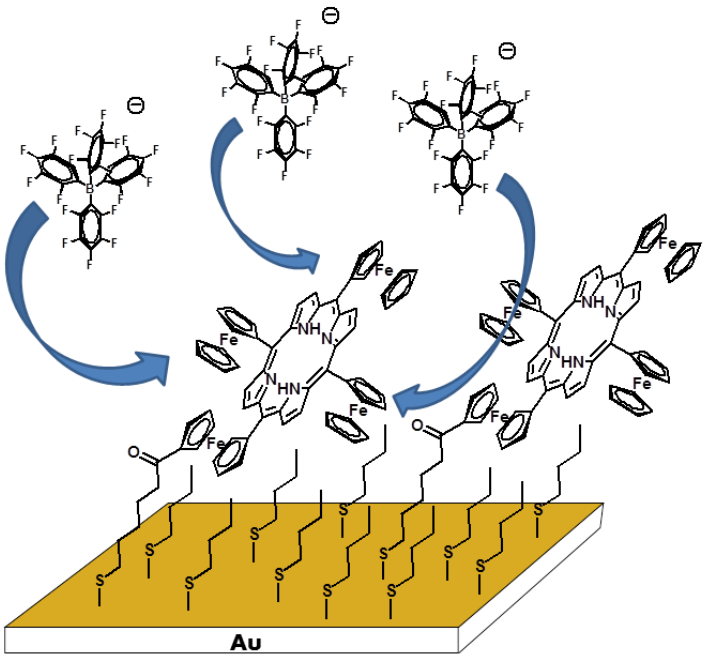

Figure 28. Representation of the simultaneous, slow arrival of three tetrakis(pentafluorophenyl)borate anions required for the occurrence of the first oxidation process.

However, k_{ET} were all obtained under the same assumptions that are not affected by different electrolytes. Therefore, albeit not completely reliable in absolute, these values can be efficiently compared. A significant decrease of two orders of magnitude in the rate of the electron transfer was found switching from Na_2SO_4 to $Li[B(C_6F_5)_4]$ solutions (see Table 5). This difference strongly supports the idea that quenching of the photo-catalytic activity of the porphyrin is kinetically hampered by the exclusion of bulky anions from the monolayer, which prevents the association with the redox site. Under these circumstances, the electron delivery is slower than the excited state lifetime of the porphyrin and reduction of O_2 does not take place.

Conclusions

Three new unsymmetric metal-free tetraferrocenyl containing porphyrins of general formula $H_2Fc_3Fc(COR)P$ have been prepared and characterized by variety of spectroscopic methods. The redox properties of all new compounds were also examined by electrochemical methods, while the nature of mixed-valence species of general formula $[H_2Fc_3Fc(COR)P]^{n+}$ was probed by spectroelectrochemical and chemical oxidation approaches. The electronic structure and nature of the excited states in target compounds were modeled by DFT and TDDFT calculations. It was suggested that the fourth oxidation process is associated with the substituted ferrocenyl group, while it remains ambiguous if the first oxidation process is centered at adjacent or opposite unsubstituted ferrocenyl moiety.

Stable and well-packed monolayers were formed on gold surface and the photoelectrochemical and electrochemical properties of the resulting modified electrodes were evaluated. Interestingly, a cathodic photocurrent was generated at zero applied bias potential using O_2 as the sacrificial electron acceptor. Such a photo-catalytic activity toward dioxygen can be tuned by the supporting electrolyte. Indeed, it was found to be quenched using a bulky anion like tetrakis(pentafluorophenyl)borate, as a consequence of its low ability to penetrate into the monolayer and associate to the oxidized porphyrin. Thus, the electron transfer rate at the gold-monolayer interface is slower than the porphyrin excited state lifetime and reduction of O_2 does not take place. In particular the results of this study offered elucidation for the electron transfer kinetic on TFcP SAM that should be taken into consideration in the development of application of these active molecules. The clarification of the fate of dioxygen and the eventual formation of

partially reduced oxygen species is currently underway.

Experimental section:

Materials: All reactions were performed under dry argon atmosphere with flame-dried glassware. All solvents and reagents were purchased from commercial sources and used without additional purification. Dry toluene was obtained by distillation over sodium, dry DCM was obtained by distillation over calcium hydride prior to experiments, and dry THF was obtained by distillation over Na with benzophenone. Silica gel (60 Å, 63-100 μm) needed for column chromatography was purchased from Dynamic Adsorbents, while basic aluminum oxide (Activity I, 58 Å, 150 mesh) was purchased from Fischer Inc. The tetrabutylammonium tetrakis(pentafluorophenyl)borate (TBAF) was used in anhydrous DCM for electrochemical studies, after preparation according to literature procedures.[15]

Computational Aspects: All computations were performed using Gaussian 09 software running under Windows or UNIX OS.[168] Molecular orbital contributions were compiled from single point calculations using the QMForge program.[169] In all single-point calculations and geometry optimizations, Becke's exchange functional and the Pedrew 86 correlation functional (BP86)[170] was used because as it was shown before, GGA-based exchange-correlation functionals provide good electronic structure description for ferrocene-containing molecules,[172-183] including ferrocenylporphyrins.[139] Use of hybrid B3LYP[184,185] or PBE1PBE[186] exchange-correlation functionals lead to heavy infusion of porphyrin-centered π-electron density into the HOMO region, which was not supported by the experimental data. Wachters' full-electron basis set was used for iron,[187] while for

all other atoms 6-311G(d) basis set[188] was employed. The first 120 states were predicted in TDDFT calculations.

Instrumentation: A Bruker AMX 300 NMR instrument was used to obtain spectra at 300 MHz frequency for protons and 75 MHz for carbons. Each spectrum was referenced to TMS as an internal standard and chemical shifts were recorded in parts per million. All UV-Vis data was obtained on a JASCO-720 spectrophotometer at room temperature. An OLIS DCM 17 CD spectropolarimeter with 1.4 T DeSa magnet was used to obtain all MCD data. Electrochemical measurements were conducted using a CHI-620C electrochemical analyzer utilizing the three-electrode scheme. Either carbon or platinum working, auxiliary and reference electrodes were used in 0.05 M solution of TBAF in DCM with redox potentials corrected using an internal standard (decamethylferrocene) in all cases. Spectroelectrochemical data were collected using a custom-made 0.1 mm cell, a working electrode made of platinum mesh, and a 0.15 M solution of TBAF in DCM. A PalmSense potentiostat was employed in CV and DPV experiments of SAMs. Photocurrent generation experimetns were carried out using a PG-310 potentiostat (HEKA Elektronik, Lambrecht, Germany). The samples were excited by a xenon lamp located in a Fluoromax-2 fluorimeter (Jobin Yvo, France).

Preparation of SAMs: The gold foils were electrochemically polished according to a well-established protocol.[189] SAMs were prepared as previously described,[137] *i. e.* b*y* soaking the gold electrode in a 0.2 mM solution of the porphyrin in dichloromethane containing 5 equivalents of 1-butanethiol for 20 hours. The gold foils were then

thoroughly rinsed with DCM and dried with N_2. Film formation was monitored by cyclic voltammetry using $K_3[Fe(CN)_6]$ as redox probe. SAMs resulted well-packed and porphyrin density (Γ) was estimated in (8±2) x 10^{-11} mol/cm^2 in excellent agreement with our previously reported work.[137]

Photocurrent generation (PG) experiments: Photocurrent experiments were carried out either in a 0.1 M solution of Na_2SO_4 or in a 0.05 M solution of $Li[B(C_6F_5)_4]$ in double-distilled water using the atmospheric dioxygen dissolved in water as the electron acceptor. A functionalized gold foil was used as the working electrode, whereas an Ag/AgCl and a Pt wire were employed as reference and counter electrodes, respectively. Measurements were undertaken alternating phases of 45 seconds of light with 30 seconds of darkness at zero applied bias potential. The whole visible spectrum was investigated and data were collected every 10 nm. A step graph of the photocurrent intensity as a function of time was obtained in which every step is taken at different wavelengths. The plot of the height of each step as a function of the wavelength affords the action spectrum of the desired compound. The height of a step is calculated as the difference between the average of the intensities on the step and the average of the intensities of the adjacent phases of darkness. Each action spectrum was normalized by the immersed area of the gold electrode.

Electrochemistry of SAMs: CV and DPV experiments were carried out using a three-electrode scheme with SCE as the reference electrode and a platinum wire as the counter electrode. The same modified gold surfaces employed in PG experiments were used as

working electrodes. A 0.1 M solution of Na_2SO_4 or a 0.05 M solution of $Li[B(C_6F_5)_4]$ in double-distilled water were employed as the solvent-electrolyte couples. Γ was calculated by the integral of the peak of the first oxidation process as previously described.[137] k_{ET} values were determined performing subsequent CV experiments at variable scan rates through the Laviron method (see next section).

Because of the complete insolubility of $FcH^+PF_6^-$ in aqueous $Li[B(C_6F_5)_4]$ solution, potentials were not referred to the redox couple FcH^+/FcH. However, in the case of Na_2SO_4/H_2O, potentials could be eventually adjusted by -0,180 V.

Data analysis: The Laviron method[165] was employed to estimate the electron transfer rate constant of the first redox process, whereas the second process was too slow for k_{ET} determination with this approach. Such a method was applied under the assumption that the first process involves the simultaneous removal of three electrons, while redox centers were treated as non-interacting. Also, since CV peaks were too broad at scan rates higher than 100 mV/s, a linear region in the graph of the overpotential ($\eta = E_p - E_{1/2}$) *vs* $\log(\upsilon_s)$ could not be reached, so that the transfer coefficient (α) could not be experimentally determined. Therefore, k_{ET} were estimated assuming the ideal situation in which $\alpha = 0.5$, *i.e.* symmetric energy barriers for the redox reactions were considered.[164] Under these simplifications, the electron transfer rate constant was determined as the intercept of the straight line obtained by the plot of ΔE_p *vs* $\log(\upsilon_s)$ according to the equation:[190]

$$\Delta E_p = \left[\frac{2.3RT}{\alpha(1-\alpha)nF}\right]\left\{\alpha log(1-\alpha) + (1-\alpha)log\alpha + log\frac{nF}{RT} - logk_{ET} + log\nu_s\right\}$$

where n is number of electrons transferred during the process (n=3 for the first process of the mixed SAM), $\Delta E_p = E_a - E_c$, T is the temperature in Kelvin, R is the ideal gas constant in J/(K·mol), F is the Faraday constant in C/mol and υ_s is the scan rate in V/s.

Syntheses

Synthesis of 1'-(6-bromohexanoyl)ferrocencarboxaldehyde, 5-[1'-(6-bromohexanoyl)ferrocenyl]-10,15,20-triferrocenylporphyrin and its thioacetyl derivative were previously described.[14]

1'-acetylferrocencarboxaldehyde: Aluminium chloride (0.37 g, 1.2 equivalents) was slowly added in portions to a solution of FcCHO (0.5 g, 2.34 mmol) in 15 ml of anhydrous DCM under a nitrogen stream. In another flask, 2 equivalents of freshly distilled acetyl chloride (4.68 mmol, 334 μl) were dissolved in 15 ml of anhydrous CH_2Cl_2 under a nitrogen stream. To this solution, 2.4 equivalents of $AlCl_3$ (0.75 g) were slowly added. The solution containing the acetyl chloride was then added dropwise to that containing FcCHO in 20 minutes at 0^oC. After this period, the reaction was carried out at room temperature and under a nitrogen atmosphere for 3 hours. The reaction was then quenched by the addition of about 100 g of ice and 5 g of NH_4Cl, and extracted with methylene chloride. The crude product was chromatographed on silica gel using an hexane-AcOEt (3:2 v/v) mixture as the eluent. The solvent was removed under reduced

pressure and the product was dissolved in diethyl ether and filtered. The solvent was evaporated again and the red solid was recrystallized by pentane to obtain 455 mg of the pure product (76% yield).

^{1}HNMR ($CDCl_3$): δ (ppm) 9.96 (s, 1H, CHO), 4.87 (t, 2H, CH α), 4.83 (t, 2H, CH α'), 4.63 (t, 2H, CH β'), 4.59 (t, 2H, CH β), 2.39 (s, 3H, CH_3).
MS (E.I.): *m/z* 256 (M^+)

5-[(1'-acetyl)ferrocenyl]-10,15,20-triferrocenylporphyrin: 200 mg of 1'-acetylferrocencarboxaldehyde (0.78 mmol) and 835 mg of FcCHO (3.89 mmol) were mixed in 125 ml of dry methylene chloride together with 325 μl of pyrrole (4.67 mmol). To this solution, 58 μl of $BF_3{\cdot}Et_2O$ (10%) were slowly added. All additions were performed under a nitrogen stream. The reaction mixture was stirred for 20 hours at room temperature, in the dark and in a nitrogen atmosphere. After this period, 480 mg of chloranil were added and the mixture was stirred at room temperature for 30 minutes. The solution was concentrated and filtered over neutral Al_2O_3 deactivated with 5% of water using chloroform as eluent. The crude product was then chromatographed over Al_2O_3 deactivated with 10% of water, using the mixture hexane-$CHCl_3$ 3:2 v/v as eluent. From the first fraction H_2TFcP was collected in 15% yield. The second compound eluted was the unreacted FcCHO, while the third one was the target mono-substituted porphyrin. The solution containing the porphyrin was evaporated under reduced pressure and the green solid was dissolved in the minimum volume of toluene and precipitated with hexane. The precipitate was then filtered to obtain 63 mg of a dark green powder (7% yield).

^{1}HNMR ($CDCl_3$): δ (ppm) 9.66 (m, 6H, H β-pyrrolic), 9.67 (d, 2H, H β-pyrrolic), 9.54 (d, 2H, H β-pyrrolic), 5.39 (t, 2H, CH α'), 5.36 (t, 8H, CH α), 4.80 (t, 8H, CH β), 4.78 (t, 2H, CH β' 4.02 (s, 5H, Cp *trans*) 4.00 (s, 10 H, Cp *cis*), 3.27 (t, 2H, CH_2Br), 2.54 (t, 2H, CH_2CO), -0.5 (s, 2H, internal NH).

Bibliography

[1]Furuta, H., Asano, T., Ogawa, T. "N-Confused Porphyrin": A New Isomer of Tetraphenylporphyrin. *J. Am. Chem. Soc.* **1994,** *116,* 767-768.

[2]Chmielewski, P. J., Latos-Grażyński, L., Rachlewicz, K., Glowiak, T. Tetra-p-tolylporphyrin with an Inverted Pyrrole Ring: A novel Isomer of Porphyrin. *Angew. Chem., Int. Ed. Engl.* **1994,** *33,* 779-781.

[3]Latos-Grażyński, L. "Core Modified Heteroanalogues of Porphyrins and Metalloporphyrins" In *The Porphyrin Handbook*; Kadish, K. M., Smith, K. M. and Guilard, R., Eds.; Academic Press: New York, **2000**; pp 361− 416.

[4]Furuta, H., Maeda, H. and Osuka, A. Confusion, Inversion, and Creation: A new Spring from Porphyin Chemistry. *Chem. Commun*. **2002**, 1795– 1804

[5]Harvey, J. D. and Ziegler, C. J. Developments in the Metal Chemistry of N-Confused Porphyrin. *Coord. Chem. Rev*. **2003**, *247*, 1– 19

[6]Chmielewski, P. J. and Latos-Grażyński, L. Core Modified Porphyrins—A Macrocyclic Platform for Organometallic Chemistry. *Coord. Chem. Rev*. **2005**, *249*, 2510– 2533

[7]Maeda, H. and Furuta, H. A Dozen Years of N-Confusion: From Synthesis to Supramolecular Chemistry. *Pure Appl. Chem*. **2006**, *78*, 29– 44

[8]Harvey, J. D. and Ziegler, C. J. The Metal Complexes of N-Confused Porphyrin as Heme Model Compounds. *J. Inorg. Biochem*. **2006**, *100*, 869– 880.

[9]Furuta, H., Ishizuka, T., Osuka, A., Dejima, H., Nakagawa, H., Ishikawa, Y. NH Tautomerism of N-Confused Porphyrin. *J. Am. Chem. Soc.* **2001.** *123,* 6207-6208.

[10]Alemán, E. A.; Rajesh, C. S.; Ziegler, C. S.; Modarelli, D. A. Ultrafast Spectroscopy of Free-Base Nconfused Tetraphenylporphyrins. *J. Phys. Chem*. **2006**, *110*, 8605–8612.

[11]Vyas, S.; Hadad, C.M.; Modarelli, D. A. A Computational Study of the Ground and Excited State Structure and Absorption Spectra of Free-Base N-Confused Porphine and Free-Base N-Confused Tetraphenylporphyrin. *J. Phys. Chem. A*, **2008**, *112* (29), 6533–6549.

[12]Shaw, J. L.;Garrison, S. A.; Aleman, E. A.; Ziegler, C. J.; Modarelli, D. A. Synthesis and Spectroscopy of a Series of Substituted N-Confused Tetraphenylporphyrin. *J. Org. Chem*. **2004**, *69*, 7423.

[13]Ghosh, A. N-Confused Porphyins and Siglet Carbenes: Is there a Connection? *Angew. Chem., Int. Ed. Engl.* **1995,** *34*, 1028-1030.

[14]Ghosh, A.; Wondimagegn, T.; Nilsen, H. Molecular Structures, Tautomerism, and Carbon Nucleophilicity of Free-Base Inverted Porphyrins and Carbapophyrins: A Density Function Theoretical Study. *J. Phys. Chem. B.* **1998**, *102*, 10459-10467.

[15]Zandler, M. E.; D'Souza, F. Electronic and Structural Properties of the Metalloporphyrin Structural Isomers: Semiempirical AM1 and PM3 calculations. *J. Mol. Struct.: THEOCHEM* **1997**, *401*, 301-314.

[16]Szterenberg, L.; Latos-Grażyński, L. Structre and Stability of 2-Aza-21-carbaporphyin Tautomers Prearranged for Coordination. *Inorg. Chem*. **1997**, *36*, 6287-6291.

[17]Kobayashi, N.; Nakai, K. Applications of Magnetic Circular Dichroism Spectroscopy to Porphyrins and Phthalocyanines. *Chem. Commun*. **2007**, 4077-4092.

[18]Mack, J.; Stillman, M. J.; Kobayashi, N. Application of MCD Spectrosopy to Porphyrinoids. *Coord. Chem. Rev*. **2007**, *251*, 429-453.

[19]Nemykin, V. N.; Rohde, G. T.; Barrett, C. D.; Hadt, R. G.; Sabin, J. R.; Reina, G.; Galloni, P.; Floris, B. Long-Range Electronic Communication in Free-Base *meso*-Poly(Ferrocenyl)-Containing Porphyrins. *Inorg. Chem*. **2010**, *49*, 7497-7509.
[20]Nemykin, V. N.; Rohde, G. T.; Barrett, C. D.; Hadt, R. G.; Bizzarri, C.; Galloni, P.; Floris, B.; Nowik, I.; Herber, R. H.; Marrani, A. G.; Zanoni, R.; Loim, N. M. Electron-Transfer Processes in Metal-Free Tetraferrocenylporphyrin. Understanding Internal Interactions to Access Mixed-Valence States Potentially Useful for Quantum Cellular Automata. *J. Am. Chem*. *Soc*. **2009**, *131*, 14969–14978.
[21]Nemykin, V. N.; Galloni, P.; Floris, B.; Barrett, C. D.; Hadt, R. G.; Subbotin, R. I.; Marrani, A. G.; Zanoni, R.; Loim, N. M. Metal-Free and Transition-Metal Tetraferrocenylporphyrins Part 1: Synthesis, Characterization, Electronic Structure, and Conformational Flexibility of Neutral Compounds. *Dalton Trans*. **2008**, 4233–4246.
[22]Nemykin, V. N.; Kobayashi, N. A Tetraazaporphyrin with an Intense, Broad Near-IR Band. *Chem. Commun*. **2001**, 165–166.
[23]Gorski, A.; Vogel, E.; Sessler, J. L.; Waluk, J. Magnetic Circular Dichroism of Octaethylcorrphycene and Its Doubly Protonated and Deprotonated Forms. *J. Phys. Chem. A* **2002**, *106*, 8139.
[24]Lukyanets, E. A.; Nemykin, V. N. The Key Role of Peripheral Substituents in the Chemistry of Phthalocyanines and Their Analogs. *J. Porphyrins Phthalocyanines*. **2010**, *14*, 1–40.
[25]Mack, J.; Bunya, M.; Lansky, D.; Goldberg, D. P.; Kobayashi, N. The MCD Spectroscopy of Porphyrins and Phthalocyanines. *Heterocycles*. **2008**, *76*, 1369-1380.
[26]Stillman, M.; Mack, J.; Kobayashi, N. Theoretical Aspects of the Spectroscopy of Porphyrins and Phthalocyanines. *J. Porph. Phthalocyanines*. **2002**, *6*, 296-300.
[27]Nakamura, Y.; Aratani, N.; Shinokubo, H.; Takagi, A.; Kawai, T.; Matsumoto, T.; Yoon, Z. S.; Kim, D. Y.; Ahn, T. K.; Kim, D.; Kobayashi, N. A Directly Fused Tetrameric Porphyrin Sheet and Its Anomalous Electonic Properties that Arise from the Planar Cyclooctatetraene. *J. Am. Chem. Soc*. **2006**, *128*, 4119-4127.
[28]Kuzuhara, D.; Mack, J.; Yamada, H.; Okujima, T.; Ono, N.; Kobayashi, N. Synthesis, Structures, and Optical and Electrochemical Properties of Benzoporphycenes. *Chem. Eur. J*. **2009**, *15*, 10060-10069.
[29]Xue, Z.-L.; Shen, Z.; Mack, J.; Kuzuhara, D.; Yamada, H.; Okujima, T.; Ono, N.; You, X.-Z.; Kobayashi, N. A Facile One-Pot Synthesis of *meso*-Aryl-Substituted [14]Triphyrin(2.1.1). *J. Am. Chem. Soc*. **2008**, *130*, 16478-16479.
[30]Sripothongnak, S.; Ziegler, C. J.; Dahlby, M. R.; Nemykin, V. N. Controllable and Reversible Inversion of the Electronic Structure in Nickel N-Confused Porphyrin. *Inorg. Chem*. **2011**, *50*, 6902-6909.
[31]Gouterman, M. J. Optical Spectra and Electronic Structure of porphyrins and Related Rings. In *The Porphyrins*; Dolphin, D., Ed.; Academic Press: New York, 1978; Vol. *III,* pp 1-165.
[32]Seybold, P. G.; Gouterman, M. Porphyrins: XIII: Fluorescence Spectra and Quantum Yields. *J. Mol. Spectrosc*. **1969**, *31*, 1–13.
[33]Gouterman, M. Spectra of Porphrins. *J. Mol. Spectrosc*. **1961**, *6*, 138–163.
[34]Waluk, J.; Michl, J. Perimeter Model and Magnetic Circular Dichroism of Porphyrin Analouges. *J. Org. Chem*. **1991**, *56*, 2729-2743.

[35]Michl, J. Magnetic Circular Dichrosim of Cyclic π-Electron Systems. 1. Algebraic Solution of the Perimeter Model for the B Terms of Systems with a (4N + 2)-Electron [n]Annulene Perimeter. *J. Am. Chem. Soc*. **1978**, *100*, 6801-6811.
[36]Michl, J. Magnetic Circular Dichrosim of Cyclic π-Electron Systems. 2. Algebraic Solution of the Perimeter Model for the B Terms of Systems with a (4N + 2)-Electron [n]Annulene Perimeter. *J. Am. Chem. Soc*. **1978**, *100*, 6812-6818.
[37]Geier, G. R., III; Haynes, D. M.; Lindsey, J. S. An Efficient One-Flask Synthesis of N-Confused Tetraphenylporphyrin. *Org. Lett*. **1999**, *1*, 1455−1458.
[38]Qu, W.; Ding, T.; Cetin, A.; Harvey, J. D.; Taschner, M. J.; Ziegler, C. J. Facile Peripheral Modification of N-Confused Porphyrin. *J. Org. Chem*. **2006**, *71*, 811-814.
[39]Firsh, M.J.; Trucks, G. W.; Schlegel, H. B.; Scuseria, G. E.; Robb, M. A.; Cheeseman, J. R.; Scalmani, G.; Barone, V.; Mennucci, B.; Petersson, G. A.; *Gaussian 09*, Revision A. 1; Gaussian, Inc.: Wallingford, CT, 2009.
[40]Becke, A. D. Density-Functional Exchange-Energy Approximation with Correct Asymptotic Behavior. *Phys. Rev. A*. **1988**, *38*, 3098-3100.
[41]Perdew, J. Density-Functional Approximation for the Correlation Energy of the Inhomogeneous Electron Gas. *P. Phys. Rev. B*. **1986**, *33*, 8822-8824.
[42]McLean, A.D.; Chandler, G.S. Contracted Gaussian Basis Sets for Molecular Calculations. I. Second Row Atoms, Z = 11-18. *J. Phys. Chem*. **1980**, 72. 5639-5640.
[43]Tomasi, J.; Mennucci, B.; Cammi, R. Quantum Mechanical Continuum Solvation Models. *Chem. Rev.* **2005**, *105*, 2999-3093.
[44]Chmielewski, P. J.; Latos-Grażyński, L. N-Methyltetraphenyl-porphyrin with an Inverted N-Methylpyrrole Ring: The First Isomer of N-MethyltetraphenylPorphyrin. *J.Chem.Soc., Perkin Trans.2* **1995**, 503-509.
[45]Ikawa, Y.; Moriyama, S.; Harada, H.; Furuta. H. Acid-Base Properties and DNA-Binding of Water Soluble N-Confused Porphyrins with cationic Side-Arms. *Org. Biomol. Chem*., **2008**, *6*, 4157-4166.
[46]Belair, J. P., Ziegler, C. S., Rajesh, C. S., Modarelli, D. A. Photophysical Characterization of Free-Base N-Confused Tetraphenylporphyrins. *J. Phys Chem. A* **22002,** *160*, 6445-6451.
[47]Nemykin, V.N., Sabin, J.R. Profiling Energetics and Spectroscopic Signatures in Prototropic Tautomers of Asymmetric Phthalocyanine Analogues. *J Phys Chem A*. **2012**, *116*, 7364-7371.
[47]Toganoh, M., Yamamoto, T., Hihara, T., Akimaru H., Furuta H. Regulation of NH-tautomerism in N-confused porphyrin by *N*-alkylation. *Org. Biomol. Chem.* **2012**, *10*, 4367-4374.
[48]Sripothongnak, S., Ziegler, C. J., Dahlby, M., R., Nemykin, V., N. Controllable and Reversible Inversion of the Electronic Structure in Nickel *N*-Confused Porphyrin: A Case When MCD Matters. *Inorg. Chem.* **2011**. *50*. 6902-6909.
[49]A. D. Becke, *Phys. Rev. A.* **1988**. *38*, 3098-3100
[50]C. Lee, W. Yang, and R. G. Parr, *Phys. Rev. B.* **1988**. *37*, 785-789
[52]Wu, Y.; Zhu, W. *Chem. Soc. Rev.* **2013**, *42*, 2039-2058.
[53]Balasingam, S. K.; Lee, M.; Kang, M. G.; Jun, Y. *Chem. Commun.* **2013**, *49*, 1471-1487.
[54]Li, L.-L.; Diau, E. W.-G. *Chem. Soc. Rev.* **2013**, *42*, 291-304.
[55]Gratzel, M. *Acc. Chem. Res.* **2009**, *42*, 1788-1798.

[56]Garcia-Iglesias, M.; Cid, J.-J.; Yum, J.-H.; Forneli, A.; Vazquez, P.; Nazeeruddin, M. K.; Palomares, E.; Gratzel, M.; Torres, T. *Energy Environ. Sci.* **2011**, *4*, 189-194.
[57]Hagfeldt, A.; Gratzel, M.; Nogueria, A. F.; Furtado, L. F. O.; Formiga, A. L. B.; Nakamura, M.; Araki, K.; Toma, H. E.; Panigrahi, S.; Pal, T. *Chemtracts* **2004**, *17*, 175-182.
[58]Chen, X.; Li, C.; Graetzel, M.; Kostecki, R.; Mao, S. S. *Chem. Soc. Rev.* **2012**, *41*, 7909-7937.
[59]Nazeeruddin, M. K.; Baranoff, E.; Graetzel, M. *Solar Energy* **2011**, *85*, 1172-1178.
[60]Lee, M. M.; Teuscher, J.; Miyasaka, T.; Murakami, T. N.; Snaith, H. J. *Science* **2012**, *338*, 643-647.
[61]Crabtree, R. H. *Organometallics* **2011**, *30*, 17-19.
[62]Jacko, A. C.; McKenzie, Ross H.; Powell, B. J. *J. Mater. Chem.* **2010**, *20*, 10301-10307.
[63]Wong, W.-Y.; Ho, C.-L. *Acc. Chem. Res.* **2010**, *43*, 1246-1256.
[64]Kaim, W.; Sarkar, B. *Coord. Chem. Rev.* **2007**, *251***,** 584-594.
[65]Fabre, B. *Acc. Chem. Res.*, **2010**, *43*, 1509-1578.
[66]*Ferrocenes: Ligands, Materials and Biomolecules*, Stepnicka P. (Ed.), John Wiley & Sons, Ltd., Chichester, England, 2008; 655 pp.
[67]Nemykin, V. N.; Kobayashi, N. *Chem. Commun*. **2001**, 165-166;
[68]Lukyanets, E. A.; Nemykin, V. N. *J. Porphyrins Phthalocyanines*, **2010**, *14*, 1-40.
[69]Sun, L.; Wang, S.; Tian, H. *Chem. Lett.* **2007**, *36*, 250-251.
[70]Jin, Z.; Nolan, K.; McArthur, C. R.; Lever, A. B. P.; Leznoff, C. C.; *J. Organomet. Chem*. **1994**, *468*, 205-212;
[71]Poon, K.-W.; Yan, Y.; Li, X. Y.; Ng, D. K. P. *Organometallics*, **1999,** *18*, 3528-3533;
[72]Nemykin, V. N.; Lukyanets, E. A. *ARKIVOC*, **2010**, (i), 136-208;
[73]An, M.; Kim, S.; Hong, J.-D. *Bull. Korean Chem. Soc.* **2010**, *31*, 3272-3278;
[74]Gonzalez-Cabello, A.; Claessens, C. G.; Martin-Fuch, G.; Ledoux-Rack, I.; Vazquez, P.; Zyss, J.; Agullo-Lopez, F.; Torres, T. *Synthetic Metals* **2003**, *137*, 1487-1488;
[75]Omeroglu, I.; Arslan, T.; Biyiklioglu, Z.; Tosun, G. *J. Organomet. Chem.* **2014**, *749*, 261-265.
[76]Nemykin, V. N.; Purchel, A. A.; Spaeth, A. D.; Barybin, M. V. *Inorg. Chem.* **2013**, *52*, 11004-11012.
[77]Lau, J. T. F.; Jiang, X.-J.; Ng, D. K. P.; Lo, P.-C. *Chem. Commun.* **2013**, *49*, 4274-4276.
[78]Salan, U.; Altindal, A.; Bulut, M.; Bekaroglu, O. *J. Porphyrins Phthalocyanines* **2006**, *10*, 1263-1270.
[79]Pomarico, G.; Vecchi, A.; Mandoj, F.; Bortolini, O.; Cicero, D. O.; Galloni, P.; Paolesse, R. *Chem. Commun.* **2014**, *50*, 4076-4078.
[80]Gryko, D. T.; Piechowska, J.; Jaworski, J. S.; Galezowski, M.; Tasior, M.; Cembor, M.; Butenschoen, H. *New J. Chem.* **2007**, *31*, 1613-1619.
[81]Su, M.; Li, Q.; Wang, Y.; Chen, S.; Zhao, H.; Bian, Z. *Chin. J. Org. Chem.* **2013**, *33*, 815-819.
[82]Loim, N. M.; Abramova, N. V.; Sokolov, V. I. *Mendeleev Commun.* **1996**, 46-47.
[83]Burrell, A. K.; Campbell, W. M.; Jameson G. B.; Officer, D. L.; Boyd, P. D. W.; Zhao, Z.; Cocks, P. A.; Gordon, K. C. *Chem. Commun.* **1999**, 637-638.

[84]Narayanan, S.J.; Venkatraman, S.; Dey, S. R.; Sridevi, B.; Anand, V. R. G.; Chandrashekar, T. K. *Synlett* **2000**, 1834-1836.
[85]Rhee, S. W.; Na, Y. H.; Do, Y.; Kim, J. *Inorg. Chim. Acta* **2000**, *309*, 49-56.
[86]Shoji, O.; Okada, S.; Satake, A.; Kobuke Y. *J. Am. Chem. Soc.* **2005**, *127*, 2201-2210.
[87]Shoji, O.; Tanaka, H.; Kawai, T.; Kobuke, Y. *J. Am. Chem. Soc.* **2005**, *127*, 8598-8599.
[88]Dammer, S. J.; Solntsev, P. V.; Sabin, J. R.; Nemykin, V. N. *Inorg. Chem.* **2013**, *52*, 9496-9510.
[89]Kubo, M.; Mori, Y.; Otani, M.; Murakami, M.; Ishibashi, Y.; Yasuda, M.; Hosomizu, K.; Miyasaka, H.; Imahori, H.; Nakashima, S. *J. Phys. Chem. A* **2007**, *111*, 5136-5143.
[90]Nemykin, V. N.; Barrett, C. D.; Hadt, R. G.; Subbotin, R. I.; Maximov, A. Y.; Polshin, E. V.; Koposov, A. Y. *Dalton Trans.* **2007**, 3378-3389.
[91]Rochford, J.; Rooney, A. D.; Pryce Mary, T. *Inorg. Chem.* **2007**, *46*, 7247-7249.
[92]Nemykin, V. N.; Galloni, P.; Floris, B.; Barrett, C. D.; Hadt, R. G.; Subbotin, R. I.; Marrani, A. G.; Zanoni, R.; Loim, N. M. *Dalton Trans.* **2008**, 4233-4246.
[93]Nemykin, V. N.; Rohde, G. T.; Barrett, C. D.; Hadt, R. G.; Bizzarri, C.; Galloni, P.; Floris, B.; Nowik, I.; Herber, R. H.; Marrani, A. G.; Zanoni, R.; Loim, N. M. *J. Am. Chem. Soc.* **2009**, *131*, 14969-14978.
[94]Galloni, P.; Floris, B.; de Cola, L.; Cecchetto, E.; Williams, R. M. *J. Phys. Chem. C* **2007**, *111*, 1517-1523.
[95]Nemykin Victor, N.; Rohde Gregory, T.; Barrett Christopher, D.; Hadt Ryan, G.; Sabin Jared, R.; Reina, G.; Galloni, P.; Floris, B. *Inorg. Chem.*, **2010**, *49*, 7497-7509.
[96]Rohde, G. T.; Sabin, J. R.; Barrett, C. D.; Nemykin, V. N. *New J. Chem.*, **2011**, *35*, 1440-1448;
[97]Solntsev, P. V.; Neisen, B. D.; Sabin, J. R.; Gerasimchuk, N. N.; Nemykin, V. N. *J. Porphyrins Phthalocyanines*, **2011**, *15*, 612-621.
[98]Sharma, R.; Gautam, P.; Mobin, S. M.; Misra, R. *Dalton Trans.* **2013**, *42*, 5539-5545;
[99]Pareek, Y.; Ravikanth, M. *J. Organomet. Chem.* **2013**, *724*, 67-74;
[100]Samanta, S.; Mittra, K.; Sengupta, K.; Chatterjee, S.; Dey, A. *Inorg. Chem.* **2013**, *52*, 1443-1453;
[101]Devillers, C. H.; Milet, A.; Moutet, J.-C.; Pecaut, J.; Royal, G.; Saint-Aman, E.; Bucher, C. *Dalton Trans.* **2013**, *42*, 1196-1209;
[102]Osipova, E. Yu.; Rodionov, A. N.; Simenel, A. A.; Belousov, Y. A.; Nikitin, O. M.; Kachala, V. V. *J. Porphyrins Phthalocyanines* **2012**, *16*, 1225-1232;
[103]Nemykin, V. N.; Chen, P.; Solntsev, P. V.; Purchel, A. A.; Kadish, K. M. *J. Porphyrins Phthalocyanines* **2012**, *16*, 793-801;
[104]Bakar, M. A.; Sergeeva, N. N.; Juillard, T.; Senge, M. O. *Organometallics* **2011**, *30*, 3225-3228;
[105]Lyons, D. M.; Mohanraj, J.; Accorsi, G.; Armaroli, N.; Boyd, P. D. W. *New J. Chem.* **2011**, *35*, 632-639;
[106]Subbaiyan, N. K.; Wijesinghe, C. A.; D'Souza, F. *J. Am. Chem. Soc.* **2009**, *131*, 14646-14647.
[107]Burrell, A. K.; Campbell, W.; Officer, D. L. *Tetrahedron Lett.* **1997**, *38*, 1249-1252;
[108]Burrell, A. K.; Campbell, W. M.; Officer, D. L.; Scott, S. M.; Gordon, K. C.; McDonald, M. R. *J. Chem. Soc., Dalton Trans.* **1999**, 3349-3354;
[109]Jiao, L.; Courtney, B. H.; Fronczek, F. R.; Smith, K. M. *Tetrahedron Lett.* **2006**, *47*, 501-504;

[110]Wang, H. J.H.; Jaquinod, L.; Olmstead, M. M.; Vicente, M. G. H.; Kadish, K. M.; Ou, Z.; Smith, K. M. *Inorg. Chem.* **2007**, *46*, 2898-2913;
[111]Gryko, D. T.; Zhao, F.; Yasseri, A. A.; Roth, K. M.; Bocian, D. F.; Kuhr, W. G.; Lindsey, J. S. *J. Org. Chem.* **2000**, *65*, 7356-7362;
[112]Schmidt, E. S.; Calderwood, T. S.; Bruice, T. C. *Inorg. Chem.* **1986**, *25*, 3718-3720;
[113]Cheng, K.-L.; Li, H.-W.; Ng, D. K. P. *J. Organomet. Chem.* **2004**, *689*, 1593-1598;
[114]Giasson, R.; Lee, E. J.; Zbao, X.; Wrighton, M. S. *J. Phys. Chem.* **1993**, *97*, 2596-2601;
[115]Muraoka, T.; Kinbara, K.; Aida, T. *Nature* **2006**, *440*, 512-515.
[116]Maiya, G. B.; Barbe, J. M.; Kadish, K. M. *Inorg. Chem.* **1989**, *28*, 2524-2527.
[117]Solntsev, P. V.; Sabin, J. R.; Dammer, S. J.; Gerasimchuk, N. N.; Nemykin, V. N. *Chem. Commun.*, **2010**, *46*, 6581-6583;
[118]Kadish, K. M.; Xu, Q. Y.; Barbe, J. M. *Inorg. Chem*. **1987**, 26, 2565-2566;
[119]Xu, Q. Y.; Barbe, J. M.; Kadish, K. M. *Inorg. Chem*. **1988**, 27, 2373-2378.
[120]Vecchi, A.; Galloni, P.; Floris, B.; Nemykin, V. N. *J. Porphyrins Phthalocyanines* **2013**, *17*, 165-196.
[121]Suijkerbuijk, Bart M. J. M.; Klein Gebbink, Robertus J. M. *Angew. Chem., Int. Ed.* **2008**, *47*, 7396-7421.
[122]Ziegler, C. J.; Chanawanno, K.; Hasheminsasab, A.; Zatsikha, Y. V.; Maligaspe, E.; Nemykin, V. N. *Inorg. Chem.* **2014**, *53*, 4751-4755.
[123]Bandi, V.; El-Khouly, M. E.; Ohkubo, K.; Nesterov, V. N.; Zandler, M. E.; Fukuzumi, S.; D'Souza, F. *J. Phys. Chem. C* **2014**, *118*, 2321-2332.
[124]Misra, R.; Dhokale, B.; Jadhav, T.; Mobin, S. M. *Dalton Trans.* **2013**, *42*, 13658-13666.
[125]Galangau, O.; Fabre-Francke, I.; Munteanu, S.; Dumas-Verdes, C.; Clavier, G.; Meallet-Renault, R.; Pansu, R. B.; Hartl, F.; Miomandre, F. *Electrochimica Acta* **2013**, *87*, 809-815.
[126]Liu, J.-Y.; El-Khouly, M. E.; Fukuzumi, S.; Ng, D. K. P. *ChemPhysChem* **2012**, *13*, 2030-2036.
[127]Ziessel, R.; Bura, T.; Olivier, J.-H. *Synlett* **2010**, 2304-2310.
[128]Martin, R.; Cao, R.; Montforts, F.-P.; Noeske, P.-L. *New J. Chem.* **2013**, *37*, 1610-1615.
[129]Sugawa, K.; Hirono, S.; Akiyama, T.; Yamada, S. *Photochem. Photobiol. Sci.* **2012**, *11*, 318-322.
[130]Cho, Y.-J.; Ahn, T. K.; Song, H.; Kim, K. S.; Lee, C. Y.; Seo, W. S.; Lee, K.; Kim, S. K.; Kim, D.; Park, J. T. *J. Am. Chem. Soc.* **2005**, *127*, 2380-2381.
[131]Liu, L.; Xie, H.; Bostic, H. E.; Jin, L.; Best, M. D.; Zhang, X. P.; Zhan, W. *ChemPhysChem* **2013**, *14*, 2777-2785.
[132]Isosomppi, M.; Tkachenko, N. V.; Efimov, A.; Kaunisto, K.; Hosomizu, K.; Imahori, H.; Lemmetyinen, H. *J. Mater. Chem.* **2005**, *15*, 4546-4554.
[133]Wang, W.; Hu, Y.; Wang, C.; Lu, X. *Electrochimica Acta* **2012**, *65*, 244-250.
[134]Samanta, S.; Das, P. K.; Chatterjee, S.; Sengupta, K.; Mondal, B.; Dey, A. *Inorg. Chem.* **2013**, *52*, 12963-12971.
[135]Imahori, H.; Kimura, M.; Hosomizu, K.; Sato, T.; Ahn, T. K.; Kim, S. K.; Kim, D.; Nishimura, Y.; Yamazaki, I.; Araki, Y.; Ito, O.; Fukuzumi, S. *Chem. Eur. J.* **2004**, *10*, 5111-5122.

[136]Sengupta, K.; Chatterjee, S.; Samanta, S.; Bandyopadhyay, S.; Dey, A. *Inorg. Chem.* **2013**, *52*, 2000-2014.
[137]Zhu, P.; Ma, P.; Wang, Y.; Wang, Q.; Zhao, X.; Zhang, X. *Eur. J. Inorg. Chem.* **2011**, 4241-4247.
[138]Vecchi, A.; Gatto, E.; Floris, B.; Conte, V.; Venanzi, M.; Nemykin, V. N.; Galloni, P. *Chem. Commun.* **2012**, *48*, 5145-5147.
[139]P. Galloni, A. Vecchi, A. Coletti, E. Gatto, B. Floris, V. Conte, In *Handbook of Porphyrin Science*, Kadish, K. M.; Smith, K. M.; Guilard, R. Eds.; World Scientific, Singapore, **2014**, Vol. *33*, Chapter 174.
[140]Zhang, L.; Qi, D.; Zhang, Y.; Bian, Y.; Jiang, J. *J. Mol. Graphics Modelling* **2011**, *29*, 717-725.
[141]Nemykin, V. N.; Hadt, R. G. *J Phys Chem A*, **2010**, *114*, 12062-12066.
[142]Barriere, F.; Geiger, W. E. *J. Am. Chem. Soc*. **2006**, *128*, 3980-3989;
[143]Geiger, W. E.; Connelly, N. G. *Advances in Organometallic Chemistry* **1985**, *24*, 87-130.
[144]Poppitz, E. A.; Hildebrandt, A.; Korb, M.; Lang, H. *J. Organomet. Chem.* **2014**, *752*, 133-140.
[145]Solntsev, P. V.; Dudkin, S. V.; Sabin, J. R.; Nemykin, V. N. *Organometallics*, **2011**, *30*, 3037-3046.
[146]Hildebrandt, A.; Lehrich, S. W.; Schaarschmidt, D.; Jaeschke, R.; Schreiter, K.; Spange, S.; Lang, H. *Eur. J. Inorg. Chem.* **2012**, *2012*, 1114-1121.
[147]Hildebrandt, A.; Schaarschmidt, D.; Claus, R.; Lang, H. *Inorg. Chem.* **2011**, *50*, 10623-10632.
[148]Hildebrandt, A.; Schaarschmidt, D.; Lang, H. *Organometallics* **2011**, *30*, 556-563. (h) Goetsch, W. R.; Solntsev, P. V.; Van Stappen, C.; Purchel, A. A.; Dudkin, S. V.; Nemykin, V. N. *Organometallics* **2014**, *33*, 145-157.
[149]Connelly, N. G.; Geiger, W. E. *Chem. Rev.* **1996**, *96*, 877-910.
[150]D'Alessandro, D.; Keene, R. *Chem. Soc. Rev.*, **2006**, *35*, 424-440.
[151]D'Alessandro, D. M.; Keene, F. R. *Dalton Trans.* **2004**, 3950-3954.
[152]Donoli, A.; Bisello, A.; Cardena, R.; Prinzivalli, C.; Crisma, M.; Santi, S. *Organometallics* **2014**, *33*, 1135-1143.
[153]Alvarez, J.; Ren, T.; Kaifer, A. E. *Organometallics* **2001**, *20*, 3543-3549.
[154]Piglosiewicz, I. M.; Beckhaus, R.; Wittstock, G.; Saak, W.; Haase, D. Inorg. Chem. **2007**, *46*, 7610-7620.
[155]Jiao, J.; Long, G. J.; Rebbouh, L.; Grandjean, F.; Beatty, A. M.; Fehlner, T. P. *J. Am. Chem. Soc.* **2005**, *127*, 17819-17831.
[156]Zhao, Y.; Guo, D.; Liu, Y.; He, C.; Duan, C. *Chem. Commun.* **2008**, 5725-5727.
[157]Schneider, B.; Demeshko, S.; Neudeck, S.; Dechert, S.; Meyer, F. *Inorg. Chem.* **2013**, *52*, 13230-13237.
[158]Tahara, K.; Akita, T.; Katao, S.; Kikuchi, J.-I. *Dalton Trans.* **2014**, *43*, 1368-1379.
[159]Hush, N. S. *Prog. Inorg. Chem.* **1967**, *8*, 391-444;
[160]Creutz, C. *Prog. Inor. Chem.*, **1983**, *30*, 1-73;
[161]Hush, N. S. *Coord. Chem. Rev.* **1985**, *64*, 135-157.
[162]Robin, M. B.; Day, P. *Advances in Radiochemistry*. **1967,** *10*, 247-422.
[163]Gouterman, M. *J. Mol. Spectrosc.* **1961**, *6*, 138–163.
[164]Jiao, J.; Taniguchi, M.; Lindsay, J. S.; Bocian, D. F. *Langmuir* **2010**, *26*, 15718-15721.

[165]Eckermann, A. L.; Feld, D. J.; Shaw, J. A.; Meade, T. J. *Coord. Chem. Rev.* **2010**, *254*, 1769-1802.
[166]Laviron, E. *Electroanal. Chem.* **1979**, *101*, 19-28.
[167]Devaraj, N. K.; Decreau, R. A.; Ebina, W.; Collman, J. P.; Chidsey, C. E. D. *J. Phys. Chem. B* **2006**, *110*, 15955-15962; b) Roth, K. M.; Gryko, D. T.; Clausen, C.; Li, J.; Lindsay, J. S.; Kuhr, W. G.; Bocian, D. F. *J. Phys. Chem. B* **2002**, *106*, 8639-8648.
[168]*Gaussian 09, Revision A.1*, Frisch, M. J.; Trucks, G. W.; Schlegel, H. B.; Scuseria, G. E.; Robb, M. A.; Cheeseman, J. R.; Scalmani, G.; Barone, V.; Mennucci, B.; Petersson, G. A.; Nakatsuji, H.; Caricato, M.; Li, X.; Hratchian, H. P.; Izmaylov, A. F.; Bloino, J.; Zheng, G.; Sonnenberg, J. L.; Hada, M.; Ehara, M.; Toyota, K.; Fukuda, R.; Hasegawa, J.; Ishida, M.; Nakajima, T.; Honda, Y.; Kitao, O.; Nakai, H.; Vreven, T.; Montgomery, J. A. Jr.; Peralta, J. E.; Ogliaro, F.; Bearpark, M.; Heyd, J. J.; Brothers, E.; Kudin, K. N.; Staroverov, V. N.; Kobayashi, R.; Normand, J.; Raghavachari, K.; Rendell, A.; Burant, J. C.; Iyengar, S. S.; Tomasi, J.; Cossi, M.; Rega, N.; Millam, J. M.; Klene, M.; Knox, J. E.; Cross, J. B.; Bakken, V.; Adamo, C.; Jaramillo, J.; Gomperts, R.; Stratmann, R. E.; Yazyev, O.; Austin, A. J.; Cammi, R.; Pomelli, C.; Ochterski, J. W.; Martin, R. L.; Morokuma, K.; Zakrzewski, V. G.; Voth, G. A.; Salvador, P.; Dannenberg, J. J.; Dapprich, S.; Daniels, A. D.; Farkas, O.; Foresman, J. B.; Ortiz, J. V.; Cioslowski, J.; Fox, D. J. Gaussian, Inc., Wallingford CT, **2009**.
[169]QMForge program: http://qmforge.sourceforge.net/
[170]Becke, A. D. *Phys. Rev. A* **1988**, *38*, 3098-3100.
[171]Perdew, J. P. *Phys. Rev. B*, **1986**, *33*, 8822-8824.
[172]Herber, R. H.; Nowik, I. Grosland, J. O.; Hadt, R. G..; Nemykin, V. N. *J. Organomet. Chem.* **2008**, *693*, 1850-1856.
[173]Nemykin, V. N.; Makarova, E. A.; Grosland, J. O.; Hadt, R. G.; Koposov, A. Y. *Inorg. Chem.* **2007**, *46*, 9591-9601.
[174]Nemykin, V. N.; Maximov, A. Y.; Koposov, A. Y. *Organometallics* **2007**, *26*, 3138-3148.
[175]Nemykin, V. N.; Olsen, J. G.; Perera, E.; Basu, P. *Inorg. Chem.* **2006**, *45*, 3557 - 3568.
[176]Nemykin, V. N.; Hadt, R. G. *Inorg. Chem.* **2006**, *45*, 8297 - 8307.
[177]Li, Y. L.; Han, L.; Mei, Y.; Zhang, J. Z. H. *Chem. Phys. Lett.* **2009**, *482*, 217-222.
[178]Fabrizi de Biani, F.; Manca, G.; Marchetti, L.; Leoni, P.; Bruzzone, S.; Guidotti, C.; Atrei, A.; Albinati, A.; Rizzato, S. *Inorg. Chem.* **2009**, *48*, 10126-10137.
[179]Li, F.; Sa, R.; Wu, K. *Mol. Phys.* **2008**, *106*, 2537-2544.
[180]Santi, S.; Orian, L.; Donoli, A.; Durante, C.; Bisello, A.; Ganis, P.; Ceccon, A.; Crociani, L.; Benetollo, F. *Organometallics* **2007**, *26*, 5867-5879.
[181]Zhang, W.-W.; Yu, Y.-G.; Lu, Z.-D.; Mao, W.-L.; Li, Y.-Z.; Meng, Q.-J. *Organometallics* **2007**, *26*, 865-873.
[182]Parac, M.; Grimme, S. *J. Phys. Chem. A* **2002**, *106*, 6844-6850;
[183]Solntsev, P. V.; Spurgin, K. L.; Sabin, J. R.; Heikal, A. A.; Nemykin, V. N. *Inorg. Chem.* **2012**, *51*, 6537-6547.
[184]Lehrich, S. W.; Hildebrandt, A.; Rueffer, T.; Korb, M.; Low, P. J.; Lang, H. *Organometallics* **2014**, *in press* DOI: 10.1021/om500072q .
[185]Becke, A. D. *J. Chem. Phys.*, **1993**, *98*, 5648-5652;
[186]Lee, C.; Yang, W.; Parr, R. G. *Phys. Rev. B* **1988**, *37*, 785-789.

[187]Adamo, C.; Barone, V. *J. Chem. Phys.*, **1999**, *110*, 6158-6169.
[188]Wachters, A. J. H. *J. Chem. Phys.* **1970**, *52*, 1033.
[189]McLean, A. D.; Chandler, G. S. *J. Chem. Phys.* **1980**, *72*, 5639-5648. Hay, P. J.; Wadt, W. R. *J. Chem. Phys.*, **1985**, *82*, 299-310.
[190]Xiao, Y.; Lai, R. Y.; Plaxco, K. W. *Nat. Protoc.*, **2007**, *2*, 2875-2880.
[191]Orain, C.; Le Poul, P.; Le Mest, Y.; Le Poul, N. *J. Electroanal. Chem.* **2013**, *710*, 48-58.

Supporting Information Table 6. TDDFT predicted energies and expansion coefficients for vertical excitation energies in compound **1**.

Excited State 1: Singlet-A 1.3913 eV 891.13 nm f=0.0429 <S**2>=0.000
268 -> 281 0.12015
271 -> 281 -0.12195
278 -> 281 0.14328
279 -> 281 0.21476
280 -> 281 0.55129
280 -> 282 -0.25621
This state for optimization and/or second-order correction.
Total Energy, E(TD-HF/TD-KS) = -7741.03667240
Copying the excited state density for this state as the 1-particle RhoCI density.

Excited State 2: Singlet-A 1.4574 eV 850.73 nm f=0.0438 <S**2>=0.000
268 -> 282 0.10837
274 -> 281 -0.13880
277 -> 281 -0.21425
277 -> 282 0.10389
278 -> 282 -0.10779
279 -> 281 -0.31512
280 -> 281 0.27356
280 -> 282 0.43528

Excited State 3: Singlet-A 1.4711 eV 842.80 nm f=0.0103 <S**2>=0.000
276 -> 281 0.11664
278 -> 281 -0.41365
279 -> 281 0.46325
279 -> 282 -0.15173
280 -> 282 0.22454

Excited State 4: Singlet-A 1.4844 eV 835.26 nm f=0.0074 <S**2>=0.000
276 -> 281 0.14857
277 -> 281 0.57147
278 -> 281 0.30144
278 -> 282 -0.10440
280 -> 282 0.16685

Excited State 5: Singlet-A 1.4995 eV 826.85 nm f=0.0056 <S**2>=0.000
275 -> 281 0.58641
276 -> 281 -0.30529

278 -> 281 0.10745
279 -> 281 0.10691
280 -> 282 0.13519

Excited State 6: Singlet-A 1.5050 eV 823.82 nm f=0.0008 <S**2>=0.000
275 -> 281 0.27913
276 -> 281 0.58856
277 -> 281 -0.19090
278 -> 281 0.15227

Excited State 7: Singlet-A 1.5322 eV 809.21 nm f=0.0376 <S**2>=0.000
272 -> 281 0.13203
275 -> 281 -0.24741
275 -> 282 0.12554
276 -> 281 -0.10543
276 -> 282 0.21136
277 -> 281 -0.22708
278 -> 281 0.35924
279 -> 281 0.29591
279 -> 282 0.10043
280 -> 281 -0.10965
280 -> 282 0.18459

Excited State 8: Singlet-A 1.5446 eV 802.67 nm f=0.0037 <S**2>=0.000
277 -> 281 0.10678
277 -> 282 0.38149
278 -> 282 0.17573
279 -> 282 0.53856

Excited State 9: Singlet-A 1.5621 eV 793.72 nm f=0.0125 <S**2>=0.000
275 -> 282 0.37719
276 -> 282 0.41970
277 -> 281 0.10174
278 -> 282 0.32981
279 -> 281 -0.13169

Excited State 10: Singlet-A 1.5644 eV 792.51 nm f=0.0108 <S**2>=0.000
274 -> 281 0.24291
276 -> 282 0.25015
277 -> 282 0.49952

278 -> 282 -0.22851
279 -> 282 -0.22710

Excited State 11: Singlet-A 1.5685 eV 790.48 nm f=0.0034 <S**2>=0.000
274 -> 281 -0.15944
275 -> 282 -0.35326
276 -> 282 0.44859
277 -> 282 -0.19482
278 -> 281 -0.10271
278 -> 282 -0.26129
279 -> 282 0.13422

Excited State 12: Singlet-A 1.5897 eV 779.90 nm f=0.0066 <S**2>=0.000
272 -> 281 -0.21564
273 -> 281 0.32857
275 -> 282 0.40580
278 -> 282 -0.36169
279 -> 282 0.16169

Excited State 13: Singlet-A 1.5957 eV 776.99 nm f=0.0408 <S**2>=0.000
271 -> 281 -0.11658
274 -> 281 0.56430
274 -> 282 -0.12981
277 -> 282 -0.19755
279 -> 282 0.18802
280 -> 281 0.11316
280 -> 282 0.15243

Excited State 14: Singlet-A 1.6168 eV 766.86 nm f=0.0104 <S**2>=0.000
273 -> 281 0.59280
274 -> 281 0.10608
275 -> 282 -0.16142
278 -> 282 0.20824
279 -> 282 -0.10899

Excited State 15: Singlet-A 1.6281 eV 761.52 nm f=0.0138 <S**2>=0.000
271 -> 281 -0.11267
272 -> 281 0.60872
273 -> 282 0.17309
274 -> 282 0.16460

275 -> 282 0.11004
278 -> 281 -0.10225
278 -> 282 -0.13417

Excited State 16: Singlet-A 1.6529 eV 750.10 nm f=0.0102 <S**2>=0.000
271 -> 281 0.16148
272 -> 281 -0.12099
274 -> 282 0.64489

Excited State 17: Singlet-A 1.6788 eV 738.53 nm f=0.0119 <S**2>=0.000
272 -> 281 -0.10815
272 -> 282 0.36996
273 -> 282 0.56767

Excited State 18: Singlet-A 1.6899 eV 733.70 nm f=0.0066 <S**2>=0.000
272 -> 282 0.58243
273 -> 282 -0.35556

Excited State 19: Singlet-A 1.7038 eV 727.70 nm f=0.0211 <S**2>=0.000
268 -> 281 0.12498
269 -> 281 0.13056
271 -> 281 0.45246
271 -> 282 0.44301

Excited State 20: Singlet-A 1.7253 eV 718.61 nm f=0.0206 <S**2>=0.000
269 -> 282 0.11935
271 -> 281 -0.40079
271 -> 282 0.50731
274 -> 282 0.10203

Excited State 21: Singlet-A 1.7641 eV 702.83 nm f=0.0020 <S**2>=0.000
269 -> 281 0.14135
270 -> 281 0.67917

Excited State 22: Singlet-A 1.7947 eV 690.82 nm f=0.0046 <S**2>=0.000
268 -> 281 -0.15422
269 -> 281 0.63253
269 -> 282 0.12314
270 -> 281 -0.13194
270 -> 282 0.17132

Excited State 23: Singlet-A 1.8145 eV 683.28 nm f=0.0051 <S**2>=0.000
268 -> 282 0.11664
269 -> 281 -0.13736
270 -> 282 0.66464

Excited State 24: Singlet-A 1.8469 eV 671.30 nm f=0.0103 <S**2>=0.000
268 -> 281 0.10489
268 -> 282 -0.10675
269 -> 281 -0.10622
269 -> 282 0.66710

Excited State 25: Singlet-A 1.9952 eV 621.41 nm f=0.0185 <S**2>=0.000
267 -> 281 0.33245
267 -> 282 0.12805
268 -> 281 -0.39372
268 -> 282 0.41673
280 -> 283 0.10847

Excited State 26: Singlet-A 2.0560 eV 603.02 nm f=0.0539 <S**2>=0.000
267 -> 281 0.18070
267 -> 282 -0.27994
268 -> 281 0.37158
268 -> 282 0.38933
280 -> 281 -0.11536
280 -> 283 -0.22015

Excited State 27: Singlet-A 2.1060 eV 588.72 nm f=0.0219 <S**2>=0.000
267 -> 282 -0.16265
268 -> 281 0.18321
280 -> 283 0.64166

Excited State 28: Singlet-A 2.2695 eV 546.32 nm f=0.0045 <S**2>=0.000
279 -> 283 0.69804

Excited State 29: Singlet-A 2.2923 eV 540.86 nm f=0.0028 <S**2>=0.000
277 -> 283 0.23763
278 -> 283 0.66168

Excited State 30: Singlet-A 2.2989 eV 539.31 nm f=0.0016 <S**2>=0.000

277 -> 283 0.65910
278 -> 283 -0.22905

Excited State 31: Singlet-A 2.3101 eV 536.70 nm f=0.0004 <S**2>=0.000
276 -> 283 0.69619

Excited State 32: Singlet-A 2.3154 eV 535.47 nm f=0.0012 <S**2>=0.000
275 -> 283 0.69809

Excited State 33: Singlet-A 2.3851 eV 519.83 nm f=0.0039 <S**2>=0.000
274 -> 283 0.68586
280 -> 284 -0.10599

Excited State 34: Singlet-A 2.4004 eV 516.52 nm f=0.0324 <S**2>=0.000
273 -> 283 -0.19738
280 -> 284 0.63944

Excited State 35: Singlet-A 2.4149 eV 513.40 nm f=0.0058 <S**2>=0.000
273 -> 283 0.67388
280 -> 284 0.18173

Excited State 36: Singlet-A 2.4254 eV 511.20 nm f=0.0002 <S**2>=0.000
271 -> 283 -0.15281
272 -> 283 0.68592

Excited State 37: Singlet-A 2.4861 eV 498.70 nm f=0.0372 <S**2>=0.000
266 -> 281 -0.40621
267 -> 282 -0.12033
271 -> 283 0.51383
272 -> 283 0.11094

Excited State 38: Singlet-A 2.4872 eV 498.49 nm f=0.0222 <S**2>=0.000
266 -> 281 0.57681
271 -> 283 0.36635

Excited State 39: Singlet-A 2.5469 eV 486.81 nm f=0.0007 <S**2>=0.000
266 -> 282 0.70591

Excited State 40: Singlet-A 2.5570 eV 484.88 nm f=0.0827 <S**2>=0.000
267 -> 281 0.19085

278 -> 284 -0.22121
279 -> 284 0.60484

Excited State 41: Singlet-A 2.5742 eV 481.63 nm f=0.0476 <S**2>=0.000
267 -> 281 -0.13501
278 -> 284 0.57041
279 -> 284 0.30938

Excited State 42: Singlet-A 2.5890 eV 478.89 nm f=0.0087 <S**2>=0.000
277 -> 284 0.68565

Excited State 43: Singlet-A 2.5981 eV 477.20 nm f=0.0050 <S**2>=0.000
275 -> 284 0.22824
276 -> 284 0.64397
278 -> 284 0.12452

Excited State 44: Singlet-A 2.6049 eV 475.97 nm f=0.0123 <S**2>=0.000
275 -> 284 0.62246
276 -> 284 -0.26481
278 -> 284 0.12735

Excited State 45: Singlet-A 2.6300 eV 471.42 nm f=0.0475 <S**2>=0.000
267 -> 281 -0.15430
268 -> 283 -0.11464
269 -> 283 0.55382
270 -> 283 0.21604
275 -> 284 0.14737
278 -> 284 -0.14586

Excited State 46: Singlet-A 2.6438 eV 468.96 nm f=0.1171 <S**2>=0.000
264 -> 281 -0.20432
264 -> 282 0.10210
267 -> 281 -0.15757
267 -> 282 -0.18208
268 -> 283 -0.13541
269 -> 283 -0.28028
270 -> 283 0.23487
271 -> 283 -0.12428
275 -> 284 0.10205
278 -> 284 -0.17351

280 -> 285 0.32042

Excited State 47: Singlet-A 2.6598 eV 466.15 nm f=0.0043 <S**2>=0.000
265 -> 281 0.58709
265 -> 282 -0.18247
270 -> 283 0.16124
280 -> 285 0.25329

Excited State 48: Singlet-A 2.6652 eV 465.20 nm f=0.0703 <S**2>=0.000
264 -> 282 -0.13049
265 -> 281 -0.26232
267 -> 281 0.19649
267 -> 283 0.10075
268 -> 282 -0.10134
268 -> 283 0.13271
269 -> 283 0.15189
270 -> 283 0.22531
271 -> 284 0.11559
273 -> 284 -0.15140
274 -> 284 0.22885
280 -> 285 0.33216

Excited State 49: Singlet-A 2.6759 eV 463.34 nm f=0.0135 <S**2>=0.000
265 -> 281 0.13754
269 -> 283 -0.10999
274 -> 284 0.64120

Excited State 50: Singlet-A 2.6965 eV 459.79 nm f=0.0064 <S**2>=0.000
268 -> 283 0.33013
269 -> 283 0.12882
270 -> 283 -0.26447
270 -> 284 -0.12653
273 -> 284 0.40281
280 -> 285 0.26530

Excited State 51: Singlet-A 2.7002 eV 459.17 nm f=0.0317 <S**2>=0.000
264 -> 281 0.46167
267 -> 282 0.15797
269 -> 283 -0.10329
270 -> 283 0.17184

272 -> 284 0.19234
273 -> 284 0.32649

Excited State 52: Singlet-A 2.7104 eV 457.44 nm f=0.0197 <S**2>=0.000
264 -> 281 -0.22793
268 -> 283 0.11676
270 -> 283 0.21059
271 -> 284 0.21878
272 -> 284 0.36242
273 -> 284 0.22199
280 -> 285 -0.29703

Excited State 53: Singlet-A 2.7129 eV 457.01 nm f=0.0129 <S**2>=0.000
264 -> 281 -0.14146
270 -> 283 -0.16003
271 -> 284 -0.27276
272 -> 284 0.53788
273 -> 284 -0.17486
280 -> 285 0.14999

Excited State 54: Singlet-A 2.7209 eV 455.68 nm f=0.0471 <S**2>=0.000
264 -> 281 0.15156
264 -> 282 0.21632
265 -> 282 0.18316
267 -> 281 -0.15411
267 -> 283 -0.11041
268 -> 283 0.32931
271 -> 284 0.33633
273 -> 284 -0.29053

Excited State 55: Singlet-A 2.7314 eV 453.92 nm f=0.0242 <S**2>=0.000
264 -> 281 -0.10384
264 -> 282 -0.11585
265 -> 281 0.19930
265 -> 282 0.60600
273 -> 284 0.12847

Excited State 56: Singlet-A 2.7644 eV 448.51 nm f=0.1299 <S**2>=0.000
264 -> 281 -0.23912
267 -> 282 0.19349

267 -> 283 -0.10084
268 -> 283 0.33975
270 -> 283 0.15509
270 -> 284 0.18852
271 -> 284 -0.32680
272 -> 284 -0.13088

Excited State 57: Singlet-A 2.7990 eV 442.97 nm f=0.2091 <S**2>=0.000
264 -> 281 0.14286
264 -> 282 0.36348
267 -> 282 -0.26179
267 -> 283 0.24249
268 -> 283 0.14988
271 -> 284 -0.28957

Excited State 58: Singlet-A 2.8384 eV 436.81 nm f=0.1855 <S**2>=0.000
264 -> 281 0.13782
264 -> 282 -0.39388
267 -> 282 -0.17979
267 -> 283 -0.12728
268 -> 283 0.10866
280 -> 286 0.40815

Excited State 59: Singlet-A 2.8646 eV 432.81 nm f=0.1009 <S**2>=0.000
264 -> 282 -0.12699
267 -> 282 -0.15109
267 -> 283 -0.18021
280 -> 286 -0.35843
280 -> 287 0.39494
280 -> 288 -0.13464
280 -> 289 0.18642

Excited State 60: Singlet-A 2.8660 eV 432.60 nm f=0.0315 <S**2>=0.000
264 -> 282 0.10050
279 -> 285 0.20709
280 -> 286 0.34541
280 -> 287 0.48110
280 -> 289 -0.18754

Excited State 61: Singlet-A 2.8747 eV 431.30 nm f=0.0097 <S**2>=0.000

279 -> 285 0.48389
280 -> 288 0.47346

Excited State 62: Singlet-A 2.8824 eV 430.14 nm f=0.0138 <S**2>=0.000
267 -> 283 0.16466
269 -> 284 0.23945
279 -> 285 0.44082
280 -> 288 -0.41882

Excited State 63: Singlet-A 2.8877 eV 429.36 nm f=0.0092 <S**2>=0.000
269 -> 284 0.59921
278 -> 285 -0.12615
279 -> 285 -0.14195
280 -> 287 0.13407
280 -> 288 0.19036
280 -> 290 0.10124

Excited State 64: Singlet-A 2.8994 eV 427.62 nm f=0.0012 <S**2>=0.000
269 -> 284 0.10931
278 -> 285 0.68292

Excited State 65: Singlet-A 2.9089 eV 426.22 nm f=0.0266 <S**2>=0.000
267 -> 283 0.17508
277 -> 285 0.62391
280 -> 290 0.18336

Excited State 66: Singlet-A 2.9100 eV 426.07 nm f=0.0762 <S**2>=0.000
267 -> 283 0.30699
269 -> 284 -0.14577
270 -> 284 0.17919
277 -> 285 -0.30553
280 -> 287 0.10924
280 -> 289 0.32269
280 -> 290 0.23345

Excited State 67: Singlet-A 2.9190 eV 424.75 nm f=0.0004 <S**2>=0.000
276 -> 285 0.69844

Excited State 68: Singlet-A 2.9253 eV 423.84 nm f=0.0100 <S**2>=0.000
275 -> 285 0.66870

280 -> 289 -0.14694

Excited State 69: Singlet-A 2.9302 eV 423.12 nm f=0.0613 <S**2>=0.000
264 -> 282 0.10235
267 -> 283 -0.19374
270 -> 284 0.12977
275 -> 285 0.21313
280 -> 286 0.11545
280 -> 289 0.42337
280 -> 290 -0.32158

Excited State 70: Singlet-A 2.9473 eV 420.67 nm f=0.0332 <S**2>=0.000
263 -> 281 0.14198
267 -> 282 -0.12330
267 -> 283 -0.10250
270 -> 283 -0.21296
270 -> 284 0.51511
271 -> 285 -0.15243
280 -> 289 -0.19581

Excited State 71: Singlet-A 2.9751 eV 416.75 nm f=0.0223 <S**2>=0.000
263 -> 281 0.41184
268 -> 284 -0.40417
274 -> 285 0.17558
280 -> 290 0.23717
280 -> 291 0.12826

Excited State 72: Singlet-A 2.9926 eV 414.31 nm f=0.1721 <S**2>=0.000
263 -> 282 -0.14075
264 -> 282 0.11863
267 -> 281 0.18908
267 -> 283 -0.22672
268 -> 282 -0.11043
268 -> 284 0.26181
280 -> 290 0.40142

Excited State 73: Singlet-A 3.0000 eV 413.29 nm f=0.0013 <S**2>=0.000
263 -> 281 -0.10356
271 -> 285 -0.19279
274 -> 285 0.65144

Excited State 74: Singlet-A 3.0258 eV 409.76 nm f=0.0034 <S**2>=0.000
273 -> 285 0.70164

Excited State 75: Singlet-A 3.0323 eV 408.88 nm f=0.0316 <S**2>=0.000
268 -> 284 0.14686
272 -> 285 -0.26572
279 -> 286 0.11709
280 -> 291 0.57609

Excited State 76: Singlet-A 3.0367 eV 408.29 nm f=0.0054 <S**2>=0.000
271 -> 285 -0.18962
272 -> 285 0.62929
280 -> 291 0.22345

Excited State 77: Singlet-A 3.0434 eV 407.39 nm f=0.0020 <S**2>=0.000
278 -> 287 -0.11978
279 -> 286 0.64006
279 -> 287 -0.18989

Excited State 78: Singlet-A 3.0562 eV 405.68 nm f=0.0298 <S**2>=0.000
262 -> 281 -0.11969
262 -> 282 0.14848
263 -> 281 0.40528
267 -> 284 -0.17902
268 -> 284 0.34228
280 -> 291 -0.16969
280 -> 292 -0.18228

Excited State 79: Singlet-A 3.0617 eV 404.96 nm f=0.0042 <S**2>=0.000
277 -> 286 0.17542
278 -> 286 -0.24594
278 -> 287 -0.10980
279 -> 286 0.11064
279 -> 287 0.49479
279 -> 288 -0.33471

Excited State 80: Singlet-A 3.0692 eV 403.97 nm f=0.0002 <S**2>=0.000
277 -> 286 0.60490
278 -> 286 0.25066

278 -> 287 0.23970

Excited State 81: Singlet-A 3.0825 eV 402.22 nm f=0.0065 <S**2>=0.000
263 -> 282 -0.24915
267 -> 284 -0.13005
275 -> 287 0.12534
276 -> 286 -0.24672
277 -> 286 -0.17093
277 -> 287 0.22774
277 -> 288 -0.16711
278 -> 286 0.13569
278 -> 287 0.37918
279 -> 287 0.10310

Excited State 82: Singlet-A 3.0835 eV 402.09 nm f=0.0207 <S**2>=0.000
263 -> 282 0.50168
267 -> 284 0.27671
276 -> 286 -0.14828
278 -> 287 0.19939
280 -> 292 -0.11175

Excited State 83: Singlet-A 3.0866 eV 401.69 nm f=0.0010 <S**2>=0.000
275 -> 286 0.11217
275 -> 287 -0.12483
276 -> 286 0.22894
276 -> 287 -0.20001
277 -> 287 0.43190
277 -> 288 -0.14465
278 -> 286 0.19560
278 -> 287 -0.13890
278 -> 288 -0.27375
279 -> 288 -0.12401
279 -> 289 0.10708

Excited State 84: Singlet-A 3.0882 eV 401.47 nm f=0.0008 <S**2>=0.000
275 -> 286 0.12454
276 -> 286 0.38610
276 -> 287 -0.21098
278 -> 288 0.48324

Excited State 85: Singlet-A 3.0940 eV 400.72 nm f=0.0010 <S**2>=0.000
275 -> 286 -0.40407
275 -> 287 -0.19484
276 -> 287 0.40433
277 -> 287 0.20379
277 -> 288 -0.22370
278 -> 288 0.15192

Excited State 86: Singlet-A 3.1003 eV 399.91 nm f=0.0026 <S**2>=0.000
276 -> 287 0.12852
279 -> 289 0.62437

Excited State 87: Singlet-A 3.1059 eV 399.18 nm f=0.0012 <S**2>=0.000
275 -> 286 0.27645
275 -> 287 0.20697
276 -> 287 0.22921
276 -> 288 0.46045
277 -> 287 0.11854
277 -> 288 -0.14281
278 -> 286 -0.14728
278 -> 289 0.11177

Excited State 88: Singlet-A 3.1078 eV 398.95 nm f=0.0007 <S**2>=0.000
275 -> 287 0.28957
275 -> 288 0.36269
276 -> 288 -0.22818
276 -> 289 0.10105
277 -> 287 0.15974
277 -> 288 0.14192
278 -> 288 0.20820
279 -> 287 -0.17283
279 -> 288 -0.16066
279 -> 289 0.13427

Excited State 89: Singlet-A 3.1163 eV 397.85 nm f=0.0010 <S**2>=0.000
275 -> 286 -0.13999
275 -> 287 0.24041
275 -> 288 0.22420
275 -> 289 -0.27753
276 -> 288 0.18637

277 -> 287 -0.12778
278 -> 286 0.30102
278 -> 287 -0.14659
278 -> 289 -0.22105
279 -> 287 0.12164

Excited State 90: Singlet-A 3.1203 eV 397.35 nm f=0.0013 <S**2>=0.000
275 -> 287 0.19139
275 -> 288 0.10516
275 -> 289 0.15843
276 -> 287 -0.12417
276 -> 288 -0.17873
277 -> 288 -0.21104
277 -> 289 -0.23056
277 -> 290 0.19369
278 -> 286 -0.14511
278 -> 289 -0.22932
279 -> 287 0.11124
279 -> 288 0.32047

Excited State 91: Singlet-A 3.1252 eV 396.72 nm f=0.0014 <S**2>=0.000
275 -> 286 0.14755
275 -> 288 0.16456
276 -> 287 0.18319
276 -> 288 -0.24811
277 -> 289 -0.15474
278 -> 286 0.14092
278 -> 289 0.47568
279 -> 290 0.13685

Excited State 92: Singlet-A 3.1268 eV 396.51 nm f=0.0000 <S**2>=0.000
274 -> 286 -0.14685
275 -> 287 -0.18251
275 -> 288 0.38782
275 -> 289 0.14373
276 -> 289 -0.35719
277 -> 289 -0.12563
278 -> 286 -0.12124
278 -> 287 0.20590
278 -> 288 -0.14167

Excited State 93: Singlet-A 3.1318 eV 395.89 nm f=0.0000 <S**2>=0.000
275 -> 288 0.19676
277 -> 289 0.57115
277 -> 290 0.22654
279 -> 288 0.15615

Excited State 94: Singlet-A 3.1355 eV 395.42 nm f=0.0017 <S**2>=0.000
277 -> 287 -0.14726
277 -> 288 -0.30636
277 -> 290 -0.17079
279 -> 287 -0.13522
279 -> 288 -0.17902
279 -> 290 0.49849
280 -> 292 0.11569

Excited State 95: Singlet-A 3.1473 eV 393.94 nm f=0.0029 <S**2>=0.000
262 -> 281 -0.14042
262 -> 282 0.14720
271 -> 285 -0.10815
277 -> 288 0.10381
280 -> 292 0.57975

Excited State 96: Singlet-A 3.1521 eV 393.34 nm f=0.0007 <S**2>=0.000
274 -> 286 -0.13909
275 -> 287 -0.13845
276 -> 289 0.19839
277 -> 290 -0.13110
278 -> 290 0.57689

Excited State 97: Singlet-A 3.1574 eV 392.67 nm f=0.0008 <S**2>=0.000
273 -> 286 -0.10232
274 -> 286 0.57286
275 -> 289 0.14668
275 -> 290 -0.13899
276 -> 289 -0.22314
278 -> 290 0.20068

Excited State 98: Singlet-A 3.1659 eV 391.63 nm f=0.0040 <S**2>=0.000
262 -> 281 -0.18054

274 -> 286 0.23736
274 -> 287 0.16637
275 -> 289 -0.31722
275 -> 290 0.34937
276 -> 290 -0.28311
278 -> 287 0.11009

Excited State 99: Singlet-A 3.1677 eV 391.40 nm f=0.0368 <S**2>=0.000
261 -> 281 -0.26291
262 -> 281 0.49272
275 -> 289 -0.14005
276 -> 290 -0.29349

Excited State 100: Singlet-A 3.1710 eV 391.00 nm f=0.0107 <S**2>=0.000
261 -> 281 -0.13562
262 -> 281 0.22076
274 -> 286 0.10911
274 -> 287 -0.11068
275 -> 290 0.37653
276 -> 286 0.12396
276 -> 289 0.15286
276 -> 290 0.39364
278 -> 287 0.10265

Excited State 101: Singlet-A 3.1772 eV 390.23 nm f=0.0043 <S**2>=0.000
274 -> 287 0.59683
274 -> 288 -0.14712
276 -> 290 0.24756
277 -> 290 -0.11933

Excited State 102: Singlet-A 3.1829 eV 389.54 nm f=0.0057 <S**2>=0.000
260 -> 281 -0.17439
262 -> 282 0.10710
268 -> 284 0.10379
268 -> 285 -0.28231
269 -> 285 -0.20997
270 -> 283 -0.10640
270 -> 285 0.13662
271 -> 285 0.40552
273 -> 286 -0.12070

274 -> 288 -0.13257

Excited State 103: Singlet-A 3.1888 eV 388.81 nm f=0.0003 <S**2>=0.000
261 -> 281 -0.16153
273 -> 286 0.56379
274 -> 288 0.15015
276 -> 289 -0.14208
278 -> 290 0.10020

Excited State 104: Singlet-A 3.1906 eV 388.59 nm f=0.0009 <S**2>=0.000
260 -> 281 -0.14200
273 -> 286 -0.18213
273 -> 287 0.17547
274 -> 288 0.52562
277 -> 288 -0.10888
279 -> 290 -0.16802

Excited State 105: Singlet-A 3.1980 eV 387.69 nm f=0.0097 <S**2>=0.000
260 -> 281 0.43692
260 -> 282 -0.17790
261 -> 281 0.29783
262 -> 281 0.15087
267 -> 284 -0.11775
271 -> 285 0.10518
272 -> 286 0.11782
273 -> 287 0.11300
280 -> 292 0.10054

Excited State 106: Singlet-A 3.1984 eV 387.64 nm f=0.0088 <S**2>=0.000
259 -> 281 -0.19002
260 -> 281 -0.23630
260 -> 282 0.12362
261 -> 281 0.40225
263 -> 282 -0.13655
267 -> 284 0.17646
272 -> 287 -0.14575
273 -> 286 0.16882
273 -> 287 -0.14578

Excited State 107: Singlet-A 3.2005 eV 387.39 nm f=0.0006 <S**2>=0.000

272 -> 286 0.54226
273 -> 287 -0.37649
279 -> 291 0.10852

Excited State 108: Singlet-A 3.2046 eV 386.89 nm f=0.0037 <S**2>=0.000
261 -> 281 -0.16552
271 -> 286 0.16883
271 -> 287 0.10859
271 -> 288 -0.11287
271 -> 289 -0.12232
272 -> 286 0.10981
272 -> 287 -0.14160
272 -> 288 0.14304
273 -> 288 0.14557
274 -> 288 0.11309
275 -> 289 -0.11145
275 -> 290 0.24614
275 -> 291 0.14045
276 -> 286 -0.17112
276 -> 289 -0.11747
276 -> 290 0.14074
276 -> 291 0.15252
279 -> 291 -0.14624

Excited State 109: Singlet-A 3.2085 eV 386.43 nm f=0.0010 <S**2>=0.000
271 -> 286 0.11472
272 -> 287 0.37883
273 -> 288 0.21562
274 -> 288 0.11646
274 -> 289 0.23089
275 -> 286 -0.10188
275 -> 289 -0.15203
275 -> 290 -0.11683
276 -> 291 0.11363
277 -> 290 -0.11148
278 -> 289 0.10280
279 -> 291 -0.14158

Excited State 110: Singlet-A 3.2105 eV 386.18 nm f=0.0031 <S**2>=0.000
259 -> 281 -0.11843

260 -> 281 -0.12826
262 -> 282 -0.14855
271 -> 286 0.17621
272 -> 286 0.14134
272 -> 287 0.19865
273 -> 287 0.36140
273 -> 288 -0.22110
274 -> 288 -0.16386
276 -> 289 -0.14069
279 -> 291 0.18816

Excited State 111: Singlet-A 3.2136 eV 385.81 nm f=0.0064 <S**2>=0.000
260 -> 281 0.17617
260 -> 282 0.10676
262 -> 282 0.33750
271 -> 286 0.18516
272 -> 286 -0.17806
273 -> 287 -0.18190
273 -> 288 -0.32369
277 -> 288 -0.10181
279 -> 291 0.12654

Excited State 112: Singlet-A 3.2183 eV 385.25 nm f=0.0021 <S**2>=0.000
259 -> 281 -0.10536
262 -> 282 -0.14849
272 -> 287 -0.19090
273 -> 287 -0.10176
273 -> 288 -0.24251
274 -> 289 0.51762
279 -> 291 -0.10398

Excited State 113: Singlet-A 3.2187 eV 385.21 nm f=0.0024 <S**2>=0.000
259 -> 281 -0.11056
269 -> 285 -0.14459
270 -> 285 0.11775
271 -> 286 0.44054
271 -> 287 -0.23666
271 -> 288 0.12649
272 -> 289 -0.11242
275 -> 289 0.16090

275 -> 290 0.10758
276 -> 290 -0.11028
276 -> 291 -0.15760
279 -> 291 -0.20868

Excited State 114: Singlet-A 3.2217 eV 384.84 nm f=0.0007 <S**2>=0.000
262 -> 282 0.12135
271 -> 286 0.19345
272 -> 287 -0.23053
272 -> 288 -0.20740
273 -> 288 0.18297
274 -> 289 0.17760
277 -> 290 -0.17585
277 -> 291 0.14446
279 -> 291 0.40602

Excited State 115: Singlet-A 3.2218 eV 384.82 nm f=0.0023 <S**2>=0.000
259 -> 281 -0.19541
260 -> 282 -0.14549
262 -> 282 -0.17992
267 -> 284 -0.10319
269 -> 285 -0.19010
270 -> 285 0.14795
272 -> 286 -0.17694
272 -> 287 0.12398
272 -> 288 0.29782
273 -> 287 -0.19893
277 -> 290 -0.12111
277 -> 291 0.10138
279 -> 291 0.23341

Excited State 116: Singlet-A 3.2249 eV 384.46 nm f=0.0005 <S**2>=0.000
268 -> 285 -0.16081
269 -> 285 0.37391
270 -> 285 -0.27709
271 -> 285 0.13886
271 -> 287 -0.19557
272 -> 287 0.10297
272 -> 288 0.28571
274 -> 289 0.15286

275 -> 290 0.12242

Excited State 117: Singlet-A 3.2255 eV 384.39 nm f=0.0045 <S**2>=0.000
259 -> 281 0.11682
260 -> 282 0.13690
262 -> 282 0.17251
268 -> 285 0.11238
269 -> 285 -0.20836
270 -> 285 0.15822
271 -> 285 -0.10902
271 -> 286 -0.15263
272 -> 286 0.11201
272 -> 288 0.31978
273 -> 287 0.14822
274 -> 288 -0.10739
274 -> 289 0.23203

Excited State 118: Singlet-A 3.2306 eV 383.79 nm f=0.0012 <S**2>=0.000
269 -> 285 0.11720
271 -> 286 0.20836
271 -> 287 0.37366
271 -> 288 0.18969
273 -> 288 -0.22628
273 -> 289 -0.11878
275 -> 291 -0.10090
276 -> 289 0.10496
277 -> 290 -0.15615
277 -> 291 0.19758
278 -> 291 -0.17684
279 -> 291 -0.12450

Excited State 119: Singlet-A 3.2338 eV 383.40 nm f=0.0007 <S**2>=0.000
261 -> 282 0.14149
271 -> 286 -0.16876
271 -> 287 0.19812
271 -> 288 0.13696
272 -> 288 -0.14523
273 -> 289 0.16660
275 -> 290 0.12401
275 -> 291 0.10820

278 -> 291 0.45642

Excited State 120: Singlet-A 3.2386 eV 382.84 nm f=0.0147 <S**2>=0.000
259 -> 281 0.19026
260 -> 281 0.13424
261 -> 282 0.51736
262 -> 282 -0.21627
274 -> 290 0.12973
279 -> 291 0.14355

Optimized coordinates for compound 1:

Fe	-0.09722800	-5.99958200	-2.58662400
C	-0.96802400	-7.01530800	-1.05609300
C	-0.17951900	-5.92658900	-0.55028500
C	-1.96097600	-6.47330000	-1.94393700
C	-1.77785600	-5.04922900	-1.98973400
H	-0.83006200	-8.07050500	-0.81196800
H	0.63138800	-6.00645400	0.17502600
H	-2.70234500	-7.04386800	-2.50662300
H	-2.36114100	-4.34557800	-2.58593400
C	-0.68740400	-4.68265300	-1.10321800
C	1.81902400	-6.40249600	-3.16465300
C	0.91513400	-7.41993400	-3.63330400
C	0.21303500	-5.37567200	-4.50138900
C	-0.07621000	-6.78496000	-4.46120000
H	2.68815300	-6.56495800	-2.52415100
H	0.96865100	-8.48458300	-3.39817400
H	-0.36189900	-4.61641800	-5.03447500
H	-0.91200200	-7.28325800	-4.95600900
C	1.38383300	-5.14016000	-3.70143600
H	1.84553400	-4.16979000	-3.51032400
Fe	-5.74965600	0.78271400	1.77940700
C	-6.18948500	2.59294700	0.96828100
C	-4.76925000	2.40309200	1.06968800
C	-6.71468300	1.53557100	0.14817500
C	-5.62275000	0.69770100	-0.25739300
H	-6.76678200	3.38593700	1.44731900
H	-4.07348000	3.02633000	1.63326200
H	-7.76417200	1.37441900	-0.10639400
H	-5.69936800	-0.17045500	-0.91279600
C	-4.38990500	1.23967200	0.28841700
C	-6.57615700	0.87829400	3.62735100
C	-7.16332800	-0.20421400	2.86028200

C	-4.86489800	-0.58084600	3.02599200
C	-6.08678500	-1.09596400	2.48256100
H	-7.11128400	1.72826700	4.05482300
H	-3.87215500	-1.01459500	2.89364300
H	-6.22402200	-2.01168000	1.90698100
C	-5.16379700	0.63828400	3.72886400
H	-4.43911500	1.27883400	4.23489100
Fe	6.00723200	-0.76877000	2.93911100
C	6.24382000	1.08200600	3.76671300
C	4.91958200	0.57833400	4.01949600
C	7.18834400	0.14768300	4.32088100
C	6.44628200	-0.93090600	4.91815000
H	6.49260100	2.01580300	3.25866900
H	3.98513800	1.04305000	3.70039300
H	8.27568500	0.23903300	4.29009300
H	6.87316400	-1.80604200	5.41178800
C	5.04421200	-0.66501000	4.73034300
H	4.21985200	-1.30117800	5.05741000
C	6.28732900	-0.63190800	0.92596700
C	7.28678400	-1.47196600	1.52534500
C	5.20357500	-2.37674400	2.01178200
C	6.61714300	-2.55429100	2.19471600
H	6.48141300	0.24882800	0.31230600
H	8.36563000	-1.30998500	1.48168400
H	4.41752200	-3.02050500	2.40937700
H	7.09525000	-3.35326400	2.76450600
C	4.97567300	-1.19521800	1.19965200
N	1.43570900	-1.66720900	-0.05100900
N	-1.40182200	-1.05789300	-0.32912000
N	2.16235500	1.11310900	0.04035100
N	-0.67496800	1.72480600	-0.22952500
C	1.02541900	-2.90082700	-0.51624800
C	2.78096900	-1.80408500	0.20261200
C	-1.43798700	-2.43226300	-0.47170400
C	-2.65902900	-0.55661600	-0.03378600
C	3.33561900	0.60612800	0.57452500
C	2.22432800	2.48837500	-0.07234700
C	-2.04299900	1.85999000	-0.23984100
C	-0.18271400	2.96480800	-0.58805800
C	-0.32880800	-3.28986200	-0.72579200
C	2.15828400	-3.81334800	-0.63486700
C	3.24812500	-3.14305900	-0.15488200
C	-2.80138900	-2.82564500	-0.23242700
C	-2.98918200	0.82126100	0.02943900
C	-3.53398200	-1.69210600	0.05888000
C	3.65287200	-0.77324500	0.67517000

C	4.17055500	1.73879000	0.86075400
C	3.51075300	2.87766800	0.44107800
C	-2.43377700	3.20678900	-0.65728900
C	1.18605900	3.35164200	-0.53037000
C	-1.27249800	3.88168600	-0.90810900
Fe	1.32143300	6.01551400	-2.44118300
C	1.65847700	6.73399700	-4.31309000
C	1.38063200	5.32253700	-4.35627700
C	0.52819400	7.39226200	-3.71259600
C	-0.44941000	6.38687500	-3.38817000
H	2.57334900	7.21889400	-4.65900900
H	2.04649100	4.54824400	-4.74167000
H	0.43155500	8.46432000	-3.53112900
H	-1.42410200	6.56657300	-2.93014000
C	0.07870300	5.10869500	-3.78554400
H	-0.41075700	4.14311200	-3.64718200
C	2.85708000	5.09301300	-1.50838200
C	3.02514000	6.51928100	-1.46591600
C	1.01032100	5.99529800	-0.42577500
C	1.87938500	7.07637400	-0.79888000
H	3.54356000	4.37877400	-1.96583500
H	3.85888000	7.08075800	-1.89174400
H	0.07572600	6.08991500	0.12873100
H	1.69494900	8.13622900	-0.61233700
C	1.61636700	4.74104200	-0.83995800
H	2.11365200	-4.82225000	-1.03852600
H	4.27759500	-3.49700000	-0.10464800
H	-3.15954100	-3.85325800	-0.23418800
H	-4.58702300	-1.63966900	0.32194400
H	5.14580500	1.67365800	1.33578300
H	3.85691900	3.90623000	0.52408800
H	-3.45368000	3.56328000	-0.80036100
H	-1.15219700	4.89550400	-1.28273800
H	-0.55525900	-0.47772600	-0.34941300
H	1.33915600	0.53308800	-0.15877100
C	-8.57637600	-0.39032100	2.44026600
O	-8.90523400	-1.33465300	1.71421300
C	-9.60415400	0.61236000	2.95815800
H	-9.66395600	0.57011700	4.06180100
H	-9.32300600	1.64711600	2.68877600
H	-10.58996900	0.37520300	2.53070700

Supporting Information Table 7: Geometry optimization coordinates for the tautomers of methylated N-confused porphyrins.

2-MeNCTPP-c

N	1.77613	0.88356	0.00222
N	-1.77613	-0.88356	0.00222
N	0.88356	-1.77613	-0.00222
C	-0.25718	3.00768	0.00122
C	-2.25105	2.00089	-0.00826
C	2.02244	2.25357	0.00827
C	3.04997	0.29193	-0.00102
C	-3.00768	-0.25718	-0.00122
C	-2.00089	-2.25105	0.00826
C	2.25105	-2.00089	-0.00826
C	0.25718	-3.00768	0.00122
C	-1.28053	4.07522	-0.00809
C	3.45269	2.42085	0.00923
C	-4.07522	-1.28053	0.00809
C	-3.42695	-2.4999	0.00955
C	2.4999	-3.42695	-0.00955
C	1.28053	-4.07522	-0.00809
H	-3.86532	-3.48657	0.00397
H	3.48657	-3.86532	-0.00397
H	3.89105	3.40753	0.00365
C	-1.06663	-3.22073	0.0088
C	1.06663	3.22073	0.0088
C	-3.22073	1.06663	-0.0088
C	3.22073	-1.06663	-0.0088
H	1.10124	-5.13009	-0.00664
H	-5.13009	-1.10124	0.00664
H	-1.10124	5.13009	-0.00664
C	-4.70914	1.46169	-0.02206
C	-5.39205	1.6482	1.18016
C	-5.3745	1.63316	-1.23592
C	-6.74018	2.00543	1.16842
H	-4.86741	1.51219	2.13697
C	-6.72279	1.99146	-1.24783
H	-4.83636	1.48637	-2.18354
C	-7.40572	2.17748	-0.04594
H	-7.27869	2.15184	2.11599

H	-7.24702	2.12699	-2.20505
H	-8.46866	2.4592	-0.05494
C	-1.46172	-4.70918	0.01522
C	-1.64359	-5.38778	-1.19014
C	-1.63763	-5.37893	1.22602
C	-2.00195	-6.73566	-1.18461
H	-1.50558	-4.85928	-2.14454
C	-1.99514	-6.72747	1.23172
H	-1.49415	-4.84428	2.17612
C	-2.17744	-7.40585	0.02669
H	-2.14593	-7.27044	-2.13464
H	-2.13337	-7.25539	2.18654
H	-2.45994	-8.46862	0.03081
C	1.46164	4.70918	0.01872
C	1.6358	5.37656	1.23146
C	1.64541	5.39009	-1.18467
C	1.99299	6.72473	1.24072
H	1.4901	4.83966	2.18001
C	2.00367	6.73842	-1.17558
H	1.50835	4.8642	-2.14059
C	2.17734	7.40583	0.03683
H	2.12967	7.25099	2.19657
H	2.14889	7.27492	-2.12455
H	2.45903	8.46879	0.04438
C	4.65258	-1.63347	-0.01964
C	5.2955	-1.88129	-1.23278
C	5.30675	-1.89902	1.18331
C	6.59204	-2.39518	-1.24288
H	4.7792	-1.67255	-2.18099
C	6.60406	-2.41214	1.17339
H	4.80025	-1.70359	2.13955
C	7.24671	-2.66037	-0.03943
H	7.09863	-2.59113	-2.19905
H	7.11976	-2.62103	2.12202
H	8.26902	-3.0655	-0.04764
N	-2.4999	3.42695	-0.00955
C	-0.88356	1.77613	-0.00222
H	-0.39979	0.85272	0.23897
C	-3.61302	4.38583	-0.05858
H	-4.17727	4.23178	-0.95456

H	-4.2466	4.24057	0.79134
H	-3.22541	5.38311	-0.04821
C	4.16255	1.20613	0.00426
H	5.13988	0.77055	0.00189
H	0.43185	-0.88397	-0.00064

2-MeNCTPP-a

N	1.77613	0.88356	0.00222
N	-1.77613	-0.88356	0.00222
N	0.88356	-1.77613	-0.00222
C	-0.25718	3.00768	0.00122
C	-2.25105	2.00089	-0.00826
C	2.02244	2.25357	0.00827
C	3.04997	0.29193	-0.00102
C	-3.00768	-0.25718	-0.00122
C	-2.00089	-2.25105	0.00826
C	2.25105	-2.00089	-0.00826
C	0.25718	-3.00768	0.00122
C	-1.28053	4.07522	-0.00809
C	3.45269	2.42085	0.00923
C	-4.07522	-1.28053	0.00809
C	-3.42695	-2.4999	0.00955
C	2.4999	-3.42695	-0.00955
C	1.28053	-4.07522	-0.00809
H	-3.86532	-3.48657	0.00397
H	3.48657	-3.86532	-0.00397
H	3.89105	3.40753	0.00365
C	-1.06663	-3.22073	0.0088
C	1.06663	3.22073	0.0088
C	-3.22073	1.06663	-0.0088
C	3.22073	-1.06663	-0.0088
H	1.10124	-5.13009	-0.00664
H	-5.13009	-1.10124	0.00664
H	-1.10124	5.13009	-0.00664
C	-4.70914	1.46169	-0.02206
C	-5.39205	1.6482	1.18016
C	-5.3745	1.63316	-1.23592
C	-6.74018	2.00543	1.16842
H	-4.86741	1.51219	2.13697

C	-6.72279	1.99146	-1.24783
H	-4.83636	1.48637	-2.18354
C	-7.40572	2.17748	-0.04594
H	-7.27869	2.15184	2.11599
H	-7.24702	2.12699	-2.20505
H	-8.46866	2.4592	-0.05494
C	-1.46172	-4.70918	0.01522
C	-1.64359	-5.38778	-1.19014
C	-1.63763	-5.37893	1.22602
C	-2.00195	-6.73566	-1.18461
H	-1.50558	-4.85928	-2.14454
C	-1.99514	-6.72747	1.23172
H	-1.49415	-4.84428	2.17612
C	-2.17744	-7.40585	0.02669
H	-2.14593	-7.27044	-2.13464
H	-2.13337	-7.25539	2.18654
H	-2.45994	-8.46862	0.03081
C	1.46164	4.70918	0.01872
C	1.6358	5.37656	1.23146
C	1.64541	5.39009	-1.18467
C	1.99299	6.72473	1.24072
H	1.4901	4.83966	2.18001
C	2.00367	6.73842	-1.17558
H	1.50835	4.8642	-2.14059
C	2.17734	7.40583	0.03683
H	2.12967	7.25099	2.19657
H	2.14889	7.27492	-2.12455
H	2.45903	8.46879	0.04438
C	4.65258	-1.63347	-0.01964
C	5.2955	-1.88129	-1.23278
C	5.30675	-1.89902	1.18331
C	6.59204	-2.39518	-1.24288
H	4.7792	-1.67255	-2.18099
C	6.60406	-2.41214	1.17339
H	4.80025	-1.70359	2.13955
C	7.24671	-2.66037	-0.03943
H	7.09863	-2.59113	-2.19905
H	7.11976	-2.62103	2.12202
H	8.26902	-3.0655	-0.04764
N	-2.4999	3.42695	-0.00955

C	-0.88356	1.77613	-0.00222
H	-0.39979	0.85272	0.23897
C	-3.61302	4.38583	-0.05858
H	-4.17727	4.23178	-0.95456
H	-4.2466	4.24057	0.79134
H	-3.22541	5.38311	-0.04821
H	0.88397	0.43185	0.00064
C	4.16255	1.20613	0.00426
H	5.13988	0.77055	0.00189

2-MeNCTPP-b

N	1.77613	0.88356	0.00222
N	-1.77613	-0.88356	0.00222
N	0.88356	-1.77613	-0.00222
C	-0.25718	3.00768	0.00122
C	-2.25105	2.00089	-0.00826
C	2.00089	2.25105	0.00826
C	3.00768	0.25718	-0.00122
C	-3.00768	-0.25718	-0.00122
C	-2.00089	-2.25105	0.00826
C	2.25105	-2.00089	-0.00826
C	0.25718	-3.00768	0.00122
C	-1.28053	4.07522	-0.00809
C	3.42695	2.4999	0.00955
C	-4.07522	-1.28053	0.00809
C	-3.42695	-2.4999	0.00955
C	2.4999	-3.42695	-0.00955
C	1.28053	-4.07522	-0.00809
H	-3.86532	-3.48657	0.00397
H	3.48657	-3.86532	-0.00397
H	3.86532	3.48657	0.00397
C	-1.06663	-3.22073	0.0088
C	1.06663	3.22073	0.0088
C	-3.22073	1.06663	-0.0088
C	3.22073	-1.06663	-0.0088
H	1.10124	-5.13009	-0.00664
H	-5.13009	-1.10124	0.00664
H	-1.10124	5.13009	-0.00664
C	-4.70914	1.46169	-0.02206

C	-5.39205	1.6482	1.18016
C	-5.3745	1.63316	-1.23592
C	-6.74018	2.00543	1.16842
H	-4.86741	1.51219	2.13697
C	-6.72279	1.99146	-1.24783
H	-4.83636	1.48637	-2.18354
C	-7.40572	2.17748	-0.04594
H	-7.27869	2.15184	2.11599
H	-7.24702	2.12699	-2.20505
H	-8.46866	2.4592	-0.05494
C	-1.46172	-4.70918	0.01522
C	-1.64359	-5.38778	-1.19014
C	-1.63763	-5.37893	1.22602
C	-2.00195	-6.73566	-1.18461
H	-1.50558	-4.85928	-2.14454
C	-1.99514	-6.72747	1.23172
H	-1.49415	-4.84428	2.17612
C	-2.17744	-7.40585	0.02669
H	-2.14593	-7.27044	-2.13464
H	-2.13337	-7.25539	2.18654
H	-2.45994	-8.46862	0.03081
C	1.46164	4.70918	0.01872
C	1.6358	5.37656	1.23146
C	1.64541	5.39009	-1.18467
C	1.99299	6.72473	1.24072
H	1.4901	4.83966	2.18001
C	2.00367	6.73842	-1.17558
H	1.50835	4.8642	-2.14059
C	2.17734	7.40583	0.03683
H	2.12967	7.25099	2.19657
H	2.14889	7.27492	-2.12455
H	2.45903	8.46879	0.04438
C	4.65258	-1.63347	-0.01964
C	5.2955	-1.88129	-1.23278
C	5.30675	-1.89902	1.18331
C	6.59204	-2.39518	-1.24288
H	4.7792	-1.67255	-2.18099
C	6.60406	-2.41214	1.17339
H	4.80025	-1.70359	2.13955
C	7.24671	-2.66037	-0.03943

H	7.09863	-2.59113	-2.19905
H	7.11976	-2.62103	2.12202
H	8.26902	-3.0655	-0.04764
N	-2.4999	3.42695	-0.00955
C	-0.88356	1.77613	-0.00222
H	-0.39979	0.85272	0.23897
C	-3.61302	4.38583	-0.05858
H	-4.17727	4.23178	-0.95456
H	-4.2466	4.24057	0.79134
H	-3.22541	5.38311	-0.04821
C	4.25212	1.16435	0.00416
H	5.22945	0.72878	0.00178
H	-0.88397	-0.43185	0.00064

2-MeNCTPP-h

C	0.98742	-2.78283	-0.24375
C	3.27211	-2.786	-0.18584
C	-0.83539	-1.10319	-0.03727
C	-0.80524	1.06917	0.10692
C	5.06639	-1.10262	0.09328
C	5.03543	1.07328	0.14626
C	0.97579	2.83636	0.08163
C	3.25352	2.83557	0.06691
C	1.47122	-3.96222	-0.84107
C	-2.23028	-0.67923	0.08717
C	6.44689	-0.67534	0.33294
C	6.43299	0.67865	0.343
C	1.43629	4.20307	0.18203
C	2.79548	4.20303	0.16894
H	7.27092	1.34831	0.4768
H	0.7824	5.05689	0.27787
H	-3.0914	-1.33142	0.12553
C	4.58648	2.42818	0.12143
C	-0.40556	-2.41706	-0.19836
C	4.65593	-2.43265	-0.02884
C	-0.35528	2.42728	0.12886
H	3.45157	5.05649	0.25251
H	7.29791	-1.32426	0.48211
H	0.92029	-4.75318	-1.32949

C	5.6782	-3.51293	0.07749
C	5.55139	-4.49743	1.07415
C	6.78276	-3.5815	-0.789
C	6.49913	-5.51193	1.2034
H	4.70852	-4.44995	1.75854
C	7.72802	-4.60026	-0.66328
H	6.88782	-2.8351	-1.57102
C	7.59034	-5.56908	0.33253
H	6.38945	-6.25495	1.98915
H	8.57146	-4.63834	-1.34776
H	8.32763	-6.36127	0.43072
C	5.62327	3.51024	0.19836
C	5.93624	4.28244	-0.93095
C	6.30418	3.77504	1.3972
C	6.90031	5.28995	-0.8652
H	5.41967	4.08361	-1.86609
C	7.27049	4.77972	1.46387
H	6.0665	3.18967	2.28132
C	7.57146	5.54098	0.33263
H	7.12908	5.87558	-1.75197
H	7.7842	4.97153	2.40249
H	8.32296	6.32439	0.38498
C	-1.40015	-3.50963	-0.37965
C	-1.34862	-4.66269	0.42606
C	-2.39505	-3.43851	-1.37211
C	-2.27004	-5.69588	0.25963
H	-0.59204	-4.73064	1.20238
C	-3.31172	-4.47552	-1.54252
H	-2.43052	-2.56919	-2.02135
C	-3.25541	-5.60671	-0.72583
H	-2.22102	-6.56977	0.90421
H	-4.06697	-4.40217	-2.32074
H	-3.97143	-6.41341	-0.85833
C	-1.39601	3.50268	0.22104
C	-1.66437	4.34311	-0.87076
C	-2.13081	3.6896	1.40293
C	-2.63506	5.3425	-0.78323
H	-1.10904	4.20346	-1.79428
C	-3.10293	4.68658	1.49111
H	-1.92947	3.04915	2.25732

C	-3.35796	5.51718	0.39792
H	-2.82925	5.9813	-1.64108
H	-3.65748	4.81772	2.41679
H	-4.11458	6.29438	0.46629
N	2.81696	-3.98051	-0.81106
C	2.13684	-2.06224	0.16047
H	2.14772	-1.11402	0.66332
C	3.59396	-4.99302	-1.52265
H	4.32725	-4.51823	-2.17717
H	4.11944	-5.65522	-0.83195
H	2.90428	-5.58022	-2.13276
C	-2.21451	0.67322	0.16668
H	-3.05989	1.34071	0.25709
N	0.	0.	0.
H	0.71954	0.0075	-0.69441
N	2.11508	2.05243	0.
H	2.60857	1.40043	0.57564
N	4.23964	0.	0.
H	3.77885	0.4218	-0.78087

2-MeNCTPP-i

N	0.	0.	0.
N	4.23964	0.	0.
N	2.11508	2.05243	0.
C	0.98742	-2.78283	-0.24375
C	3.27211	-2.786	-0.18584
C	-0.83637	-1.10241	-0.03849
C	-0.80524	1.06917	0.10692
C	5.06639	-1.10262	0.09328
C	5.03543	1.07328	0.14626
C	0.97579	2.83636	0.08163
C	3.25352	2.83557	0.06691
C	1.47122	-3.96222	-0.84107
C	-2.23028	-0.67923	0.08717
C	6.44689	-0.67534	0.33294
C	6.43299	0.67865	0.343
C	1.43629	4.20307	0.18203
C	2.79548	4.20303	0.16894
H	7.27092	1.34831	0.4768

H	0.7824	5.05689	0.27787
H	-3.0914	-1.33142	0.12553
C	4.58648	2.42818	0.12143
C	-0.40556	-2.41706	-0.19836
C	4.65593	-2.43265	-0.02884
C	-0.35528	2.42728	0.12886
H	3.45157	5.05649	0.25251
H	7.29791	-1.32426	0.48211
H	0.92029	-4.75318	-1.32949
C	5.6782	-3.51293	0.07749
C	5.55139	-4.49743	1.07415
C	6.78276	-3.5815	-0.789
C	6.49913	-5.51193	1.2034
H	4.70852	-4.44995	1.75854
C	7.72802	-4.60026	-0.66328
H	6.88782	-2.8351	-1.57102
C	7.59034	-5.56908	0.33253
H	6.38945	-6.25495	1.98915
H	8.57146	-4.63834	-1.34776
H	8.32763	-6.36127	0.43072
C	5.62327	3.51024	0.19836
C	5.93624	4.28244	-0.93095
C	6.30418	3.77504	1.3972
C	6.90031	5.28995	-0.8652
H	5.41967	4.08361	-1.86609
C	7.27049	4.77972	1.46387
H	6.0665	3.18967	2.28132
C	7.57146	5.54098	0.33263
H	7.12908	5.87558	-1.75197
H	7.7842	4.97153	2.40249
H	8.32296	6.32439	0.38498
C	-1.40015	-3.50963	-0.37965
C	-1.34862	-4.66269	0.42606
C	-2.39505	-3.43851	-1.37211
C	-2.27004	-5.69588	0.25963
H	-0.59204	-4.73064	1.20238
C	-3.31172	-4.47552	-1.54252
H	-2.43052	-2.56919	-2.02135
C	-3.25541	-5.60671	-0.72583
H	-2.22102	-6.56977	0.90421

H	-4.06697	-4.40217	-2.32074
H	-3.97143	-6.41341	-0.85833
C	-1.39601	3.50268	0.22104
C	-1.66437	4.34311	-0.87076
C	-2.13081	3.6896	1.40293
C	-2.63506	5.3425	-0.78323
H	-1.10904	4.20346	-1.79428
C	-3.10293	4.68658	1.49111
H	-1.92947	3.04915	2.25732
C	-3.35796	5.51718	0.39792
H	-2.82925	5.9813	-1.64108
H	-3.65748	4.81772	2.41679
H	-4.11458	6.29438	0.46629
N	2.81696	-3.98051	-0.81106
C	2.13684	-2.06224	0.16047
H	2.14772	-1.11402	0.66332
C	3.59396	-4.99302	-1.52265
H	4.32725	-4.51823	-2.17717
H	4.11944	-5.65522	-0.83195
H	2.90428	-5.58022	-2.13276
C	-2.21451	0.67322	0.16668
H	-3.05989	1.34071	0.25709

24-MeNCTPP-a

N	0.	0.	0.
N	3.96753	0.	0.
N	1.98377	1.98377	0.
C	0.87442	-2.80742	-0.00729
C	3.10801	-2.79404	-0.01674
C	-0.81031	-1.12426	0.00351
C	-0.82366	1.10935	-0.00095
C	4.79119	-1.10934	-0.00593
C	4.77784	1.12423	0.00855
C	0.85952	2.79409	-0.00422
C	3.09311	2.80742	0.00529
C	1.31518	-4.21899	-0.01977
C	-2.19794	-0.7119	0.00573
C	6.20279	-0.66859	0.00437
C	6.16548	0.71187	0.00892

C	1.27188	4.18173	-0.00241
C	2.65235	4.21904	-0.00086
H	6.99742	1.40004	0.00489
H	0.58372	5.01365	0.00504
H	-3.02989	-1.40005	-0.00139
C	4.37326	2.40854	0.01197
C	-0.40573	-2.40856	0.00118
C	4.39232	-2.38946	-0.01637
C	-0.42479	2.38951	-0.00567
H	3.28271	5.08363	0.00252
H	7.06739	-1.29895	0.00151
H	0.68482	-5.08359	-0.02025
C	5.54899	-3.40607	-0.03191
C	6.07735	-3.87991	1.16924
C	6.06833	-3.85322	-1.24677
C	7.12527	-4.80018	1.15545
H	5.6682	-3.52661	2.12685
C	7.11591	-4.77451	-1.26075
H	5.6519	-3.47999	-2.19357
C	7.64451	-5.24793	-0.05992
H	7.5422	-5.17324	2.10218
H	7.52492	-5.1272	-2.21877
H	8.47072	-5.97358	-0.07054
C	5.38994	3.5652	0.02098
C	5.85502	4.09448	-1.1832
C	5.84574	4.08379	1.23295
C	6.77621	5.14164	-1.17531
H	5.49606	3.6849	-2.13852
C	6.76647	5.13194	1.241
H	5.47916	3.66688	2.18212
C	7.23184	5.66081	0.03715
H	7.14332	5.55845	-2.12442
H	7.12536	5.54089	2.19674
H	7.95813	6.48651	0.04312
C	-1.42234	-3.5653	0.00851
C	-1.87552	-4.08798	1.22008
C	-1.89015	-4.0904	-1.19606
C	-2.79579	-5.13596	1.22699
H	-1.50594	-3.67429	2.16956
C	-2.81145	-5.13805	-1.18931

H	-1.53321	-3.67846	-2.15106
C	-3.26421	-5.66097	0.02193
H	-3.15257	-5.54841	2.18192
H	-3.18043	-5.5516	-2.13921
H	-3.98985	-6.48723	0.02763
C	-1.4543	3.53478	-0.01394
C	-1.91955	4.04573	-1.22594
C	-1.92173	4.06121	1.19019
C	-2.85151	5.08333	-1.23372
H	-1.55026	3.63101	-2.17509
C	-2.85471	5.09846	1.18259
H	-1.55528	3.6585	2.14553
C	-3.31954	5.60966	-0.02908
H	-3.2178	5.48655	-2.18899
H	-3.22339	5.51305	2.13215
H	-4.0544	6.42773	-0.03546
N	2.69565	-4.18167	-0.02114
C	1.98377	-1.98375	-0.00889
C	2.49757	-0.01039	-0.00234
H	2.14614	-0.87241	0.52522
H	2.13388	0.8742	0.47738
H	0.99997	0.00707	-0.00156
H	2.14272	-0.04051	-1.01134
H	1.9762	-0.91379	-0.0048
C	-2.3419	0.85139	0.00384
H	-3.19024	1.50348	0.00535

24-MeNCTPP-c

N	0.	0.	0.
N	3.96753	0.	0.
N	1.98377	1.98377	0.
C	0.87442	-2.80742	-0.00729
C	3.10801	-2.79404	-0.01674
C	-0.81031	-1.12426	0.00351
C	-0.82366	1.10935	-0.00095
C	4.79119	-1.10934	-0.00593
C	4.77784	1.12423	0.00855
C	0.85952	2.79409	-0.00422
C	3.09311	2.80742	0.00529

C	1.31518	-4.21899	-0.01977
C	-2.19794	-0.7119	0.00573
C	6.20279	-0.66859	0.00437
C	6.16548	0.71187	0.00892
C	1.27188	4.18173	-0.00241
C	2.65235	4.21904	-0.00086
H	6.99742	1.40004	0.00489
H	0.58372	5.01365	0.00504
H	-3.02989	-1.40005	-0.00139
C	4.37326	2.40854	0.01197
C	-0.40573	-2.40856	0.00118
C	4.39232	-2.38946	-0.01637
C	-0.42479	2.38951	-0.00567
H	3.28271	5.08363	0.00252
H	7.06739	-1.29895	0.00151
H	0.68482	-5.08359	-0.02025
C	5.54899	-3.40607	-0.03191
C	6.07735	-3.87991	1.16924
C	6.06833	-3.85322	-1.24677
C	7.12527	-4.80018	1.15545
H	5.6682	-3.52661	2.12685
C	7.11591	-4.77451	-1.26075
H	5.6519	-3.47999	-2.19357
C	7.64451	-5.24793	-0.05992
H	7.5422	-5.17324	2.10218
H	7.52492	-5.1272	-2.21877
H	8.47072	-5.97358	-0.07054
C	5.38994	3.5652	0.02098
C	5.85502	4.09448	-1.1832
C	5.84574	4.08379	1.23295
C	6.77621	5.14164	-1.17531
H	5.49606	3.6849	-2.13852
C	6.76647	5.13194	1.241
H	5.47916	3.66688	2.18212
C	7.23184	5.66081	0.03715
H	7.14332	5.55845	-2.12442
H	7.12536	5.54089	2.19674
H	7.95813	6.48651	0.04312
C	-1.42234	-3.5653	0.00851
C	-1.87552	-4.08798	1.22008

C	-1.89015	-4.0904	-1.19606
C	-2.79579	-5.13596	1.22699
H	-1.50594	-3.67429	2.16956
C	-2.81145	-5.13805	-1.18931
H	-1.53321	-3.67846	-2.15106
C	-3.26421	-5.66097	0.02193
H	-3.15257	-5.54841	2.18192
H	-3.18043	-5.5516	-2.13921
H	-3.98985	-6.48723	0.02763
C	-1.4543	3.53478	-0.01394
C	-1.91955	4.04573	-1.22594
C	-1.92173	4.06121	1.19019
C	-2.85151	5.08333	-1.23372
H	-1.55026	3.63101	-2.17509
C	-2.85471	5.09846	1.18259
H	-1.55528	3.6585	2.14553
C	-3.31954	5.60966	-0.02908
H	-3.2178	5.48655	-2.18899
H	-3.22339	5.51305	2.13215
H	-4.0544	6.42773	-0.03546
N	2.69565	-4.18167	-0.02114
C	1.98377	-1.98375	-0.00889
C	2.96051	0.32788	1.01946
H	3.28702	-0.03306	1.97236
H	2.83161	1.38911	1.06511
H	2.02991	-0.13374	0.76298
H	1.9762	-0.91379	-0.0048
H	1.99084	0.9838	-0.00066
C	-2.3419	0.85139	0.00384
H	-3.19024	1.50348	0.00535

24-MeNCTPP-d

N	0.	0.	0.
N	3.96753	0.	0.
N	1.98377	1.98377	0.
C	0.87442	-2.80742	-0.00729
C	3.10801	-2.79404	-0.01674
C	-0.81031	-1.12426	0.00351
C	-0.82366	1.10935	-0.00095

C	4.79119	-1.10934	-0.00593
C	4.77784	1.12423	0.00855
C	0.85952	2.79409	-0.00422
C	3.09311	2.80742	0.00529
C	1.31518	-4.21899	-0.01977
C	-2.19794	-0.7119	0.00573
C	6.20279	-0.66859	0.00437
C	6.16548	0.71187	0.00892
C	1.27188	4.18173	-0.00241
C	2.65235	4.21904	-0.00086
H	6.99742	1.40004	0.00489
H	0.58372	5.01365	0.00504
H	-3.02989	-1.40005	-0.00139
C	4.37326	2.40854	0.01197
C	-0.40573	-2.40856	0.00118
C	4.39232	-2.38946	-0.01637
C	-0.42479	2.38951	-0.00567
H	3.28271	5.08363	0.00252
H	7.06739	-1.29895	0.00151
H	0.68482	-5.08359	-0.02025
C	5.54899	-3.40607	-0.03191
C	6.07735	-3.87991	1.16924
C	6.06833	-3.85322	-1.24677
C	7.12527	-4.80018	1.15545
H	5.6682	-3.52661	2.12685
C	7.11591	-4.77451	-1.26075
H	5.6519	-3.47999	-2.19357
C	7.64451	-5.24793	-0.05992
H	7.5422	-5.17324	2.10218
H	7.52492	-5.1272	-2.21877
H	8.47072	-5.97358	-0.07054
C	5.38994	3.5652	0.02098
C	5.85502	4.09448	-1.1832
C	5.84574	4.08379	1.23295
C	6.77621	5.14164	-1.17531
H	5.49606	3.6849	-2.13852
C	6.76647	5.13194	1.241
H	5.47916	3.66688	2.18212
C	7.23184	5.66081	0.03715
H	7.14332	5.55845	-2.12442

H	7.12536	5.54089	2.19674
H	7.95813	6.48651	0.04312
C	-1.42234	-3.5653	0.00851
C	-1.87552	-4.08798	1.22008
C	-1.89015	-4.0904	-1.19606
C	-2.79579	-5.13596	1.22699
H	-1.50594	-3.67429	2.16956
C	-2.81145	-5.13805	-1.18931
H	-1.53321	-3.67846	-2.15106
C	-3.26421	-5.66097	0.02193
H	-3.15257	-5.54841	2.18192
H	-3.18043	-5.5516	-2.13921
H	-3.98985	-6.48723	0.02763
C	-1.4543	3.53478	-0.01394
C	-1.91955	4.04573	-1.22594
C	-1.92173	4.06121	1.19019
C	-2.85151	5.08333	-1.23372
H	-1.55026	3.63101	-2.17509
C	-2.85471	5.09846	1.18259
H	-1.55528	3.6585	2.14553
C	-3.31954	5.60966	-0.02908
H	-3.2178	5.48655	-2.18899
H	-3.22339	5.51305	2.13215
H	-4.0544	6.42773	-0.03546
N	2.69565	-4.18167	-0.02114
C	1.98377	-1.98375	-0.00889
C	2.49757	-0.01039	-0.00234
H	2.14317	-0.52857	0.86414
H	2.13376	0.99579	0.01014
H	2.1458	-0.50594	-0.88301
H	1.9762	-0.91379	-0.0048
H	3.3044	-4.97503	-0.02458
C	-2.3419	0.85139	0.00384
H	-3.19024	1.50348	0.00535

24-MeNCTPP-h

N	1.48127	-1.62148	0.1358
N	-1.50454	1.66515	-0.40487
C	-1.37908	-2.63118	0.04615

C	-2.90755	-0.97363	-0.14514
C	1.08838	-2.94626	0.25814
C	2.85141	-1.5064	0.14373
C	-2.80386	1.47044	0.06942
C	-0.99883	2.83985	0.12915
C	2.9582	0.96122	-0.21135
C	1.49613	2.58607	-0.21673
C	-2.6748	-3.09965	-0.47245
C	2.30725	-3.69556	0.4078
C	-3.13099	2.59026	0.87306
C	-2.02988	3.42155	0.91683
C	3.71109	2.18948	-0.45573
C	2.80434	3.19433	-0.47166
H	-1.91033	4.3166	1.51003
H	4.78029	2.25918	-0.59684
H	2.34908	-4.76404	0.55741
C	0.32389	3.34786	-0.02743
C	-0.21956	-3.44626	0.18037
C	-3.56282	0.27319	-0.09505
C	3.56331	-0.31126	-0.05113
H	2.98808	4.24457	-0.64691
H	-4.05066	2.68873	1.43229
H	-2.89227	-4.11505	-0.7883
C	-5.03561	0.38282	-0.12157
C	-5.65682	1.48708	-0.73872
C	-5.8586	-0.59455	0.4733
C	-7.04427	1.61142	-0.76062
H	-5.04188	2.239	-1.22338
C	-7.24414	-0.46652	0.45133
H	-5.39996	-1.45075	0.95197
C	-7.84406	0.63542	-0.16399
H	-7.5003	2.46726	-1.2513
H	-7.85978	-1.22891	0.92123
H	-8.92662	0.73067	-0.17984
C	0.45245	4.82307	0.16615
C	1.32779	5.36377	1.12564
C	-0.33069	5.71221	-0.59222
C	1.42692	6.74284	1.30807
H	1.91889	4.69148	1.73992
C	-0.22686	7.09091	-0.41485

H	-1.01459	5.31222	-1.33526
C	0.65325	7.61175	0.53624
H	2.10399	7.13809	2.06082
H	-0.83236	7.75917	-1.02153
H	0.73176	8.68634	0.67797
C	-0.40955	-4.92635	0.18867
C	0.23401	-5.76019	-0.74265
C	-1.27553	-5.51809	1.1251
C	0.02796	-7.13949	-0.72934
H	0.88167	-5.31652	-1.4931
C	-1.47786	-6.89766	1.14077
H	-1.77885	-4.88652	1.85142
C	-0.82584	-7.7138	0.21445
H	0.52804	-7.76483	-1.46429
H	-2.14464	-7.33512	1.87913
H	-0.98591	-8.78857	0.22435
C	5.05738	-0.41294	-0.09537
C	5.7925	-0.70319	1.06476
C	5.75533	-0.23037	-1.29985
C	7.18365	-0.80874	1.02231
H	5.26569	-0.83787	2.00557
C	7.14642	-0.33099	-1.34243
H	5.19785	-0.0139	-2.20708
C	7.86527	-0.62202	-0.18143
H	7.73468	-1.03088	1.93252
H	7.66796	-0.1879	-2.28529
H	8.94853	-0.70221	-0.21469
C	-1.57487	-1.26092	0.24461
C	-1.01329	1.09679	-1.66482
H	-1.82716	0.55521	-2.14513
H	-0.6877	1.91542	-2.3128
H	0.9046	-0.79382	0.02084
H	-0.16889	0.43	-1.50133
H	-0.90522	-0.55412	0.71145
C	3.36774	-2.83407	0.3232
H	4.41779	-3.08074	0.37621
N	-3.56048	-2.15104	-0.58677
H	-4.50609	-2.19083	-0.90965
N	1.62553	1.22227	-0.09763
H	0.90067	0.79233	0.44063

24-MeNCTPP-i

N	1.48127	-1.62148	0.1358
N	-1.50454	1.66515	-0.40487
C	-1.37908	-2.63118	0.04615
C	-2.90755	-0.97363	-0.14514
C	1.08838	-2.94626	0.25814
C	2.85141	-1.5064	0.14373
C	-2.80386	1.47044	0.06942
C	-0.99883	2.83985	0.12915
C	2.9582	0.96122	-0.21135
C	1.49613	2.58607	-0.21673
C	-2.6748	-3.09965	-0.47245
C	2.30725	-3.69556	0.4078
C	-3.13099	2.59026	0.87306
C	-2.02988	3.42155	0.91683
C	3.71109	2.18948	-0.45573
C	2.80434	3.19433	-0.47166
H	-1.91033	4.3166	1.51003
H	4.78029	2.25918	-0.59684
H	2.34908	-4.76404	0.55741
C	0.32389	3.34786	-0.02743
C	-0.21956	-3.44626	0.18037
C	-3.56282	0.27319	-0.09505
C	3.56331	-0.31126	-0.05113
H	2.98808	4.24457	-0.64691
H	-4.05066	2.68873	1.43229
H	-2.89227	-4.11505	-0.7883
C	-5.03561	0.38282	-0.12157
C	-5.65682	1.48708	-0.73872
C	-5.8586	-0.59455	0.4733
C	-7.04427	1.61142	-0.76062
H	-5.04188	2.239	-1.22338
C	-7.24414	-0.46652	0.45133
H	-5.39996	-1.45075	0.95197
C	-7.84406	0.63542	-0.16399
H	-7.5003	2.46726	-1.2513
H	-7.85978	-1.22891	0.92123
H	-8.92662	0.73067	-0.17984

C	0.45245	4.82307	0.16615
C	1.32779	5.36377	1.12564
C	-0.33069	5.71221	-0.59222
C	1.42692	6.74284	1.30807
H	1.91889	4.69148	1.73992
C	-0.22686	7.09091	-0.41485
H	-1.01459	5.31222	-1.33526
C	0.65325	7.61175	0.53624
H	2.10399	7.13809	2.06082
H	-0.83236	7.75917	-1.02153
H	0.73176	8.68634	0.67797
C	-0.40955	-4.92635	0.18867
C	0.23401	-5.76019	-0.74265
C	-1.27553	-5.51809	1.1251
C	0.02796	-7.13949	-0.72934
H	0.88167	-5.31652	-1.4931
C	-1.47786	-6.89766	1.14077
H	-1.77885	-4.88652	1.85142
C	-0.82584	-7.7138	0.21445
H	0.52804	-7.76483	-1.46429
H	-2.14464	-7.33512	1.87913
H	-0.98591	-8.78857	0.22435
C	5.05738	-0.41294	-0.09537
C	5.7925	-0.70319	1.06476
C	5.75533	-0.23037	-1.29985
C	7.18365	-0.80874	1.02231
H	5.26569	-0.83787	2.00557
C	7.14642	-0.33099	-1.34243
H	5.19785	-0.0139	-2.20708
C	7.86527	-0.62202	-0.18143
H	7.73468	-1.03088	1.93252
H	7.66796	-0.1879	-2.28529
H	8.94853	-0.70221	-0.21469
C	-1.57487	-1.26092	0.24461
C	-1.01329	1.09679	-1.66482
H	-1.82716	0.55521	-2.14513
H	-0.6877	1.91542	-2.3128
H	-0.16889	0.43	-1.50133
H	-0.90522	-0.55412	0.71145
C	3.36774	-2.83407	0.3232

H	4.41779	-3.08074	0.37621
N	-3.56048	-2.15104	-0.58677
N	1.62553	1.22227	-0.09763

22-MeNCTPP-d

H	0.77496	0.92186	0.11085
N	-2.97812	2.87707	0.51828
N	-1.29454	-1.85046	0.44594
N	1.7412	-1.03192	0.08969
N	1.24755	1.79873	-0.07499
C	-1.71047	2.46076	0.02319
C	-1.70968	1.07649	-0.21895
C	-3.70904	1.8009	0.5696
C	-2.99098	0.60078	0.12257
C	-3.48832	-0.72481	0.05508
C	-2.60834	-1.83077	-0.03491
C	-2.7985	-3.02788	-0.7793
C	-1.60976	-3.72122	-0.78658
C	-0.65111	-2.97915	-0.03486
C	0.71955	-3.30677	0.13775
C	1.78423	-2.38512	0.29891
C	3.1491	-2.80481	0.62496
C	3.92259	-1.69556	0.56187
C	3.0322	-0.59455	0.20214
C	3.47422	0.73175	-0.01163
C	2.61505	1.83615	-0.19975
C	2.9548	3.18878	-0.51909
C	1.79472	3.923	-0.54872
C	0.69435	3.05623	-0.24867
C	-0.66674	3.40881	-0.11416
C	-4.94297	-0.97992	-0.02756
C	-5.52352	-2.07851	0.63679
C	-6.89334	-2.31866	0.56171
C	-7.71672	-1.46747	-0.17817
C	-7.15756	-0.37604	-0.84619
C	-5.78754	-0.1353	-0.77499
C	1.04706	-4.75582	-0.00299
C	0.36543	-5.7202	0.76166
C	0.65403	-7.0774	0.62994

C	1.62546	-7.50338	-0.27786
C	2.30337	-6.56101	-1.05331
C	2.01728	-5.20329	-0.91863
C	4.94264	1.00362	-0.04363
C	5.76936	0.37361	-0.98929
C	7.14036	0.62689	-1.02249
C	7.71312	1.515	-0.11053
C	6.9047	2.14824	0.83495
C	5.53346	1.89584	0.8673
C	-1.01003	4.85623	-0.07401
C	-0.33563	5.74437	0.78157
C	-0.66394	7.09932	0.80927
C	-1.67124	7.59341	-0.02001
C	-2.35523	6.72072	-0.86922
C	-2.03372	5.36637	-0.89116
C	-0.8869	-1.19516	1.69219
H	-0.93462	0.48512	-0.68258
H	-4.72017	1.82126	0.96325
H	-3.69572	-3.26114	-1.33373
H	-1.38292	-4.62191	-1.33704
H	3.45333	-3.80697	0.88867
H	4.98083	-1.61338	0.76162
H	3.95628	3.54214	-0.71022
H	1.69595	4.97297	-0.77634
H	-4.89162	-2.72971	1.23187
H	-7.32042	-3.16603	1.0902
H	-8.785	-1.65417	-0.23535
H	-7.78854	0.28377	-1.43447
H	-5.35458	0.69586	-1.3214
H	-0.3862	-5.39407	1.47392
H	0.12265	-7.80231	1.23988
H	1.84938	-8.5609	-0.38287
H	3.05081	-6.8836	-1.77246
H	2.53384	-4.47671	-1.53709
H	5.32504	-0.30963	-1.7063
H	7.7604	0.13387	-1.76574
H	8.78088	1.71187	-0.1362
H	7.34232	2.83526	1.55361
H	4.91049	2.38046	1.61281
H	0.43226	5.36138	1.44585

H	-0.13754	7.76642	1.48591
H	-1.92646	8.64902	-0.00045
H	-3.14357	7.09623	-1.51518
H	-2.57011	4.69062	-1.54753
H	-0.08652	-0.47757	1.52349
H	-0.52351	-1.95785	2.38615
H	-1.74921	-0.6929	2.12568

22-MeNCTPP-c

N	-2.99493	2.86403	0.51897
N	-1.28421	-1.85375	0.44664
N	1.74677	-1.01778	0.09039
H	0.87751	-0.42974	-0.11818
N	1.23686	1.81	-0.0743
C	-1.72491	2.45501	0.02388
C	-1.71616	1.07077	-0.21825
C	-3.71966	1.78368	0.5703
C	-2.99471	0.5877	0.12327
C	-3.48443	-0.74072	0.05578
C	-2.59811	-1.84161	-0.03421
C	-2.78138	-3.03979	-0.7786
C	-1.58868	-3.72629	-0.78589
C	-0.63431	-2.97872	-0.03416
C	0.73821	-3.29845	0.13845
C	1.79757	-2.37071	0.2996
C	3.16484	-2.78254	0.62565
C	3.93194	-1.66887	0.56256
C	3.03524	-0.573	0.20283
C	3.46963	0.75582	-0.01093
C	2.60412	1.85527	-0.19905
C	2.9361	3.20983	-0.5184
C	1.77182	3.93737	-0.54802
C	0.67645	3.06429	-0.24797
C	-0.68664	3.40904	-0.11347
C	-4.93759	-1.00419	-0.02687
C	-5.51181	-2.10609	0.63749
C	-6.88023	-2.35411	0.56241
C	-7.70849	-1.50767	-0.17748
C	-7.15561	-0.41304	-0.84549

C	-5.787	-0.16443	-0.7743
C	1.07404	-4.7456	-0.0023
C	0.39796	-5.71388	0.76236
C	0.69436	-7.0694	0.63063
C	1.66822	-7.4898	-0.27717
C	2.3407	-6.54355	-1.05261
C	2.04682	-5.18749	-0.91793
C	4.93646	1.03612	-0.04293
C	5.76679	0.41088	-0.9886
C	7.13631	0.67203	-1.02179
C	7.70396	1.56341	-0.10983
C	6.89191	2.192	0.83564
C	5.52215	1.93173	0.86799
C	-1.03824	4.85447	-0.07331
C	-0.36896	5.74647	0.78226
C	-0.70505	7.09951	0.80996
C	-1.71517	7.58781	-0.01931
C	-2.39414	6.7112	-0.86852
C	-2.06485	5.35872	-0.89047
C	-0.88035	-1.19612	1.69288
H	-0.93772	0.48386	-0.68188
H	-4.73088	1.79823	0.96394
H	-3.67725	-3.2782	-1.33303
H	-1.35666	-4.62566	-1.33634
H	3.47483	-3.78294	0.88937
H	4.9897	-1.58061	0.76232
H	3.93554	3.56894	-0.70953
H	1.66702	4.98675	-0.77564
H	-4.87618	-2.75365	1.23256
H	-7.30244	-3.20392	1.09089
H	-8.77568	-1.70051	-0.23466
H	-7.79037	0.24314	-1.43378
H	-5.35882	0.6692	-1.3207
H	-0.35552	-5.39208	1.47461
H	0.16715	-7.79735	1.24057
H	1.89822	-8.54601	-0.38217
H	3.08999	-6.86184	-1.77176
H	2.55919	-4.45795	-1.5364
H	5.3264	-0.27491	-1.7056
H	7.75917	0.18258	-1.76504

H	8.77057	1.76642	-0.1355
H	7.32558	2.88152	1.5543
H	4.8964	2.41276	1.61351
H	0.40112	5.3679	1.44654
H	-0.1825	7.76962	1.48661
H	-1.97646	8.64193	0.00024
H	-3.18462	7.08217	-1.51449
H	-2.59735	4.67989	-1.54683
H	-0.0841	-0.47394	1.52418
H	-0.51258	-1.9567	2.38684
H	-1.74553	-0.69882	2.12637

22-MeNCTPP-d

N	-4.04366	-0.20688	0.5725
H	-4.90019	0.23311	0.87363
N	0.54983	-2.14926	0.42798
N	2.02667	0.49316	-0.06418
N	-0.528	2.09577	0.02174
C	-2.94672	0.49269	0.04432
C	-1.96464	-0.45755	-0.20892
C	-3.75506	-1.5176	0.67594
C	-2.44682	-1.73143	0.19199
C	-1.77311	-3.01332	0.11771
C	-0.38413	-3.11973	0.03963
C	0.35937	-4.16967	-0.60954
C	1.67129	-3.80418	-0.65198
C	1.81175	-2.51592	-0.02063
C	2.99683	-1.76635	0.07097
C	3.05089	-0.33888	0.19447
C	4.25684	0.4064	0.58788
C	3.91951	1.71521	0.5392
C	2.50762	1.76567	0.12468
C	1.78701	2.95902	-0.02856
C	0.36216	3.07222	-0.20157
C	-0.31239	4.30879	-0.62518
C	-1.64188	4.04036	-0.62479
C	-1.76839	2.64311	-0.21375
C	-2.9596	1.91822	-0.10395
C	-2.58762	-4.24485	0.01514

C	-2.22998	-5.41012	0.7232
C	-2.99424	-6.57128	0.63154
C	-4.14087	-6.5989	-0.16469
C	-4.51316	-5.45336	-0.87168
C	-3.74878	-4.29216	-0.78362
C	4.27757	-2.51192	-0.07063
C	4.52983	-3.67018	0.68827
C	5.72586	-4.37368	0.55386
C	6.70191	-3.93465	-0.34225
C	6.46916	-2.7875	-1.10381
C	5.27239	-2.08583	-0.97129
C	2.55606	4.2398	-0.00294
C	3.60998	4.46919	-0.90439
C	4.32613	5.66594	-0.88104
C	4.00593	6.65812	0.04669
C	2.96139	6.44589	0.94884
C	2.24192	5.25216	0.92112
C	-4.27122	2.61284	-0.12255
C	-4.50115	3.74861	0.67768
C	-5.73764	4.39118	0.66885
C	-6.7752	3.91326	-0.13431
C	-6.56613	2.78607	-0.93113
C	-5.33034	2.14063	-0.9239
C	0.33995	-1.23492	1.55518
H	-0.99967	-0.2271	-0.62909
H	-4.45966	-2.22148	1.09343
H	-0.0962	-5.02682	-1.08292
H	2.4771	-4.31832	-1.15396
H	5.20097	-0.02483	0.88921
H	4.53315	2.56453	0.80171
H	0.17188	5.23303	-0.90567
H	-2.44907	4.69508	-0.92141
H	-1.35521	-5.38688	1.36487
H	-2.7003	-7.45304	1.19379
H	-4.73841	-7.50308	-0.23355
H	-5.39594	-5.46807	-1.50475
H	-4.02899	-3.41671	-1.36022
H	3.78231	-4.00592	1.40037
H	5.89907	-5.26038	1.15722
H	7.63492	-4.48083	-0.44648

H	7.21821	-2.44266	-1.81109
H	5.09068	-1.20592	-1.57987
H	3.85405	3.70366	-1.63404
H	5.132	5.82441	-1.59214
H	4.56442	7.58953	0.06621
H	2.70851	7.20973	1.67881
H	1.43535	5.08838	1.62897
H	-3.70375	4.11004	1.31826
H	-5.89398	5.26247	1.29822
H	-7.7384	4.4147	-0.13902
H	-7.36313	2.41403	-1.56853
H	-5.16509	1.28243	-1.5683
H	0.16925	-0.21052	1.22194
H	1.23608	-1.25329	2.1795
H	-0.50765	-1.59739	2.13828

22-MeNCTPP-h

H	0.76683	0.92849	0.11006
N	-1.28089	-1.86082	0.44422
N	1.2334	1.80897	-0.07835
C	-1.72993	2.44774	0.02358
C	-1.72044	1.06395	-0.22384
C	-3.71987	1.76994	0.57882
C	-2.9956	0.5768	0.12303
C	-3.48261	-0.75276	0.05229
C	-2.59347	-1.85062	-0.04042
C	-2.77277	-3.04979	-0.78496
C	-1.57915	-3.73439	-0.7891
C	-0.62736	-2.98512	-0.03499
C	0.74486	-3.3018	0.14013
C	1.80159	-2.3707	0.30389
C	3.16883	-2.77872	0.63586
C	3.93368	-1.66345	0.5709
C	3.03536	-0.57085	0.20424
C	3.46775	0.75795	-0.01359
C	2.60074	1.8558	-0.20504
C	2.92913	3.2105	-0.52781
C	1.76308	3.93588	-0.55709
C	0.66944	3.06153	-0.25385

C	-0.69427	3.40383	-0.11563
C	-4.93534	-1.01863	-0.03105
C	-5.50814	-2.12382	0.62937
C	-6.87652	-2.37344	0.554
C	-7.70638	-1.52528	-0.18264
C	-7.15498	-0.42721	-0.8468
C	-5.78642	-0.17707	-0.7748
C	1.08497	-4.74805	0.00052
C	0.40989	-5.71825	0.76388
C	0.71031	-7.07327	0.63318
C	1.6875	-7.4913	-0.27255
C	2.35933	-6.54304	-1.04665
C	2.06137	-5.18754	-0.91259
C	4.93421	1.04056	-0.04591
C	5.76556	0.41544	-0.99093
C	7.13489	0.67897	-1.02497
C	7.7014	1.5725	-0.11397
C	6.88829	2.20087	0.83116
C	5.51866	1.93839	0.8638
C	-1.04824	4.8486	-0.07237
C	-0.37791	5.74071	0.78248
C	-0.71649	7.09331	0.81364
C	-1.7301	7.58129	-0.01206
C	-2.40979	6.70466	-0.86108
C	-2.07797	5.35254	-0.88603
C	-0.88039	-1.19473	1.68619
H	-0.94474	0.48086	-0.69862
H	-4.72892	1.78188	0.97959
H	-3.66748	-3.29044	-1.34173
H	-1.34432	-4.63372	-1.33978
H	3.48042	-3.77801	0.90488
H	4.99126	-1.57213	0.7741
H	3.92799	3.57192	-0.72157
H	1.65622	4.98527	-0.78704
H	-4.87155	-2.77314	1.2226
H	-7.29742	-3.22632	1.07993
H	-8.77399	-1.71943	-0.24017
H	-7.79096	0.231	-1.43268
H	-5.35961	0.65988	-1.3184
H	-0.34633	-5.39846	1.47507

H	0.18328	-7.80281	1.24255
H	1.92077	-8.54753	-0.37694
H	3.11174	-6.85931	-1.76441
H	2.57373	-4.45651	-1.53036
H	5.32613	-0.27236	-1.70752
H	7.75862	0.18928	-1.76829
H	8.76832	1.7774	-0.14011
H	7.32101	2.89235	1.54949
H	4.89209	2.41963	1.60939
H	0.39526	5.36248	1.44439
H	-0.19276	7.76347	1.49039
H	-1.99353	8.63552	0.01011
H	-3.20333	7.07523	-1.50466
H	-2.61121	4.67396	-1.54299
H	-0.1538	-0.40441	1.50692
H	-0.42519	-1.93636	2.34822
H	-1.7665	-0.77704	2.16317
N	1.74817	-1.01917	0.08964
H	1.07129	-0.61756	-0.52724
N	-2.99814	2.85213	0.52779
H	-3.61932	3.56058	0.86281

22-MeNCTPP-i

N	-1.28089	-1.86082	0.44422
N	1.2334	1.80897	-0.07835
C	-1.72993	2.44774	0.02358
C	-1.72044	1.06395	-0.22384
C	-3.71987	1.76994	0.57882
C	-2.9956	0.5768	0.12303
C	-3.48261	-0.75276	0.05229
C	-2.59347	-1.85062	-0.04042
C	-2.77277	-3.04979	-0.78496
C	-1.57915	-3.73439	-0.7891
C	-0.62736	-2.98512	-0.03499
C	0.74486	-3.3018	0.14013
C	1.80159	-2.3707	0.30389
C	3.16883	-2.77872	0.63586
C	3.93368	-1.66345	0.5709
C	3.03536	-0.57085	0.20424

C	3.46775	0.75795	-0.01359
C	2.60074	1.8558	-0.20504
C	2.92913	3.2105	-0.52781
C	1.76308	3.93588	-0.55709
C	0.66944	3.06153	-0.25385
C	-0.69427	3.40383	-0.11563
C	-4.93534	-1.01863	-0.03105
C	-5.50814	-2.12382	0.62937
C	-6.87652	-2.37344	0.554
C	-7.70638	-1.52528	-0.18264
C	-7.15498	-0.42721	-0.8468
C	-5.78642	-0.17707	-0.7748
C	1.08497	-4.74805	0.00052
C	0.40989	-5.71825	0.76388
C	0.71031	-7.07327	0.63318
C	1.6875	-7.4913	-0.27255
C	2.35933	-6.54304	-1.04665
C	2.06137	-5.18754	-0.91259
C	4.93421	1.04056	-0.04591
C	5.76556	0.41544	-0.99093
C	7.13489	0.67897	-1.02497
C	7.7014	1.5725	-0.11397
C	6.88829	2.20087	0.83116
C	5.51866	1.93839	0.8638
C	-1.04824	4.8486	-0.07237
C	-0.37791	5.74071	0.78248
C	-0.71649	7.09331	0.81364
C	-1.7301	7.58129	-0.01206
C	-2.40979	6.70466	-0.86108
C	-2.07797	5.35254	-0.88603
C	-0.88039	-1.19473	1.68619
H	-0.94474	0.48086	-0.69862
H	-4.72892	1.78188	0.97959
H	-3.66748	-3.29044	-1.34173
H	-1.34432	-4.63372	-1.33978
H	3.48042	-3.77801	0.90488
H	4.99126	-1.57213	0.7741
H	3.92799	3.57192	-0.72157
H	1.65622	4.98527	-0.78704
H	-4.87155	-2.77314	1.2226

H	-7.29742	-3.22632	1.07993
H	-8.77399	-1.71943	-0.24017
H	-7.79096	0.231	-1.43268
H	-5.35961	0.65988	-1.3184
H	-0.34633	-5.39846	1.47507
H	0.18328	-7.80281	1.24255
H	1.92077	-8.54753	-0.37694
H	3.11174	-6.85931	-1.76441
H	2.57373	-4.45651	-1.53036
H	5.32613	-0.27236	-1.70752
H	7.75862	0.18928	-1.76829
H	8.76832	1.7774	-0.14011
H	7.32101	2.89235	1.54949
H	4.89209	2.41963	1.60939
H	0.39526	5.36248	1.44439
H	-0.19276	7.76347	1.49039
H	-1.99353	8.63552	0.01011
H	-3.20333	7.07523	-1.50466
H	-2.61121	4.67396	-1.54299
H	-0.1538	-0.40441	1.50692
H	-0.42519	-1.93636	2.34822
H	-1.7665	-0.77704	2.16317
N	1.74817	-1.01917	0.08964
N	-2.99814	2.85213	0.52779

21-MeNCTPP-a,b

H	0.77496	0.92186	0.11085
N	-2.97812	2.87707	0.51828
N	-1.29454	-1.85046	0.44594
N	1.7412	-1.03192	0.08969
N	1.24755	1.79873	-0.07499
C	-1.71047	2.46076	0.02319
C	-1.70968	1.07649	-0.21895
C	-3.70904	1.8009	0.5696
C	-2.99098	0.60078	0.12257
C	-3.48832	-0.72481	0.05508
C	-2.60834	-1.83077	-0.03491
C	-2.7985	-3.02788	-0.7793
C	-1.60976	-3.72122	-0.78658

C	-0.65111	-2.97915	-0.03486
C	0.71955	-3.30677	0.13775
C	1.78423	-2.38512	0.29891
C	3.1491	-2.80481	0.62496
C	3.92259	-1.69556	0.56187
C	3.0322	-0.59455	0.20214
C	3.47422	0.73175	-0.01163
C	2.61505	1.83615	-0.19975
C	2.9548	3.18878	-0.51909
C	1.79472	3.923	-0.54872
C	0.69435	3.05623	-0.24867
C	-0.66674	3.40881	-0.11416
C	-4.94297	-0.97992	-0.02756
C	-5.52352	-2.07851	0.63679
C	-6.89334	-2.31866	0.56171
C	-7.71672	-1.46747	-0.17817
C	-7.15756	-0.37604	-0.84619
C	-5.78754	-0.1353	-0.77499
C	1.04706	-4.75582	-0.00299
C	0.36543	-5.7202	0.76166
C	0.65403	-7.0774	0.62994
C	1.62546	-7.50338	-0.27786
C	2.30337	-6.56101	-1.05331
C	2.01728	-5.20329	-0.91863
C	4.94264	1.00362	-0.04363
C	5.76936	0.37361	-0.98929
C	7.14036	0.62689	-1.02249
C	7.71312	1.515	-0.11053
C	6.9047	2.14824	0.83495
C	5.53346	1.89584	0.8673
C	-1.01003	4.85623	-0.07401
C	-0.33563	5.74437	0.78157
C	-0.66394	7.09932	0.80927
C	-1.67124	7.59341	-0.02001
C	-2.35523	6.72072	-0.86922
C	-2.03372	5.36637	-0.89116
H	-4.72017	1.82126	0.96325
H	-3.69572	-3.26114	-1.33373
H	-1.38292	-4.62191	-1.33704
H	3.45333	-3.80697	0.88867

H	4.98083	-1.61338	0.76162
H	3.95628	3.54214	-0.71022
H	1.69595	4.97297	-0.77634
H	-4.89162	-2.72971	1.23187
H	-7.32042	-3.16603	1.0902
H	-8.785	-1.65417	-0.23535
H	-7.78854	0.28377	-1.43447
H	-5.35458	0.69586	-1.3214
H	-0.3862	-5.39407	1.47392
H	0.12265	-7.80231	1.23988
H	1.84938	-8.5609	-0.38287
H	3.05081	-6.8836	-1.77246
H	2.53384	-4.47671	-1.53709
H	5.32504	-0.30963	-1.7063
H	7.7604	0.13387	-1.76574
H	8.78088	1.71187	-0.1362
H	7.34232	2.83526	1.55361
H	4.91049	2.38046	1.61281
H	0.43226	5.36138	1.44585
H	-0.13754	7.76642	1.48591
H	-1.92646	8.64902	-0.00045
H	-3.14357	7.09623	-1.51518
H	-2.57011	4.69062	-1.54753
H	-0.88513	-1.15965	1.04189
C	-0.60403	0.23287	-0.88034
H	-0.01168	0.85685	-1.51648
H	0.01778	-0.19698	-0.12305
H	-1.04997	-0.54741	-1.46103

21-MeNCTPP-c,d

N	-2.97812	2.87707	0.51828
N	-1.29454	-1.85046	0.44594
N	1.7412	-1.03192	0.08969
N	1.24755	1.79873	-0.07499
C	-1.71047	2.46076	0.02319
C	-1.70968	1.07649	-0.21895
C	-3.70904	1.8009	0.5696
C	-2.99098	0.60078	0.12257
C	-3.48832	-0.72481	0.05508

C	-2.60834	-1.83077	-0.03491
C	-2.7985	-3.02788	-0.7793
C	-1.60976	-3.72122	-0.78658
C	-0.65111	-2.97915	-0.03486
C	0.71955	-3.30677	0.13775
C	1.78423	-2.38512	0.29891
C	3.1491	-2.80481	0.62496
C	3.92259	-1.69556	0.56187
C	3.0322	-0.59455	0.20214
C	3.47422	0.73175	-0.01163
C	2.61505	1.83615	-0.19975
C	2.9548	3.18878	-0.51909
C	1.79472	3.923	-0.54872
C	0.69435	3.05623	-0.24867
C	-0.66674	3.40881	-0.11416
C	-4.94297	-0.97992	-0.02756
C	-5.52352	-2.07851	0.63679
C	-6.89334	-2.31866	0.56171
C	-7.71672	-1.46747	-0.17817
C	-7.15756	-0.37604	-0.84619
C	-5.78754	-0.1353	-0.77499
C	1.04706	-4.75582	-0.00299
C	0.36543	-5.7202	0.76166
C	0.65403	-7.0774	0.62994
C	1.62546	-7.50338	-0.27786
C	2.30337	-6.56101	-1.05331
C	2.01728	-5.20329	-0.91863
C	4.94264	1.00362	-0.04363
C	5.76936	0.37361	-0.98929
C	7.14036	0.62689	-1.02249
C	7.71312	1.515	-0.11053
C	6.9047	2.14824	0.83495
C	5.53346	1.89584	0.8673
C	-1.01003	4.85623	-0.07401
C	-0.33563	5.74437	0.78157
C	-0.66394	7.09932	0.80927
C	-1.67124	7.59341	-0.02001
C	-2.35523	6.72072	-0.86922
C	-2.03372	5.36637	-0.89116
H	-4.72017	1.82126	0.96325

H	-3.69572	-3.26114	-1.33373
H	-1.38292	-4.62191	-1.33704
H	3.45333	-3.80697	0.88867
H	4.98083	-1.61338	0.76162
H	3.95628	3.54214	-0.71022
H	1.69595	4.97297	-0.77634
H	-4.89162	-2.72971	1.23187
H	-7.32042	-3.16603	1.0902
H	-8.785	-1.65417	-0.23535
H	-7.78854	0.28377	-1.43447
H	-5.35458	0.69586	-1.3214
H	-0.3862	-5.39407	1.47392
H	0.12265	-7.80231	1.23988
H	1.84938	-8.5609	-0.38287
H	3.05081	-6.8836	-1.77246
H	2.53384	-4.47671	-1.53709
H	5.32504	-0.30963	-1.7063
H	7.7604	0.13387	-1.76574
H	8.78088	1.71187	-0.1362
H	7.34232	2.83526	1.55361
H	4.91049	2.38046	1.61281
H	0.43226	5.36138	1.44585
H	-0.13754	7.76642	1.48591
H	-1.92646	8.64902	-0.00045
H	-3.14357	7.09623	-1.51518
H	-2.57011	4.69062	-1.54753
C	-0.60403	0.23287	-0.88034
H	-0.01168	0.85685	-1.51648
H	0.01778	-0.19698	-0.12305
H	-1.04997	-0.54741	-1.46103
H	-3.25104	3.80453	0.77391
H	0.93198	-0.4777	-0.10523

21-MeNCTPP-h

H	0.	0.	0.
N	0.41869	3.40833	0.
N	-0.14075	-0.92587	-0.38266
C	2.72797	-0.20011	-0.65304
C	2.12722	1.04121	-1.02254

C	4.11836	1.29075	0.07455
C	3.00161	2.03296	-0.51291
C	2.85794	3.44367	-0.42545
C	1.60043	4.06317	-0.29952
C	1.26201	5.45373	-0.37745
C	-0.07682	5.59289	-0.10822
C	-0.62061	4.29028	0.14615
C	-1.94581	3.94316	0.47609
C	-2.45443	2.62335	0.54153
C	-3.82117	2.33509	0.96897
C	-4.00112	1.0032	0.81625
C	-2.74478	0.46829	0.29822
C	-2.59268	-0.8878	-0.06194
C	-1.38275	-1.4991	-0.46539
C	-1.18391	-2.80256	-1.01928
C	0.16515	-2.97769	-1.23007
C	0.84423	-1.78918	-0.82246
C	2.23313	-1.51643	-0.79142
C	4.08297	4.27967	-0.37216
C	4.24143	5.31744	0.56647
C	5.40882	6.07756	0.60216
C	6.44665	5.81648	-0.29543
C	6.31029	4.78388	-1.22534
C	5.14394	4.02213	-1.26137
C	-2.87724	5.08486	0.73928
C	-2.64987	5.96632	1.80917
C	-3.51063	7.03781	2.04984
C	-4.61467	7.25069	1.2224
C	-4.85169	6.3844	0.15329
C	-3.99132	5.31277	-0.08589
C	-3.79968	-1.77161	-0.05532
C	-4.90251	-1.49204	-0.87992
C	-6.02313	-2.32264	-0.88187
C	-6.06361	-3.44975	-0.05887
C	-4.97441	-3.74128	0.76451
C	-3.85267	-2.9119	0.76391
C	3.18182	-2.65414	-0.81761
C	2.93787	-3.83771	-0.09652
C	3.83721	-4.90169	-0.14145
C	4.99964	-4.80596	-0.90823

C	5.26093	-3.63358	-1.62177
C	4.36603	-2.56861	-1.57339
H	4.95726	1.73687	0.60042
H	1.95818	6.2367	-0.6403
H	-0.65124	6.50728	-0.10527
H	-4.52982	3.05924	1.34383
H	-4.8849	0.42529	1.04433
H	-1.97608	-3.50119	-1.24379
H	0.6522	-3.83935	-1.66263
H	3.45353	5.50467	1.2894
H	5.51382	6.86662	1.34213
H	7.35688	6.40931	-0.26596
H	7.11222	4.57308	-1.92781
H	5.03489	3.22854	-1.99429
H	-1.79747	5.79796	2.46142
H	-3.32073	7.70303	2.88817
H	-5.28515	8.0853	1.40906
H	-5.70501	6.5456	-0.50034
H	-4.17309	4.64603	-0.9239
H	-4.86985	-0.62138	-1.52837
H	-6.86317	-2.09124	-1.53158
H	-6.93698	-4.09641	-0.05955
H	-4.99869	-4.61311	1.41308
H	-3.01101	-3.13693	1.41283
H	2.05163	-3.90826	0.52627
H	3.6343	-5.80205	0.43256
H	5.70073	-5.63565	-0.94429
H	6.16542	-3.54914	-2.21832
H	4.57091	-1.66015	-2.12924
H	0.29919	2.41429	0.14523
C	1.06656	1.2529	-2.07616
H	1.04707	0.40012	-2.76299
H	0.04355	1.37941	-1.70072
H	1.30206	2.15005	-2.65947
N	-1.80539	1.46818	0.18669
H	-1.46942	1.53398	-0.75288
N	3.96965	0.	0.
H	4.58865	-0.75132	0.22881

21-MeNCTPP-i

N	0.41869	3.40833	0.
N	-0.14075	-0.92587	-0.38266
C	2.72797	-0.20011	-0.65304
C	2.12722	1.04121	-1.02254
C	4.11836	1.29075	0.07455
C	3.00161	2.03296	-0.51291
C	2.85794	3.44367	-0.42545
C	1.60043	4.06317	-0.29952
C	1.26201	5.45373	-0.37745
C	-0.07682	5.59289	-0.10822
C	-0.62061	4.29028	0.14615
C	-1.94581	3.94316	0.47609
C	-2.45443	2.62335	0.54153
C	-3.82117	2.33509	0.96897
C	-4.00112	1.0032	0.81625
C	-2.74478	0.46829	0.29822
C	-2.59268	-0.8878	-0.06194
C	-1.38275	-1.4991	-0.46539
C	-1.18391	-2.80256	-1.01928
C	0.16515	-2.97769	-1.23007
C	0.84423	-1.78918	-0.82246
C	2.23313	-1.51643	-0.79142
C	4.08297	4.27967	-0.37216
C	4.24143	5.31744	0.56647
C	5.40882	6.07756	0.60216
C	6.44665	5.81648	-0.29543
C	6.31029	4.78388	-1.22534
C	5.14394	4.02213	-1.26137
C	-2.87724	5.08486	0.73928
C	-2.64987	5.96632	1.80917
C	-3.51063	7.03781	2.04984
C	-4.61467	7.25069	1.2224
C	-4.85169	6.3844	0.15329
C	-3.99132	5.31277	-0.08589
C	-3.79968	-1.77161	-0.05532
C	-4.90251	-1.49204	-0.87992
C	-6.02313	-2.32264	-0.88187
C	-6.06361	-3.44975	-0.05887
C	-4.97441	-3.74128	0.76451

C	-3.85267	-2.9119	0.76391
C	3.18182	-2.65414	-0.81761
C	2.93787	-3.83771	-0.09652
C	3.83721	-4.90169	-0.14145
C	4.99964	-4.80596	-0.90823
C	5.26093	-3.63358	-1.62177
C	4.36603	-2.56861	-1.57339
H	4.95726	1.73687	0.60042
H	1.95818	6.2367	-0.6403
H	-0.65124	6.50728	-0.10527
H	-4.52982	3.05924	1.34383
H	-4.8849	0.42529	1.04433
H	-1.97608	-3.50119	-1.24379
H	0.6522	-3.83935	-1.66263
H	3.45353	5.50467	1.2894
H	5.51382	6.86662	1.34213
H	7.35688	6.40931	-0.26596
H	7.11222	4.57308	-1.92781
H	5.03489	3.22854	-1.99429
H	-1.79747	5.79796	2.46142
H	-3.32073	7.70303	2.88817
H	-5.28515	8.0853	1.40906
H	-5.70501	6.5456	-0.50034
H	-4.17309	4.64603	-0.9239
H	-4.86985	-0.62138	-1.52837
H	-6.86317	-2.09124	-1.53158
H	-6.93698	-4.09641	-0.05955
H	-4.99869	-4.61311	1.41308
H	-3.01101	-3.13693	1.41283
H	2.05163	-3.90826	0.52627
H	3.6343	-5.80205	0.43256
H	5.70073	-5.63565	-0.94429
H	6.16542	-3.54914	-2.21832
H	4.57091	-1.66015	-2.12924
C	1.06656	1.2529	-2.07616
H	1.04707	0.40012	-2.76299
H	0.04355	1.37941	-1.70072
H	1.30206	2.15005	-2.65947
N	-1.80539	1.46818	0.18669
N	3.96965	0.	0.

21-MeTPP-c

N	1.61631	1.2893	0.07603
N	1.51118	-1.50788	-0.03
N	-1.64041	-1.37566	-0.04517
C	-2.84009	1.38417	-0.08323
C	-2.17877	3.37274	-0.73213
C	-1.07777	2.77106	-0.0632
C	0.21448	3.34012	0.09214
C	1.43239	2.63859	0.23594
C	2.71279	3.29246	0.50852
C	3.6611	2.32499	0.46679
C	2.95908	1.08137	0.17071
C	3.59057	-0.17459	-0.01178
C	2.88025	-1.37645	-0.16194
C	3.38775	-2.68174	-0.45857
C	2.33405	-3.55476	-0.47333
C	1.12665	-2.82984	-0.18213
C	-0.15051	-3.39859	-0.04544
C	-1.37882	-2.71934	0.13625
C	-2.60453	-3.29975	0.58087
C	-3.5642	-2.3133	0.63375
C	-2.97183	-1.08795	0.22241
C	-3.57212	0.18651	0.05179
C	0.27225	4.82964	-0.01066
C	1.10078	5.46813	-0.95027
C	1.13877	6.85919	-1.0416
C	0.35245	7.64051	-0.19288
C	-0.47983	7.02074	0.7415
C	-0.525	5.63037	0.82593
C	5.08071	-0.23955	-0.06027
C	5.80008	0.49526	-1.01848
C	7.19249	0.43445	-1.06859
C	7.89466	-0.36173	-0.16163
C	7.19384	-1.09621	0.79658
C	5.80109	-1.03563	0.8466
C	-0.23338	-4.89445	-0.05777
C	0.41506	-5.66365	0.92247
C	0.32557	-7.05586	0.91178

C	-0.41321	-7.70403	-0.07993
C	-1.0644	-6.95128	-1.05914
C	-0.97752	-5.55923	-1.04634
C	-5.04758	0.25265	-0.07433
C	-5.76756	-0.70703	-0.80914
C	-7.15552	-0.63274	-0.91877
C	-7.85283	0.40196	-0.29399
C	-7.15104	1.36873	0.43037
C	-5.76472	1.2999	0.53402
H	-2.07681	4.33259	-1.22994
H	2.84997	4.34159	0.72641
H	4.723	2.42796	0.63978
H	4.42609	-2.9069	-0.65127
H	2.36908	-4.61347	-0.68065
H	-2.71909	-4.33556	0.86317
H	-4.58678	-2.41494	0.96529
H	1.70103	4.86411	-1.62395
H	1.77762	7.33218	-1.7828
H	0.38298	8.72452	-0.26357
H	-1.09749	7.62051	1.40466
H	-1.17755	5.15216	1.54997
H	5.25729	1.10618	-1.73383
H	7.7287	1.00554	-1.82192
H	8.97959	-0.40854	-0.20075
H	7.73158	-1.71225	1.51254
H	5.26155	-1.59596	1.60491
H	0.98219	-5.16155	1.70112
H	0.8284	-7.63347	1.68287
H	-0.48236	-8.78841	-0.08859
H	-1.63823	-7.4476	-1.83717
H	-1.48103	-4.97645	-1.81238
H	-5.23058	-1.49362	-1.32978
H	-7.6895	-1.37699	-1.5038
H	-8.93501	0.46006	-0.37741
H	-7.68554	2.18273	0.91262
H	-5.22127	2.05378	1.0908
C	-1.11187	1.0963	1.73078
H	-1.53851	0.12077	1.95797
H	-0.02748	1.03632	1.82504
H	-1.50333	1.82349	2.45425

C	-3.31032	2.54007	-0.80263
N	-1.4703	1.49198	0.35229
H	0.96187	-0.6692	0.15351
H	-4.25949	2.71677	-1.26389

21-MeTPP-a

N	1.62306	-1.3768	-0.05683
N	-1.52997	-1.48264	-0.03538
N	-1.5943	1.30962	0.10269
C	1.12187	2.76413	-0.16409
C	3.26668	2.49279	-0.66039
C	2.8464	1.34502	0.05473
C	3.57252	0.13282	0.21803
C	2.96109	-1.13184	0.22958
C	3.54463	-2.41063	0.49737
C	2.58121	-3.37117	0.3317
C	1.34808	-2.73311	-0.02909
C	0.117	-3.3794	-0.23599
C	-1.16893	-2.79291	-0.28365
C	-2.39355	-3.49535	-0.53072
C	-3.44073	-2.61732	-0.39497
C	-2.90389	-1.33612	-0.07329
C	-3.58649	-0.12744	0.17142
C	-2.93248	1.115	0.32448
C	-3.58049	2.36349	0.69525
C	-2.61626	3.31848	0.64154
C	-1.38122	2.64793	0.24577
C	-0.1622	3.33576	-0.04097
C	5.05542	0.22019	0.26347
C	5.87148	-0.5945	-0.54293
C	7.26085	-0.49389	-0.48703
C	7.86501	0.42659	0.37117
C	7.0683	1.25218	1.16759
C	5.67981	1.15282	1.11194
C	0.18122	-4.87206	-0.36728
C	0.84881	-5.46237	-1.45223
C	0.92361	-6.85019	-1.57556
C	0.33477	-7.67251	-0.61338
C	-0.32905	-7.09836	0.47277

C	-0.40528	-5.71072	0.59446
C	-5.07489	-0.18168	0.24841
C	-5.72132	-1.01567	1.17691
C	-7.1135	-1.06309	1.24703
C	-7.88706	-0.28085	0.38741
C	-7.25844	0.55071	-0.54135
C	-5.86651	0.6013	-0.60953
C	-0.24657	4.79026	-0.33353
C	-1.25167	5.3096	-1.1704
C	-1.31244	6.67189	-1.45878
C	-0.37327	7.54717	-0.90988
C	0.63362	7.04824	-0.08146
C	0.70263	5.68473	0.19542
H	4.25446	2.5508	-1.10871
H	4.56674	-2.56018	0.81189
H	2.68795	-4.4339	0.48984
H	-2.45301	-4.54312	-0.78262
H	-4.49166	-2.82996	-0.52286
H	-4.6173	2.48183	0.9768
H	-2.71283	4.36918	0.87391
H	5.40893	-1.28931	-1.2373
H	7.87152	-1.12616	-1.12617
H	8.94793	0.50621	0.41285
H	7.52904	1.97504	1.8355
H	5.06386	1.79578	1.73307
H	1.30369	-4.8245	-2.20487
H	1.43903	-7.288	-2.42624
H	0.39344	-8.75338	-0.70837
H	-0.78349	-7.73089	1.23073
H	-0.91443	-5.26722	1.44546
H	-5.12362	-1.61494	1.85777
H	-7.59361	-1.70737	1.97889
H	-8.97172	-0.31864	0.44136
H	-7.85214	1.15858	-1.21891
H	-5.38093	1.24091	-1.34039
H	-1.96712	4.63153	-1.62483
H	-2.08825	7.04764	-2.12086
H	-0.42255	8.61031	-1.13121
H	1.37252	7.72124	0.34529
H	1.48346	5.30173	0.84193

C	1.05621	1.12324	1.74257
H	1.31862	1.9184	2.45207
H	-0.02042	0.96288	1.7622
H	1.55982	0.20588	2.047
H	1.0242	-0.64075	-0.411
C	2.20569	3.37951	-0.89784
N	1.48517	1.49289	0.37725
H	2.19984	4.28081	-1.47448

21-MeTPP-h

N	0.	0.	0.
N	3.12046	2.93706	0.
C	0.40722	4.32696	0.28566
C	-1.67983	3.9155	0.86824
C	-1.22203	2.78708	0.13645
C	-1.92908	1.57425	-0.06028
C	-1.33298	0.30608	-0.18898
C	-1.98214	-0.94249	-0.48001
C	-1.0478	-1.9423	-0.4256
C	0.2227	-1.35493	-0.11198
C	1.45896	-1.99938	0.03661
C	2.71203	-1.3408	0.14644
C	3.96325	-2.05315	0.3699
C	4.95035	-1.12625	0.30278
C	4.30078	0.15161	0.04553
C	5.01455	1.35034	-0.16987
C	4.43069	2.6296	-0.28719
C	5.04383	3.84872	-0.7053
C	4.101	4.84923	-0.63404
C	2.87511	4.28225	-0.17204
C	1.65774	4.9515	0.1337
C	-3.41777	1.65178	-0.02035
C	-4.1771	0.83888	0.84001
C	-5.5684	0.92979	0.86713
C	-6.22955	1.83661	0.03694
C	-5.48845	2.65817	-0.81505
C	-4.09799	2.56964	-0.83996
C	1.43399	-3.49519	0.03532
C	0.74239	-4.20272	1.03234

C	0.71136	-5.5977	1.0283
C	1.36807	-6.31134	0.02431
C	2.05639	-5.62075	-0.97529
C	2.08972	-4.22644	-0.96933
C	6.50059	1.28615	-0.31101
C	7.09601	0.50857	-1.31891
C	8.48308	0.45576	-1.45439
C	9.3021	1.17684	-0.58333
C	8.72437	1.9539	0.42245
C	7.33705	2.01101	0.55494
C	1.72524	6.41369	0.38073
C	2.76808	6.98057	1.13616
C	2.81781	8.35338	1.37316
C	1.82742	9.18972	0.85549
C	0.7817	8.64178	0.10946
C	0.72631	7.26935	-0.11983
H	-2.65604	3.91587	1.34445
H	-3.03019	-1.04107	-0.71955
H	-1.20434	-2.99413	-0.61341
H	4.0621	-3.1118	0.56131
H	6.01182	-1.28	0.43245
H	6.06577	3.93632	-1.04299
H	4.22706	5.88715	-0.90358
H	-3.66822	0.14953	1.50724
H	-6.13515	0.29919	1.54707
H	-7.31364	1.90803	0.05907
H	-5.99361	3.37018	-1.46217
H	-3.52495	3.21218	-1.50144
H	0.23847	-3.65084	1.82088
H	0.17752	-6.12628	1.81367
H	1.34352	-7.39773	0.0205
H	2.56482	-6.16775	-1.76492
H	2.61894	-3.69227	-1.75315
H	6.46091	-0.04584	-2.00345
H	8.9237	-0.14591	-2.24493
H	10.38284	1.13398	-0.68808
H	9.3539	2.51364	1.10907
H	6.89202	2.60861	1.34527
H	3.52407	6.33424	1.57102
H	3.62447	8.767	1.97276

H	1.86649	10.26061	1.03766
H	0.00286	9.28474	-0.29163
H	-0.08682	6.84649	-0.69747
C	0.56102	2.60982	-1.59444
H	0.94667	3.48429	-2.12398
H	1.34241	1.84666	-1.56783
H	-0.29089	2.21468	-2.15145
H	0.74394	0.64757	0.22559
H	2.46962	2.24513	0.34868
C	-0.68733	4.88716	1.04315
N	0.11394	3.01698	-0.23929
N	2.93481	0.	0.
H	2.36692	0.64096	-0.5164
H	-0.72879	5.80388	1.59342

21-MeTPP-i

N	0.	0.	0.
N	3.12046	2.93706	0.
C	0.40722	4.32696	0.28566
C	-1.67983	3.9155	0.86824
C	-1.22203	2.78708	0.13645
C	-1.92908	1.57425	-0.06028
C	-1.33298	0.30608	-0.18898
C	-1.98214	-0.94249	-0.48001
C	-1.0478	-1.9423	-0.4256
C	0.2227	-1.35493	-0.11198
C	1.45896	-1.99938	0.03661
C	2.71203	-1.3408	0.14644
C	3.96325	-2.05315	0.3699
C	4.95035	-1.12625	0.30278
C	4.30078	0.15161	0.04553
C	5.01455	1.35034	-0.16987
C	4.43069	2.6296	-0.28719
C	5.04383	3.84872	-0.7053
C	4.101	4.84923	-0.63404
C	2.87511	4.28225	-0.17204
C	1.65774	4.9515	0.1337
C	-3.41777	1.65178	-0.02035
C	-4.1771	0.83888	0.84001

C	-5.5684	0.92979	0.86713
C	-6.22955	1.83661	0.03694
C	-5.48845	2.65817	-0.81505
C	-4.09799	2.56964	-0.83996
C	1.43399	-3.49519	0.03532
C	0.74239	-4.20272	1.03234
C	0.71136	-5.5977	1.0283
C	1.36807	-6.31134	0.02431
C	2.05639	-5.62075	-0.97529
C	2.08972	-4.22644	-0.96933
C	6.50059	1.28615	-0.31101
C	7.09601	0.50857	-1.31891
C	8.48308	0.45576	-1.45439
C	9.3021	1.17684	-0.58333
C	8.72437	1.9539	0.42245
C	7.33705	2.01101	0.55494
C	1.72524	6.41369	0.38073
C	2.76808	6.98057	1.13616
C	2.81781	8.35338	1.37316
C	1.82742	9.18972	0.85549
C	0.7817	8.64178	0.10946
C	0.72631	7.26935	-0.11983
H	-2.65604	3.91587	1.34445
H	-3.03019	-1.04107	-0.71955
H	-1.20434	-2.99413	-0.61341
H	4.0621	-3.1118	0.56131
H	6.01182	-1.28	0.43245
H	6.06577	3.93632	-1.04299
H	4.22706	5.88715	-0.90358
H	-3.66822	0.14953	1.50724
H	-6.13515	0.29919	1.54707
H	-7.31364	1.90803	0.05907
H	-5.99361	3.37018	-1.46217
H	-3.52495	3.21218	-1.50144
H	0.23847	-3.65084	1.82088
H	0.17752	-6.12628	1.81367
H	1.34352	-7.39773	0.0205
H	2.56482	-6.16775	-1.76492
H	2.61894	-3.69227	-1.75315
H	6.46091	-0.04584	-2.00345

H	8.9237	-0.14591	-2.24493
H	10.38284	1.13398	-0.68808
H	9.3539	2.51364	1.10907
H	6.89202	2.60861	1.34527
H	3.52407	6.33424	1.57102
H	3.62447	8.767	1.97276
H	1.86649	10.26061	1.03766
H	0.00286	9.28474	-0.29163
H	-0.08682	6.84649	-0.69747
C	0.56102	2.60982	-1.59444
H	0.94667	3.48429	-2.12398
H	1.34241	1.84666	-1.56783
H	-0.29089	2.21468	-2.15145
C	-0.68733	4.88716	1.04315
N	0.11394	3.01698	-0.23929
N	2.93481	0.	0.
H	-0.72879	5.80388	1.59342

23-MeNCTPP-a

N	-0.68324	2.09033	0.00222
N	0.73194	-1.97166	0.09913
N	-2.05359	-0.68012	0.40255
C	2.3092	1.98765	-0.12646
C	3.0589	-0.14938	-0.14491
C	0.15549	3.1844	0.17571
C	-2.00444	2.42259	0.22925
C	2.01956	-2.37393	0.27436
C	-0.0401	-3.05752	0.39614
C	-3.02798	0.16968	-0.13988
C	-2.25659	-1.97554	-0.08427
C	3.72397	1.88276	-0.5638
C	-0.69927	4.25415	0.58978
C	2.07526	-3.74418	0.74742
C	0.78688	-4.17648	0.83378
C	-3.87144	-0.63747	-0.9619
C	-3.41409	-1.93449	-0.90999
H	0.43183	-5.14035	1.18205
H	-4.67871	-0.25144	-1.56787
H	-0.34971	5.23529	0.8764

C	-1.44255	-3.1098	0.17197
C	1.5533	3.18629	0.00909
C	3.16094	-1.54704	0.0034
C	-3.11236	1.57738	0.04082
H	-3.77518	-2.77859	-1.48348
H	2.97026	-4.287	1.01807
H	4.34074	2.70627	-0.89014
C	4.48784	-2.19811	-0.126
C	4.64135	-3.35002	-0.91939
C	5.624	-1.68243	0.52433
C	5.88396	-3.96785	-1.05354
H	3.78185	-3.7447	-1.45209
C	6.86198	-2.30746	0.39908
H	5.52492	-0.7911	1.13277
C	6.99818	-3.45186	-0.39036
H	5.98132	-4.84994	-1.68118
H	7.72479	-1.89815	0.91805
H	7.96682	-3.93465	-0.49108
C	-2.11237	-4.43299	0.04677
C	-3.33402	-4.67876	0.70198
C	-1.54573	-5.46856	-0.71804
C	-3.96878	-5.91512	0.58738
H	-3.77321	-3.89492	1.30173
C	-2.18382	-6.70283	-0.83621
H	-0.61835	-5.28895	-1.25215
C	-3.40103	-6.93238	-0.17235
H	-4.90505	-6.08572	1.11225
H	-1.74131	-7.48431	-1.44823
H	-3.89651	-7.89594	-0.25619
C	2.25979	4.49454	0.0059
C	1.82803	5.55216	-0.8157
C	3.3825	4.7017	0.815
C	2.50125	6.77303	-0.82382
H	0.97294	5.40128	-1.47781
C	4.05345	5.92336	0.80743
H	3.72093	3.90092	1.46565
C	3.61062	6.96417	-0.0115
H	2.15646	7.57268	-1.47415
H	4.92097	6.0638	1.45674
H	4.1356	7.91556	-0.01889

C	-4.46156	2.18867	-0.10424
C	-5.56774	1.63478	0.56821
C	-4.68137	3.31985	-0.91337
C	-6.83807	2.1944	0.44576
H	-5.42927	0.76531	1.20173
C	-5.95158	3.88137	-1.03302
H	-3.84992	3.74549	-1.45679
C	-7.03577	3.32245	-0.3534
H	-7.68389	1.753	0.97225
H	-6.09662	4.7501	-1.66987
H	-8.02604	3.75954	-0.44853
C	1.9421	0.66312	0.11572
H	1.01512	0.26654	0.46387
N	4.15296	0.64752	-0.57581
C	-1.41153	-0.41506	1.6992
H	-0.19521	-0.33925	1.57309
H	-1.89859	0.64049	2.11299
H	-0.39919	1.23354	-0.43886
H	-1.71173	-1.36768	2.41973
C	-1.99492	3.7977	0.6325
H	-2.87152	4.35867	0.94038

23-MeNCTPP-b

N	1.77613	0.88356	0.00222
N	-1.77613	-0.88356	0.00222
N	0.88356	-1.77613	-0.00222
C	-0.25718	3.00768	0.00122
C	-2.25105	2.00089	-0.00826
C	2.00089	2.25105	0.00826
C	3.00768	0.25718	-0.00122
C	-3.00768	-0.25718	-0.00122
C	-2.00089	-2.25105	0.00826
C	2.25105	-2.00089	-0.00826
C	0.25718	-3.00768	0.00122
C	-1.28053	4.07522	-0.00809
C	3.42695	2.4999	0.00955
C	-4.07522	-1.28053	0.00809
C	-3.42695	-2.4999	0.00955
C	2.4999	-3.42695	-0.00955
C	1.28053	-4.07522	-0.00809

H	-3.86532	-3.48657	0.00397
H	3.48657	-3.86532	-0.00397
H	3.86532	3.48657	0.00397
C	-1.06663	-3.22073	0.0088
C	1.06663	3.22073	0.0088
C	-3.22073	1.06663	-0.0088
C	3.22073	-1.06663	-0.0088
H	1.10124	-5.13009	-0.00664
H	-5.13009	-1.10124	0.00664
H	-1.10124	5.13009	-0.00664
C	-4.70914	1.46169	-0.02206
C	-5.39205	1.6482	1.18016
C	-5.3745	1.63316	-1.23592
C	-6.74018	2.00543	1.16842
H	-4.86741	1.51219	2.13697
C	-6.72279	1.99146	-1.24783
H	-4.83636	1.48637	-2.18354
C	-7.40572	2.17748	-0.04594
H	-7.27869	2.15184	2.11599
H	-7.24702	2.12699	-2.20505
H	-8.46866	2.4592	-0.05494
C	-1.46172	-4.70918	0.01522
C	-1.64359	-5.38778	-1.19014
C	-1.63763	-5.37893	1.22602
C	-2.00195	-6.73566	-1.18461
H	-1.50558	-4.85928	-2.14454
C	-1.99514	-6.72747	1.23172
H	-1.49415	-4.84428	2.17612
C	-2.17744	-7.40585	0.02669
H	-2.14593	-7.27044	-2.13464
H	-2.13337	-7.25539	2.18654
H	-2.45994	-8.46862	0.03081
C	1.46164	4.70918	0.01872
C	1.6358	5.37656	1.23146
C	1.64541	5.39009	-1.18467
C	1.99299	6.72473	1.24072
H	1.4901	4.83966	2.18001
C	2.00367	6.73842	-1.17558
H	1.50835	4.8642	-2.14059
C	2.17734	7.40583	0.03683

H	2.12967	7.25099	2.19657
H	2.14889	7.27492	-2.12455
H	2.45903	8.46879	0.04438
C	4.65258	-1.63347	-0.01964
C	5.2955	-1.88129	-1.23278
C	5.30675	-1.89902	1.18331
C	6.59204	-2.39518	-1.24288
H	4.7792	-1.67255	-2.18099
C	6.60406	-2.41214	1.17339
H	4.80025	-1.70359	2.13955
C	7.24671	-2.66037	-0.03943
H	7.09863	-2.59113	-2.19905
H	7.11976	-2.62103	2.12202
H	8.26902	-3.0655	-0.04764
C	-0.88356	1.77613	-0.00222
H	-0.39154	0.85789	-0.24645
N	-2.4999	3.42695	-0.00955
C	0.21954	-0.46465	0.0001
H	0.95843	0.30924	-0.0045
H	-0.39618	-0.37508	-0.8704
H	-0.84132	-0.60196	-0.02481
H	-0.42808	-0.20253	0.85491
C	4.25212	1.16435	0.00416
H	5.3021	0.95836	0.0042

23-MeNCTPP-d

N	1.77613	0.88356	0.00222
N	-1.77613	-0.88356	0.00222
N	0.88356	-1.77613	-0.00222
C	-0.25718	3.00768	0.00122
C	-2.25105	2.00089	-0.00826
C	2.00089	2.25105	0.00826
C	3.00768	0.25718	-0.00122
C	-3.00768	-0.25718	-0.00122
C	-2.00089	-2.25105	0.00826
C	2.25105	-2.00089	-0.00826
C	0.25718	-3.00768	0.00122
C	-1.28053	4.07522	-0.00809
C	3.42695	2.4999	0.00955

C	-4.07522	-1.28053	0.00809
C	-3.42695	-2.4999	0.00955
C	2.4999	-3.42695	-0.00955
C	1.28053	-4.07522	-0.00809
H	-3.86532	-3.48657	0.00397
H	3.48657	-3.86532	-0.00397
H	3.86532	3.48657	0.00397
C	-1.06663	-3.22073	0.0088
C	1.06663	3.22073	0.0088
C	-3.22073	1.06663	-0.0088
C	3.22073	-1.06663	-0.0088
H	1.10124	-5.13009	-0.00664
H	-5.13009	-1.10124	0.00664
H	-1.10124	5.13009	-0.00664
C	-4.70914	1.46169	-0.02206
C	-5.39205	1.6482	1.18016
C	-5.3745	1.63316	-1.23592
C	-6.74018	2.00543	1.16842
H	-4.86741	1.51219	2.13697
C	-6.72279	1.99146	-1.24783
H	-4.83636	1.48637	-2.18354
C	-7.40572	2.17748	-0.04594
H	-7.27869	2.15184	2.11599
H	-7.24702	2.12699	-2.20505
H	-8.46866	2.4592	-0.05494
C	-1.46172	-4.70918	0.01522
C	-1.64359	-5.38778	-1.19014
C	-1.63763	-5.37893	1.22602
C	-2.00195	-6.73566	-1.18461
H	-1.50558	-4.85928	-2.14454
C	-1.99514	-6.72747	1.23172
H	-1.49415	-4.84428	2.17612
C	-2.17744	-7.40585	0.02669
H	-2.14593	-7.27044	-2.13464
H	-2.13337	-7.25539	2.18654
H	-2.45994	-8.46862	0.03081
C	1.46164	4.70918	0.01872
C	1.6358	5.37656	1.23146
C	1.64541	5.39009	-1.18467
C	1.99299	6.72473	1.24072

H	1.4901	4.83966	2.18001
C	2.00367	6.73842	-1.17558
H	1.50835	4.8642	-2.14059
C	2.17734	7.40583	0.03683
H	2.12967	7.25099	2.19657
H	2.14889	7.27492	-2.12455
H	2.45903	8.46879	0.04438
C	4.65258	-1.63347	-0.01964
C	5.2955	-1.88129	-1.23278
C	5.30675	-1.89902	1.18331
C	6.59204	-2.39518	-1.24288
H	4.7792	-1.67255	-2.18099
C	6.60406	-2.41214	1.17339
H	4.80025	-1.70359	2.13955
C	7.24671	-2.66037	-0.03943
H	7.09863	-2.59113	-2.19905
H	7.11976	-2.62103	2.12202
H	8.26902	-3.0655	-0.04764
C	-0.88356	1.77613	-0.00222
H	-0.39154	0.85789	-0.24645
N	-2.4999	3.42695	-0.00955
C	0.21954	-0.46465	0.0001
H	0.48925	0.07011	0.88677
H	0.52736	0.0925	-0.85997
H	-0.84132	-0.60196	-0.02481
H	-3.39829	3.86614	-0.01121
C	4.25212	1.16435	0.00416
H	5.3021	0.95836	0.0042

23-MeNCTPP-h

N	-0.54456	2.14548	-0.00543
N	-2.05757	-0.52728	0.37859
C	2.43449	1.82497	-0.05895
C	3.03636	-0.35796	-0.07251
C	0.3643	3.18168	0.16638
C	-1.8427	2.57314	0.19395
C	1.86737	-2.52776	0.26225
C	-0.23713	-3.08217	0.33847
C	-3.01002	0.37264	-0.11504

C	-2.37667	-1.81733	-0.07304
C	3.8112	1.61406	-0.54303
C	-0.41998	4.3207	0.5319
C	1.82534	-3.92587	0.67983
C	0.50979	-4.27168	0.73283
C	-3.94656	-0.3794	-0.87476
C	-3.56652	-1.7025	-0.84323
H	0.0884	-5.22185	1.03117
H	-4.75011	0.05592	-1.45151
H	-0.00781	5.28441	0.79294
C	-1.64082	-3.01034	0.1369
C	1.76158	3.07375	0.03492
C	3.05549	-1.76308	0.0396
C	-3.00443	1.78653	0.03428
H	-4.01663	-2.51958	-1.3888
H	2.67889	-4.5393	0.93293
H	4.47493	2.39165	-0.90821
C	4.34608	-2.48353	-0.10147
C	4.44955	-3.62127	-0.92264
C	5.49784	-2.04768	0.5789
C	5.65872	-4.30291	-1.0538
H	3.57899	-3.95391	-1.47926
C	6.70189	-2.73613	0.45646
H	5.43714	-1.16799	1.20925
C	6.78828	-3.86612	-0.36033
H	5.71841	-5.17258	-1.70311
H	7.57709	-2.38788	0.99873
H	7.73061	-4.39881	-0.45907
C	-2.40914	-4.28036	0.02017
C	-3.61372	-4.45909	0.72589
C	-1.9628	-5.32964	-0.80537
C	-4.33838	-5.6452	0.62133
H	-3.96888	-3.66384	1.37454
C	-2.69102	-6.51314	-0.91421
H	-1.04927	-5.20025	-1.37687
C	-3.87979	-6.6772	-0.19981
H	-5.25942	-5.7649	1.18573
H	-2.33296	-7.3059	-1.56573
H	-4.4452	-7.6014	-0.28411
C	2.557	4.32922	-0.00168

C	2.20556	5.39676	-0.84847
C	3.69781	4.47319	0.80993
C	2.96319	6.56668	-0.87772
H	1.34587	5.29226	-1.50351
C	4.45337	5.64405	0.78111
H	3.97583	3.66409	1.47862
C	4.08905	6.69591	-0.06199
H	2.67926	7.37434	-1.54728
H	5.32573	5.73649	1.42255
H	4.67983	7.60762	-0.08571
C	-4.3132	2.48332	-0.09036
C	-5.43283	2.03683	0.63689
C	-4.47909	3.59211	-0.94184
C	-6.6652	2.67793	0.52511
H	-5.32376	1.18683	1.30392
C	-5.71117	4.23504	-1.05111
H	-3.63716	3.9355	-1.53538
C	-6.8096	3.78206	-0.3176
H	-7.51227	2.31897	1.10378
H	-5.81597	5.08447	-1.72104
H	-7.77012	4.28263	-0.40471
C	1.98168	0.52988	0.22565
H	1.04931	0.22659	0.66241
C	-1.44297	-0.34763	1.70175
H	-0.45754	-0.81019	1.7111
H	-1.35146	0.7135	1.9225
H	-0.30028	1.24099	-0.3884
H	-2.07288	-0.81465	2.46825
C	-1.74467	3.95598	0.55525
H	-2.58597	4.57586	0.82822
N	0.60964	-2.04353	0.09408
H	0.41833	-1.18835	-0.38765
N	4.16568	0.36249	-0.55133
H	5.07144	0.01165	-0.78904

23-MeNCTPP-i

N	-0.54456	2.14548	-0.00543
N	-2.05757	-0.52728	0.37859
C	2.43449	1.82497	-0.05895

C	3.03636	-0.35796	-0.07251
C	0.3643	3.18168	0.16638
C	-1.8427	2.57314	0.19395
C	1.86737	-2.52776	0.26225
C	-0.23713	-3.08217	0.33847
C	-3.01002	0.37264	-0.11504
C	-2.37667	-1.81733	-0.07304
C	3.8112	1.61406	-0.54303
C	-0.41998	4.3207	0.5319
C	1.82534	-3.92587	0.67983
C	0.50979	-4.27168	0.73283
C	-3.94656	-0.3794	-0.87476
C	-3.56652	-1.7025	-0.84323
H	0.0884	-5.22185	1.03117
H	-4.75011	0.05592	-1.45151
H	-0.00781	5.28441	0.79294
C	-1.64082	-3.01034	0.1369
C	1.76158	3.07375	0.03492
C	3.05549	-1.76308	0.0396
C	-3.00443	1.78653	0.03428
H	-4.01663	-2.51958	-1.3888
H	2.67889	-4.5393	0.93293
H	4.47493	2.39165	-0.90821
C	4.34608	-2.48353	-0.10147
C	4.44955	-3.62127	-0.92264
C	5.49784	-2.04768	0.5789
C	5.65872	-4.30291	-1.0538
H	3.57899	-3.95391	-1.47926
C	6.70189	-2.73613	0.45646
H	5.43714	-1.16799	1.20925
C	6.78828	-3.86612	-0.36033
H	5.71841	-5.17258	-1.70311
H	7.57709	-2.38788	0.99873
H	7.73061	-4.39881	-0.45907
C	-2.40914	-4.28036	0.02017
C	-3.61372	-4.45909	0.72589
C	-1.9628	-5.32964	-0.80537
C	-4.33838	-5.6452	0.62133
H	-3.96888	-3.66384	1.37454
C	-2.69102	-6.51314	-0.91421

H	-1.04927	-5.20025	-1.37687
C	-3.87979	-6.6772	-0.19981
H	-5.25942	-5.7649	1.18573
H	-2.33296	-7.3059	-1.56573
H	-4.4452	-7.6014	-0.28411
C	2.557	4.32922	-0.00168
C	2.20556	5.39676	-0.84847
C	3.69781	4.47319	0.80993
C	2.96319	6.56668	-0.87772
H	1.34587	5.29226	-1.50351
C	4.45337	5.64405	0.78111
H	3.97583	3.66409	1.47862
C	4.08905	6.69591	-0.06199
H	2.67926	7.37434	-1.54728
H	5.32573	5.73649	1.42255
H	4.67983	7.60762	-0.08571
C	-4.3132	2.48332	-0.09036
C	-5.43283	2.03683	0.63689
C	-4.47909	3.59211	-0.94184
C	-6.6652	2.67793	0.52511
H	-5.32376	1.18683	1.30392
C	-5.71117	4.23504	-1.05111
H	-3.63716	3.9355	-1.53538
C	-6.8096	3.78206	-0.3176
H	-7.51227	2.31897	1.10378
H	-5.81597	5.08447	-1.72104
H	-7.77012	4.28263	-0.40471
C	1.98168	0.52988	0.22565
H	1.04931	0.22659	0.66241
C	-1.44297	-0.34763	1.70175
H	-0.45754	-0.81019	1.7111
H	-1.35146	0.7135	1.9225
H	-2.07288	-0.81465	2.46825
C	-1.74467	3.95598	0.55525
H	-2.58597	4.57586	0.82822
N	0.60964	-2.04353	0.09408
N	4.16568	0.36249	-0.55133